

1-1-2016

# Molecular Regulation Of Trophoblast Survival During Placentation And Pathologies Of Placental Insufficiency

Chandni V. Jain  
*Wayne State University,*

Follow this and additional works at: [https://digitalcommons.wayne.edu/oa\\_dissertations](https://digitalcommons.wayne.edu/oa_dissertations)

 Part of the [Other Astrophysics and Astronomy Commons](#)

---

## Recommended Citation

Jain, Chandni V., "Molecular Regulation Of Trophoblast Survival During Placentation And Pathologies Of Placental Insufficiency" (2016). *Wayne State University Dissertations*. 1642.  
[https://digitalcommons.wayne.edu/oa\\_dissertations/1642](https://digitalcommons.wayne.edu/oa_dissertations/1642)

This Open Access Dissertation is brought to you for free and open access by DigitalCommons@WayneState. It has been accepted for inclusion in Wayne State University Dissertations by an authorized administrator of DigitalCommons@WayneState.

**MOLECULAR REGULATION OF TROPHOBLAST SURVIVAL DURING  
PLACENTATION AND PATHOLOGIES OF PLACENTAL INSUFFICIENCY**

by

**CHANDNI V. JAIN**

**DISSERTATION**

Submitted to the Graduate School

of Wayne State University,

Detroit, Michigan

in partial fulfillment of the requirements

for the degree of

**DOCTOR OF PHILOSOPHY**

2016

MAJOR: PHYSIOLOGY

Approved By:

\_\_\_\_\_  
Advisor

\_\_\_\_\_  
Date

\_\_\_\_\_  
\_\_\_\_\_  
\_\_\_\_\_  
\_\_\_\_\_

**© COPYRIGHT BY**

**CHANDNI V. JAIN**

**2016**

**All Rights Reserved**

## DEDICATION

I would like to dedicate this degree to several people. First and foremost, I would like to dedicate this work to my father Mr. Ashok Kumar Jain, who has always been my inspiration. His guidance through the years has helped me to become the woman I am today and come to the United States and earn my doctoral degree. His constant support and motivation through the years means more to me than words can explain. I would also like to dedicate this degree to my mother and my in-laws who have always supported and encouraged me even in the most difficult times. Last, but not the least I would like to dedicate this work to my husband Vineet and my beautiful daughter Grisha. Vineet is a wise devoted husband who has always supported me throughout my degree. He has stood by me even in the worst of the days and always expressed how proud he has been of my achievements. Finally, this degree is for my princess Grisha, who is the greatest fortune and joy of my life. The support and good wishes of my family have made this otherwise arduous process possible, so a thank you to all of them.

## ACKNOWLEDGEMENTS

First and foremost, I want to thank my advisor Dr. Randall Armant. It has been an honor to be his Ph.D. student. In 2011, when I first moved to the United States, Dr. Armant, gave me an opportunity to volunteer in his lab and learn the much needed lab techniques. From then on there was no looking back as I joined the Physiology program in 2012 and became a Ph.D. student in Dr. Armant's lab. Through the years Dr. Armant has given the much needed guidance and motivation that have equipped me to earn this degree. He has encouraged and taught me to think critically, ask questions, resolve those questions, critically analyze the data and prove a hypothesis. I appreciate all his contributions of time, ideas, and funding to make my Ph.D. experience productive and stimulating. I would also like to extend a big thank you to Brian Kilburn who without his support this degree would not have been possible. Brian has been both a friend and a teacher, who has not only taught me many experimental techniques but has also provided incredible support in finishing my projects. His encouragement and support with his unsurpassed technical skill throughout my Ph.D. means beyond mere words can express. I would like to acknowledge Dr. Sascha Drewlo, for his guidance and support. Along way I have had the pleasure of working with many people: Dr. Hamid-Reza Kohan-Ghadr, Leena Kadam, Dr. Stephen Krawetz and members of his lab Robert Goodrich, Meritxell JodarBifet and Edward Sandler.

This research was supported by the Rumble Fellowship, NIH Grant R21HD071408, the W.K. Kellogg Foundation and PerkinElmer Health Sciences, Inc.

## TABLE OF CONTENTS

Dedication .....	ii
Acknowledgments.....	iii
List of Tables .....	viii
List of Figures.....	ix
List of Abbreviations .....	xi
Chapter 1 Introduction .....	1
Epidermal growth factor (EGF) signaling system .....	4
Mouse implantation .....	5
Human implantation.....	11
Human placentation .....	12
Chapter 2 Trophoblast Survival Signaling during Human Placentation Requires HIF-induced Transcription of HSP70 .....	16
Abstract.....	16
Introduction.....	16
Materials and Methods.....	20
Cell Culture and Treatments .....	20
Villous Explant Culture .....	21
Antibody Arrays .....	21
Western Blotting.....	21
ELISA .....	22
Immunocytochemistry .....	22
qPCR.....	23
LongRNA (LnRNA) Library Prep for Next Generation Sequencing (NGS) .....	23
Data Alignment & Mapping .....	24
Promoter Extraction.....	24

Statistics .....	24
Results .....	25
Upregulation of MMP2 at low O <sub>2</sub> .....	25
Role of MMP2 in HBEGF upregulation .....	25
MMP2 mRNA expression .....	27
Role of transcription in HBEGF upregulation .....	27
Role of MAPKs in MMP2 upregulation .....	31
Identification of differentially expressed transcripts .....	32
HSP70 function in MMP2 and HBEGF upregulation .....	39
Regulation of MMP2 in first trimester explants .....	40
Discussion .....	41
Chapter 3 Regulation of HBEGF by Micro-RNA for Survival of Developing Human Trophoblast Cells .....	49
Abstract .....	49
Introduction .....	50
Materials and Methods .....	53
Cell Culture and Treatments .....	53
Western Blotting .....	53
ELISA .....	54
Generation of 3'UTR Luciferase Reporter Vectors .....	54
Bacterial Transformations .....	55
Transfection and Luciferase Assay .....	55
Library Preparation for NGS .....	56
Sequencing Data analysis .....	56
DGCR8 Knockdown .....	57
qPCR .....	57

Statistics .....	58
Results .....	58
HBEGF regulation by protein degradation .....	58
Regulation by the HBEGF 3'UTR.....	59
Next generation sequencing to identify differentially expressed miRNAs .....	61
Global inhibition of miRNA processing .....	62
Discussion .....	63
Chapter 4 Fetal Genome Profiling at Five Weeks of Gestation after Noninvasive Isolation of Trophoblast Cells from the Endocervical Canal.....	69
Abstract .....	69
Introduction .....	69
Materials and Methods.....	72
Patient selection .....	72
Isolation of endocervical fetal trophoblast cells .....	72
Fluorescence in situ hybridization (FISH).....	73
Targeted sequencing .....	73
Nuclear isolation and DNA extraction.....	73
Library preparation for ForenSeq .....	75
ForenSeq data analysis.....	75
Results .....	77
Isolation and characterization of fetal cells .....	77
Targeted multiplex next generation sequencing .....	80
Accuracy of haplotype determination .....	81
Discussion .....	82
Chapter 5 Transcriptomic Profiling for Characterization of Cells Isolated by TRIC.....	87
Abstract .....	87



Introduction.....	87
Materials and Methods.....	90
Sample Collection.....	90
RNA Extraction .....	91
Library Preparation .....	91
Data Alignment & Mapping .....	91
qPCR.....	92
Results.....	94
TRIC provides stable RNA from isolated cells .....	94
Transcriptomic analysis of cells isolated by TRIC from normal term pregnancies .....	95
Characterization of cells isolated by TRIC .....	98
Gene Ontology Consortium analysis for fetal and maternal DEGs in normal pregnancies .....	99
Transcriptomic analysis and validation of cells isolated by TRIC in early pregnancy loss.....	100
Gene Ontology Consortium analysis for DEGs in EPL.....	106
Discussion.....	107
Chapter 6 Conclusion.....	112
Appendix - IRB Approval Letter .....	116
References.....	117
Abstract.....	152
Autobiographical Statement.....	155

## LIST OF TABLES

Table 1. MMP2 upregulation is independent of MAPKs .....	32
Table 2. Upregulated transcripts from RNASeq Analysis.....	33
Table 3. Downregulated transcripts from RNASeq Analysis.....	33
Table 4. Primer sequence for amplification of HBEGF 3'UTR and vector sequencing.....	55
Table 5. HBEGF mRNA in HTR-8/SVneo cells with or without (Control) exposure to DGCR8 siRNA measured by qPCR.....	63
Table 6. List of SNP's and STR's targeted by FORENSEQ .....	74
Table 7. Overview of samples and results for targeted sequencing approach .....	79
Table 8. Genes used for qPCR validation.....	93
Table 9. Patient and specimen characteristics.....	96
Table 10. Upregulated fetal genes in EPL compared to normal pregnancy .....	102
Table 11. Downregulated fetal genes in EPL compared to normal pregnancy .....	103

## LIST OF FIGURES

Figure 1. Heparin binding EGF-like growth factor (HBEGF)- signaling and cell differentiation during implantation in mice.....	7
Figure 2. Example for size distribution of individual libraries using Agilent Bioanalyzer .....	24
Figure 3. Upregulation of MMP2 at low O <sub>2</sub> , and its effects on HBEGF and cell survival .....	26
Figure 4. Western blots of molecular weight standards, recombinant MMP2 or MMP9, and extracts of trophoblast cells cultured at 20 % or 2% O <sub>2</sub> .....	27
Figure 5. Expression of MMP2 and HBEGF at 2% O <sub>2</sub> in HTR-8/SVneo cells.....	29
Figure 6. Expression of HIF proteins and HBEGF in presence of CoCl <sub>2</sub> in HTR-8/SVneo cells .....	30
Figure 7. Expression of HIF1A and HIF2A during altered O <sub>2</sub> concentrations or simulated hypoxia (CoCl <sub>2</sub> ) in HTR-8/SVneo cells .....	31
Figure 8. Transcriptome graph analysis of trophoblast cells exposed to 2% O <sub>2</sub> .....	37
Figure 9. Transcriptome analysis of trophoblast cells exposed to 2% O <sub>2</sub> .....	38
Figure 10. Regulation of MMP2, HBEGF and cell survival by HSP70 .....	39
Figure 11. Regulation of MMP2 in first trimester chorionic villous explants.....	41
Figure 12. Proposed Mechanism.....	43
Figure 13. Effect of O <sub>2</sub> concentration on HBEGF stability .....	59
Figure 14. Translational regulation by HBEGF 3'UTR .....	60
Figure 15. Effect of O <sub>2</sub> on miRNA expression by next generation sequencing .....	61
Figure 16. Effect of DGCR8 Knockdown on regulation of HBEGF by O <sub>2</sub> .....	63
Figure 17. Trophoblast isolation, assessment of cell purity, and fetal DNA isolation for sequencing .....	78
Figure 18. Comparison of fetal fractions obtained with/without nuclear isolation .....	79
Figure 19. Targeted sequencing of fetal cells obtained by TRIC .....	81
Figure 20. Approaches to obtain fetal DNA for prenatal testing in ongoing pregnancies in comparison to trophoblast retrieval and isolation from the cervix (TRIC).....	83

Figure 21. Assessment of RNA quality and integrity .....	95
Figure 22. Two visualizations of the comparative transcript expression profiles between fetal and maternal cells .....	97
Figure 23. Validation of RNAseq by qPCR.....	99
Figure 24. Protein-protein interaction.....	100
Figure 25. Volcano plot presentation of all the transcripts in EPL versus control fetal cells.....	101
Figure 26. Real-time qPCR validation of selected differentially expressed genes.....	106
Figure 27. Pathway Analysis for EPL.....	108

## LIST OF ABBREVIATIONS

ADAM:	a disintegrin and metalloproteinase
AGO:	Argonaute protein
ARE:	AU-rich element
AREG:	Amphiregulin
$\beta$ -hCG:	Beta subunit of human chorionic gonadotropin
BTC:	Betacellulin
CSH1:	Placental lactogen
EGF:	Epidermal growth factor
EGFR:	Epidermal growth factor receptor/ERBB1
ELISA:	Enzyme-linked immunosorbent assay
EMT:	Epithelial mesenchymal transition
EPL:	Early pregnancy loss
EREG:	Epiregulin
EVT:	Extravillous trophoblast
FGR:	Fetal growth restriction
GA:	Gestational Age
GO:	Gene Ontology
HBEGF:	Heparin-binding EGF-like growth factor
HLA-G:	Major histocompatibility complex, class I, G
HIF:	Hypoxia inducible factor
HRE:	Hypoxia responsive element
HSP:	Heat shock protein

HSPG: Heparin sulfate proteoglycan  
IGF: Insulin-like growth factor  
IPA: Ingenuity pathway analysis  
ITGA: Integrin alpha ( $\alpha$ ) subunit  
ITGB: Integrin beta ( $\beta$ ) subunit  
IUGR: Intra-uterine growth restriction  
JNK: JUN N-terminal kinase/MAPK8  
KRT7: Cytokeratin  
MAPK: Mitogen-activated protein kinase  
miRNA: microRNA  
miRNP: miRNA ribonucleoprotein complex  
MMP: Matrix metalloproteinase  
NGS: Next generation sequencing  
NRG: Neuregulin  
PIK3: Phosphoinositide-3-kinase  
PE: Preeclampsia  
PKC: Protein kinase C  
RISC: RNA-induced silencing complex  
rMMP2: Recombinant MMP2  
SDS: Sodium dodecyl sulfate  
SNP: Single nucleotide polymorphism  
STR: Short tandem repeat  
TRIC: Trophoblast Retrieval and Isolation from the Cervix

TGFA: Transforming growth factor- $\alpha$

TGFB: Transforming growth factor beta ( $\beta$ )

TNFA: tumor necrosis factor alpha ( $\alpha$ )

TUNEL: Terminal deoxynucleotidyl transferase dUTP nick end labeling

uORF: Upstream open reading frame

uPA/uPAR: Urokinase-type plasminogen activator/uPA receptor

UTR: Untranslated region

## CHAPTER 1 - INTRODUCTION

Trophoblast cells are a major embryonic component of the placenta that mediate its major functions (Chaddha et al., 2004). As placentation proceeds the trophoblast cells differentiate and change to accommodate the growing placenta and fetus that it supports. The goal of this project was to better understand mechanisms that regulate trophoblast survival in both normal and pathological human pregnancies. This chapter reviews the existing literature on growth factors and molecular mechanisms governing blastocyst implantation and placentation.

The first 10 weeks of pregnancy are a period when  $O_2$  is low within the conceptus (Burton and Jauniaux, 2004; Burton et al., 1999). Intrauterine measurements report low  $O_2$  concentrations in placental tissues (~2%) compared to the surrounding decidua (~8%) and other adult tissues (Jauniaux et al., 2001; Rodesch et al., 1992). This environment favors the proliferation of the trophoblast cells, while repressing invasion (Genbacev et al., 1996; Genbacev et al., 1997). As a result, trophoblast cells accumulate and occlude the maternal blood vessels, which maintains the relatively hypoxic state (Burton and Jauniaux, 2004). The most distal trophoblast cells contact maternal blood, exposing them to higher  $O_2$  concentrations, which promotes the invasive extravillous trophoblast (EVT) phenotype. As gestation progresses beyond 10 weeks, the spiral arteries are remodeled by EVT cells to an extent that reperfuses and fully oxygenates the placenta by dislodging the occluding trophoblast cells and removing the arterial smooth muscle (Norwitz et al., 2001). The placenta is programmed to survive this rapid increase in  $O_2$  tension after Week 10 to meet the demands of a growing fetus. Prolonged hypoxia beyond Week 10 is associated with perinatal disease arising from aberrant placental development (Soleymanlou et al., 2005). If reoxygenation does not take place in timely manner, or if the trophoblast cells are deficient in their ability to adjust to  $O_2$  fluctuation (Hung and Burton, 2006), uteroplacental insufficiency could result.



Uteroplacental insufficiency, the sub-optimal perfusion of the developing placenta due to reduced uterine artery blood flow, contributes to several perinatal disorders, including early pregnancy loss (EPL), fetal growth restriction (FGR), and preeclampsia (PE) (Hossain and Paidas, 2007; Papageorgiou et al., 2004). The incidence of EPL approaches 15% (Larsen et al., 2013). FGR occurs in 4-8% of all pregnancies in developed countries, depending on the infant size percentile used for inclusion (Kramer, 1987). PE has a frequency of about 5-7%, while the most severe forms occur at 0.5-1%. PE is clinically defined by the presence of maternal hypertension and proteinuria occurring after 20 weeks of pregnancy in a previously normotensive, non-proteinuric patient (Davey and MacGillivray, 1988). Maternal death or serious long-term morbidity can occur, while abruption, preterm delivery and FGR contribute to perinatal fetal death and infant morbidity, with the associated costs of extensive neonatal hospitalization, and lifelong disabilities (Roberts et al., 1998). Until recently, PE could be alleviated only by removal of the placenta (Roberts et al., 1998), requiring delivery of the fetus and accounting for 15% of premature deliveries and the associated infant morbidity and mortality (Meis et al., 1998). More recently, interventional efforts such as the introduction of a low dose aspirin (Bujold et al., 2014) or Pravastatin (Ramma and Ahmed, 2014) regimen prior to 16 weeks of gestation have shown promise in reducing the rate of PE in high-risk patients, providing a course of action when diagnosed early.

Histological features of placentas delivered by women with EPL, PE and FGR suggest a prior disruption of EVT function in the first trimester (Burton and Jauniaux, 2004), characterized by reduced trophoblast invasion, insufficient remodeling of the spiral arteries, and EVT cell death (Brosens et al., 1972; DiFederico et al., 1999; Ishihara et al., 2002; Khong et al., 1986). Evidence strongly indicates that remodeling of the uterine arteries becomes deficient before PE and FGR are diagnosed, yet direct confirmation of early EVT dysfunction is lacking, and the

underlying etiologic cellular and molecular mechanisms are unknown due largely to our inability to interrogate the gestational period of interest. A large number of predictors for FGR and PE have been proposed with variable results (Bastek and Elovitz, 2013; Hossain and Paidas, 2007; Papageorgiou et al., 2004; Staff et al., 2013). First trimester screening of multiple predictors remains uninformative even when combined in a multivariable model (Myatt et al., 2012). At best, screening at any GA is limited to predicting early severe PE. Therefore, no reliable biomarkers are available to alert clinicians in the first trimester to identify pregnancies that will eventually develop FGR or PE, impeding progress toward targeted management of at-risk pregnancies to lessen the impact on women and their fetuses.

While access to fetal cells for prenatal diagnosis is technically complex and in some cases high risk (Wapner, 2005), a relatively simple solution to this challenge has been advanced over the past forty years (Adinolfi and Sherlock, 2001; Bischoff and Simpson, 2006; Imudia et al., 2010; Shettles, 1971). Trophoblast cells shed into the lower uterine pole accumulate within the cervix. Scientists and clinicians have tried to harness the information of trophoblast cells in the endocervical canal, but were largely unsuccessful due to the inability to purify these cells. Trophoblast retrieval and isolation from the cervix (TRIC) (Bolnick et al., 2014) efficiently separates maternal cells from fetal cells that resemble EVT cells in endocervical specimens. TRIC provides ample amounts of fetal DNA, RNA and protein for molecular analyses. Fetal cells obtained by TRIC as early as 5 weeks of gestation can be used in genomic, epigenomic, transcriptomic, metabolomic or other global discovery paradigms. Therefore, TRIC provides the opportunity to investigate the molecular profiles of trophoblast cells in the first trimester from pregnancies with known outcomes. Indeed, a pilot study using TRIC has demonstrated significant differences between protein biomarkers produced by the fetal cells before 10 weeks of gestation in normal control pregnancies and those that ended with an EPL (Fritz et al., 2015a).

The survival and extravillous differentiation of trophoblast cells is crucial for normal pregnancy, and deficiencies are linked to diseases of placental insufficiency (e.g. EPL, FGR, PE). Heparin-binding EGF-like growth factor (HBEGF) acts as a trophoblast survival factor, protecting the first trimester trophoblast cells from apoptosis during exposure to low O<sub>2</sub> levels (Armant et al., 2006), and promoting their invasion of maternal tissues (Leach et al., 2004). Conversely the hypertensive disease, PE, in which trophoblast invasion of the uterine arteries is reduced (Khong et al., 1986) and apoptosis elevated (Allaire et al., 2000), is associated with a dramatic reduction in HBEGF expression (Leach et al., 2002a). This suggests that the survival of trophoblast cells at the beginning of pregnancy might be disrupted by reduced HBEGF in women who later develop PE. However, it is not known whether the decreased expression of HBEGF in preeclamptic placentas occurs prior to delivery, which would indicate whether dysregulation is a cause or result of disease. Recently, these findings were confirmed and extended to other components of the epidermal growth factor (EGF) family (Armant et al., 2015), of which HBEGF is a member.

### **Epidermal growth factor (EGF) signaling system**

The EGF family of growth factors and their receptors regulate a variety of biological processes that include proliferation, differentiation and survival. Growth factors in the EGF superfamily include EGF, HBEGF, transforming growth factor- $\alpha$  (TGFA), amphiregulin (AREG), betacellulin (BTC), epiregulin (EREG), epigen and the neuregulins (NRG) (Holbro and Hynes, 2004; Riese and Stern, 1998). Recent studies have examined the roles of each EGF family member in implantation and placentation.

The EGF-like growth factors activate receptor tyrosine kinases in the plasma membrane that include epidermal growth factor receptor (EGFR/ERBB1) and related ERBB family proteins (ERBB2, ERBB3, ERBB4). Growth factor binding initiates an intrinsic protein-tyrosine kinase

activity, autophosphorylation of the cytoplasmic domain and receptor dimerization to generate a downstream signaling cascade (Holbro and Hynes, 2004). The EGF-like growth factors are synthesized as membrane bound proteins that signal to their receptors on adjacent cells, through juxtacrine signaling, or they are secreted through proteolytic cleavage of their extracellular domain, carried out by metalloproteinases, for autocrine or paracrine signaling (Riese and Stern, 1998).

### **Mouse implantation**

The importance of the EGF signaling system for blastocyst implantation is suggested by the EGFR knockout (Miettinen et al., 1995; Sibilio and Wagner, 1995; Threadgill et al., 1995), which, depending on the genetic background of host mice, has a perinatal-lethal phenotype. However, the picture is less clear from studies of embryos with deletion of EGF family growth factors where several knockouts produce mice that are viable and fertile, while others have roles in early post-implantation embryonic development that make interpretation difficult. It remains to be determined whether the EGF signaling system has a specific role in the process of implantation, or if it is more involved in embryonic survival and differentiation. Alternative approaches provide evidence to support the hypothesis that this complex signaling system directly influences the success of blastocyst implantation.

Experiments in mice establish that HBEGF is present in the uterus shortly before embryo implantation, providing the earliest known signaling between the blastocyst and maternal cells (Lim and Dey, 2009). *In situ* hybridization demonstrates that HBEGF is expressed in the luminal epithelium specifically at sites surrounding blastocysts 6-7 hours prior to the attachment reaction (Das et al., 1994). HBEGF is also expressed by blastocysts prior to implantation (Liu and Armant, 2004), suggesting its role in a two-way dialogue. Experimentally induced delayed implantation in ovariectomized mice reveals no HBEGF expression at implantation sites;

however, HBEGF becomes upregulated in both the uterus (Das et al., 1994) and blastocyst (Hamatani et al., 2004) with administration of estrogen to activate the blastocyst to implant. Its receptors ERBB1 and ERBB4 are concomitantly regulated by estrogen along with HBEGF in the blastocyst (Paria et al., 1993; Paria et al., 1999). HBEGF signaling between the trophoblast and uterine epithelial cells is most likely initiated by embryonic HBEGF shedding, as depicted in Figure 1A. Crosstalk with other signaling pathways mobilizes HBEGF from intracellular stores in the trophectoderm and demonstrates the complexity of the maternal-embryo dialogue. Lysophosphatidic acid (LPA) produced in the maternal reproductive tract accelerates blastocoel formation at the morula stage and trophoblast differentiation at the early blastocyst stage through downstream intracellular  $\text{Ca}^{2+}$  signaling (Liu and Armant, 2004; Stachecki and Armant, 1996). LPA activates cognate G protein-coupled receptors that signal through phospholipase C to generate inositol-1,4,5-trisphosphate and diacylglycerol that, in turn, mobilize cytoplasmic free  $\text{Ca}^{2+}$  and activate protein kinase C (PKC), respectively (Contos et al., 2000). Signaling by both cytoplasmic  $\text{Ca}^{2+}$  and PKC is known to stimulate HBEGF shedding (Dethlefsen et al., 1998; Dong and Wiley, 2000) and the subsequent transactivation of ERBB signaling (Umata et al., 2001). Immunofluorescence microscopy demonstrates that HBEGF is sequestered from the plasma membrane during blastocyst development, but accumulates transiently at the embryo surface in response to LPA-induced intracellular  $\text{Ca}^{2+}$  release (Liu and Armant, 2004). Therefore, uterine LPA secretion could activate HBEGF shedding from blastocysts in opposition to the uterine wall, signaling its presence to the adjacent uterine epithelium (Figure 1A).

Several studies support the hypothesis that expression of HBEGF in the peri-implantation endometrial epithelium is induced by embryo derived HBEGF signaling. HBEGF is expressed in both mouse and hamster preimplantation blastocysts (Hamatani et al., 2004; Liu and Armant, 2004; Wang et al., 2002). Interestingly, when growth factor-soaked beads the approximate size

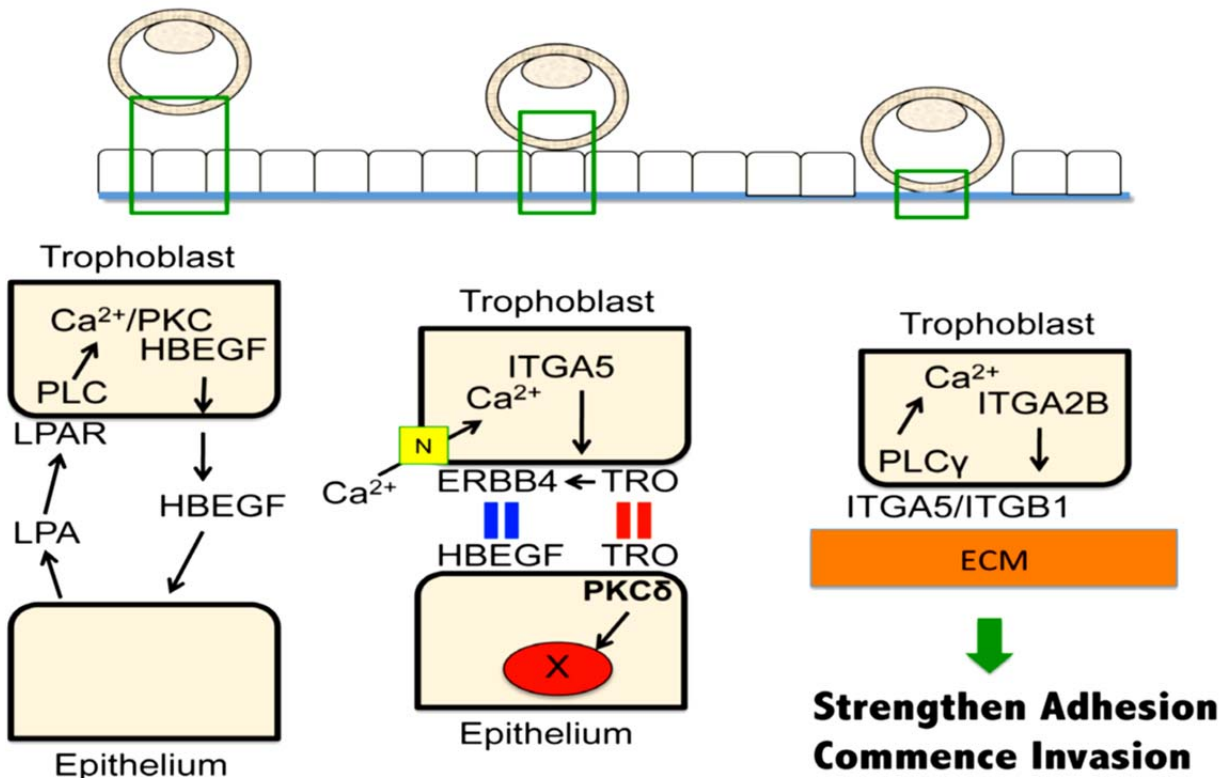


**Figure 1. Heparin binding EGF-like growth factor (HBEGF)- signaling and cell differentiation during implantation in mice.** Blastocyst-uterine interactions shown at the top of the diagram illustrate the (A) apposition, (B) attachment and (C) invasion stages of implantation. The regions within the green boxes are expanded below to summarize signaling pathways that orchestrate trophoblast and uterine epithelial cell differentiation at each stage, as discussed in the text. Arrows depict growth factor secretion or shedding, binding to receptors, intracellular trafficking, ion influx, and de-repression in the case of TRO and ERBB4. Double lines indicate juxtacrine signaling and/or cell-cell adhesion. ECM, extracellular matrix; HBEGF, heparin-binding EGF-like growth factor; ITGA, integrin alpha subunit; ITGB, integrin beta subunit; LPA, lysophosphatidic acid; LPAR, LPA receptor; N, N-type voltage-gated  $Ca^{2+}$  channel; PKC, protein kinase C; PLC, phospholipase C; TRO, trophinin; X, indicates apoptosis induced by nuclear localization of PKC $\delta$

of blastocysts are transferred into the uteri of pseudo pregnant mice only HBEGF and insulin-like growth factor-1 (IGF1) provoke discrete implantation-like responses (Paria et al., 2001). Furthermore, highly localized expression of HBEGF occurs in the uterine epithelium adjacent to apposition stage blastocysts (Das et al., 1994). These studies suggest a positive feed-forward regulation of uterine HBEGF expression initiated by the blastocyst during the apposition stage of implantation. While HBEGF secreted by the embryo is sufficient to induce HBEGF expression in the luminal epithelium, other factors secreted by embryos (e.g., IGF1) could have equivalent

activity and perhaps compensate in HBEGF deficient embryos, which are able to implant normally when transferred to wild type pseudopregnant dams (Xie et al., 2007).

HBEGF protein appears on the surface of the uterine epithelium early on gestation day 5 in mice as the attachment reaction commences (Das et al., 1994). The primary target of HBEGF in the luminal epithelium is the trophoblast (Figure 1B). Late on day 4, HBEGF signaling in the blastocyst becomes robust as a result of ERBB4 trafficking to the trophoblast surface (Wang et al., 2000). ERBBs 1-3 are already localized at the apical surface as the blastocyst forms. However, ERBB4 is the preferred receptor for HBEGF in blastocysts (Paria et al., 1999). Thus, ERBB1 and ERBB4 both become available on the trophoblast at approximately the time when uterine HBEGF first appears. These events position HBEGF and its receptors to mediate blastocyst adhesion and trophoblast differentiation.

HBEGF-induced ERBB autophosphorylation advances trophoblast adhesive differentiation (Das et al., 1994; Paria et al., 1999; Wang et al., 2000). In blastocysts cultured serum-free, HBEGF induces trafficking of integrin subunits, including ITGA5 (Figure 1B), into the plasma membrane of trophoblast cells approximately 24 hours earlier than in control embryos, which promotes their adhesion to fibronectin in the maternal extracellular matrix (Wang et al., 2000). *In vitro* experiments suggest that after apoptosis of the opposing luminal epithelial cells, ligation of the integrin ITGA5/ITGB1 by the exposed basement membrane activates phospholipase C $\gamma$  (Wang et al., 2007), leading to trafficking of ITGA2B into the plasma membrane (Rout et al., 2004), which strengthens cell adhesion as trophoblast invasion commences (Figure 1C).

Experiments have been reported suggesting that HBEGF supports the attachment reaction during implantation in addition to its ability to advance hatching and trophoblast differentiation. Using engineered cells that express membrane bound HBEGF to simulate receptive uterine



epithelial cells, it has been demonstrated that cell surface HBEGF binds to day 4 mouse blastocysts, but not to delayed blastocysts (Raab et al., 1996). HBEGF signaling activates  $\text{Ca}^{2+}$  influx across the plasma membrane through N-and calmodulin, consequently accelerating trophoblast invasion (Wang et al., 2000). It appears that there are complex autocrine, paracrine and juxtacrine pathways that integrate HBEGF signaling with input from other growth factors, as well as through cell-cell interactions between the trophectoderm and uterine epithelium during implantation (Figure 1).

Maternal HBEGF deficiency targeted to the uterus defers the window of implantation and compromises pregnancy outcome, thus, implicating the importance of two-way communication between the embryo and the uterus (Xie et al., 2007). However, another heparin-binding member of the EGF family, AREG, partially compensates for HBEGF loss. Progesterone upregulates AREG throughout the uterine luminal epithelium of the mouse early on gestation day 4 independently of the blastocyst (Das et al., 1995), but it becomes restricted to the implantation site by day 5. Studies conducted to clarify the mechanism of AREG signaling at the embryonic-maternal interface suggest that the presence of fertilized embryos in the reproductive tract elevates expression of AREG on day 4 (Lee et al., 2006). Therefore, the presence of embryos in an HBEGF-deficient uterus could induce partially-compensating production of AREG, which can activate only ERBB1 (Riese and Stern, 1998).

Another EGF family member, TGFA, has extensive sequence homology to EGF and comparable affinity for ERBB1, its only receptor. Immunohistochemical, *in situ* hybridization, northern blot and RT-PCR analyses clearly demonstrate TGFA expression in the uterus and embryo (Rappolee et al., 1988; Tamada et al., 1991). Additionally, a reduction in the number of implantation sites in rats after administration of intraluminal anti-TGFA injections supports the involvement of TGFA in implantation (Tamada et al., 1997). Addition of TGFA to *in vitro*



culture medium is favorable for preimplantation embryo development and trophoblast differentiation (Haimovici and Anderson, 1993; Machida et al., 1995). However, this involvement is controversial, as TGFA knock out mice have normal implantation (Luetteke et al., 1993; Mann et al., 1993). Similarly, AREG and EGF are not essential for implantation, indicated by mice deficient in AREG and triple knockout mice lacking TGFA, AREG and EGF, which are all fertile (Luetteke et al., 1999). These studies support the concept of a compensatory response by other EGF family members, perhaps HBEGF, during implantation.

Another group of EGF-like growth factors that mediate cell-cell interactions, the NRGs, are encoded by four distinct genes, NRG-1, NRG-2, NRG-3 and NRG-4 (Burden and Yarden, 1997; Falls, 2003). There is evidence for 15 splice variants of NRG-1 that are grouped into three subtypes (Ben-Baruch and Yarden, 1994; Meyer et al., 1997). Of the three subtypes, Type 1 is comprised of *neu* differentiation factor (NDF), heregulin and acetylcholine receptor-inducing activity (Ben-Baruch and Yarden, 1994). Type 2 consists of the glial growth factor (GGF) and type 3 comprises the sensory and motor neuron derived factor (SMDF) (Brown et al., 2004). NDF and its isoforms are expressed in the preimplantation mouse uterus (Reese et al., 1998). Mice with delayed implantation do not express NDF; however, upon administration of estrogen, the expression of NDF returns. Alternately there is evidence that SMDF has a similar cellular distribution to NDF and its expression becomes prominent at the time of implantation (Brown et al., 2004). However, no significant expression of GGF is observed in the peri-implantation uterus. In the blastocyst, both ERBB3 and ERBB4 are present on trophoblast cells, suggesting the capacity for signaling with NRG family members (Wang et al., 2000). A parallel study observed a similar expression pattern of the EGF family members BTC and EREG (Das et al., 1997), suggesting that optimal expression of NDF, BTC and EREG requires an activated blastocyst. Therefore, it remains possible that these EGF family members contribute to mouse

implantation.

### **Human implantation**

In contrast to its regulation in mice that have a short estrus cycle, HBEGF is regulated independently of the presence of an embryo in the stromal and epithelial compartments during the menstrual cycle of the human endometrium (Chobotova et al., 2002a; Leach et al., 1999; Yoo et al., 1997). There is evidence that HBEGF mediates maternal-blastocyst signaling and attachment in humans as it does in rodents owing to the switch in expression of HBEGF mRNA and protein from the subepithelial stroma during early secretory phase to glandular and luminal epithelium in the mid-secretory phase (Leach et al., 1999). ERBB4 is expressed by the trophoblast cells of human peri-implantation blastocysts, suggesting that HBEGF present in the luminal epithelium could stimulate the blastocyst through paracrine or juxtacrine signaling (Chobotova et al., 2002b). HBEGF not only accelerates the development of human embryos to the blastocyst stage, but also aids in hatching from the zona pellucida (Martin et al., 1998).

Evidence indicates that proliferation in human endometrial stromal cells is regulated by both the soluble and transmembrane forms of HBEGF, along with other EGF family members, EGF and BTC, suggesting key functions for the EGF family of growth factors in regeneration and maturation of the human endometrium and to prepare the embryo for implantation (Chobotova et al., 2002a). However, this induction is under the cooperative effect of TNF. Another study shows that the endometrial stromal cells produce both the soluble and transmembrane forms of HBEGF to regulate TNF and TGFB (Chobotova et al., 2005). This provides a survival function that prevents apoptosis of endometrial cells exposed to apoptotic factors, which highlights the importance of HBEGF and its receptors in the human endometrium.

HBEGF appears to participate in a broader dialogue that includes other molecules, exemplified by trophinin-bystin signaling. Both human trophoblast cells and the uterine

epithelium express the transmembrane protein trophinin that mediates cell adhesion through homophilic binding (Suzuki et al., 1999). Trophinin forms a complex with its cytoplasmic partner bystin and ERBB4, which inhibits ERBB tyrosine phosphorylation required for invasive trophoblast differentiation (Figure 1B). However, during the attachment reaction between the blastocyst and luminal epithelium, homophilic trophinin binding releases bystin, thus derepressing ERBB4, which can then become activated by HBEGF to promote trophoblast differentiation (Sugihara et al., 2007; Tamura et al., 2011). Meanwhile, in the luminal epithelium, homophilic trophinin binding disrupts its tethering of protein kinase C $\delta$  to the plasma membrane, freeing the latter to enter the nucleus where it induces apoptosis (Tamura et al., 2011). Thus, trophinin signaling removes the cellular barrier to blastocyst implantation as it licenses activation of trophoblast adhesion competence.

### **Human placentation**

Most components of the EGF signaling system are present throughout pregnancy. Transcripts from placental tissues obtained in all three trimesters demonstrate expression of HBEGF, with the highest abundance in first trimester decidua (Yoo et al., 1997). Strong staining for HBEGF is observed in villous and EVT cells in both normal placentas and those delivered preterm (Leach et al., 1999; Leach et al., 2002a). Other EGF family members and ERBB receptor tyrosine kinases are expressed in placental trophoblast populations (Hofmann et al., 1992; Tanimura et al., 2004), indicating that the EGF signaling system is highly active during placental development.

There is evidence to support the hypothesis that HBEGF, and possibly other EGF family members, promote trophoblast invasion (Jessmon et al., 2009). The capacity for invasion weakens as gestation progresses (Damsky et al., 1994; Librach et al., 1991), indicating the importance of the EGF signaling system in first trimester trophoblast cells (Bass et al., 1994).

EGF, TGFA and HBEGF can stimulate first trimester trophoblast cells to become invasive and differentiate to the extravillous phenotype (Bass et al., 1994; Leach et al., 2004). However, the effectiveness of EGF diminishes with trophoblast cells obtained from the second or third trimester (Bass et al., 1994), suggesting that their loss of invasion competence is intrinsic rather than a product of their environment. Invading EVT cells are necessary for adequate remodeling of the uterine spiral arteries that perfuse the developing placenta (Norwitz et al., 2001).

The widespread expression of HBEGF in placental trophoblast cells and surrounding decidua (Leach et al., 1999) could facilitate invasion and contribute to remodeling of the spiral arteries. It has been demonstrated that when the HTR-8/SVneo human first trimester cytotrophoblast cell line is cultured at 2% O<sub>2</sub>, HBEGF, but not other EGF family members, is upregulated and secreted (Armant et al., 2006). However, trophoblast cells in villous explants from term placentas do not elevate HBEGF in response to low oxygen and their survival is compromised by hypoxia (Imudia et al., 2008). Addition of HBEGF to term villous explants cultured at 2% O<sub>2</sub> inhibits apoptosis, demonstrating its capacity as a survival factor.

Because the placenta is programmed to survive at a low O<sub>2</sub> tension during the first trimester, trophoblast invasion progresses slowly at the vascular interface, delaying the full onset of placental perfusion for ten weeks (Norwitz et al., 2001). However, if reoxygenation does not occur on time, placental insufficiency ensues, and, depending on severity, can result in EPL, FGR or PE (Burton and Jauniaux, 2004). These disorders are associated with poor trophoblast invasion and increased apoptosis (Brosens et al., 1972; DiFederico et al., 1999), two functions that are strongly regulated by HBEGF signaling (Jessmon et al., 2009). Placental tissues from preeclamptic pregnancies have reduced expression of HBEGF compared to gestational age-matched normotensive placentas, as well as reduced HBEGF mRNA expression (Leach et al., 2002a). There are also deficiencies in EGF and TGFA, as well as increased production of a

secreted form of EGFR that binds EGF-like growth factors to antagonize signaling through ERBB receptors (Armant et al., 2015). These findings suggest the hypothesis that reduced HBEGF expression could contribute to the shallow trophoblast invasion and poor survival observed in preeclampsia. It remains to be established whether the reduced expression of HBEGF precedes the onset of preeclampsia, or if it is merely associated with late placental demise. There is also clinical evidence of HBEGF disruption associated with infertility in women (Aghajanova et al., 2008). The decreased HBEGF expression in infertile couples was not confirmed in a larger clinical study, but it was noted that a significant increase between the early and mid-secretory phases was absent in the infertile patients (Leach et al., 2012).

Significant advancements have been made in unraveling the molecular mechanisms governing growth factors involved in implantation and trophoblast invasion. The mouse has provided a powerful experimental model; however, its correlation with human implantation and trophoblast development is not entirely consistent. In the mouse trophoblast invasion is shallow (Redline and Lu, 1989), the arteries and blood vessels of the decidua are lined by endothelium rather than trophoblast (Adamson et al., 2002; Redline and Lu, 1989). In humans, trophoblasts are responsible for vascular remodeling (Pijnenborg et al., 2006), while uterine natural killer cells are more important in the mouse (Monk et al., 2005). The differences in trophoblast invasion and vascular remodeling in humans compared to the mouse make it a suboptimal model for studying placental insufficiencies.

A better understanding of the molecular mechanisms governing the expression of growth factors in implantation and placentation could better define the window of implantation. Furthermore, this additional information could provide a foundation for development of new treatments for clinical pathologies such as recurrent pregnancy loss and placental insufficiencies that reduce fetal growth or contribute to PE. In considering the signaling pathways disrupted by

obstetric disease it might be possible to devise new strategies for pharmaceutical intervention to improve maternal-fetal care. Therefore, continued investigation of growth factors and the molecular mechanisms that ensure successful implantation and placentation has significant clinical relevance. The significance of HBEGF signaling during human pregnancy will not be fully appreciated without more sophisticated experimental approaches that take into account its interactions with other signaling pathways. Other pathways that regulate HBEGF and alter its expression in obstetric disease might lie closer to the root cause of placental insufficiencies, and would provide superior targets for intervention strategies. Therefore, global approaches to this subject are needed in addition to a targeted analysis of the role for HBEGF in placental development and pathology.

## CHAPTER 2 - TROPHOBLAST SURVIVAL SIGNALING DURING HUMAN PLACENTATION REQUIRES HIF-INDUCED TRANSCRIPTION OF HSP70

### Abstract

Survival of trophoblast cells in the low oxygen environment of human placentation requires metalloproteinase-mediated shedding of HBEGF and downstream signaling. A matrix metalloproteinase (MMP) antibody array and quantitative RT-PCR revealed upregulation of MMP2 post-transcriptionally in human first trimester HTR-8/SVneo trophoblast cells and placental explants exposed to 2% O<sub>2</sub>. Specific MMP inhibitors established the requirement for MMP2 in HBEGF shedding and upregulation. Hypoxia inducible factors, HIF1A and EPAS1 (HIF2A), accumulated at 2% O<sub>2</sub>, and HIF target genes were identified by next-generation sequencing of RNA from trophoblast cells cultured at 2% O<sub>2</sub> for 0, 1, 2 and 4 hrs. Of nine genes containing HIF-response elements upregulated at 1 hour, only HSPA6 (HSP70B') remained elevated after 4 hours. The HSP70 chaperone inhibitor VER155008 blocked upregulation of both MMP2 and HBEGF at 2% O<sub>2</sub>, and increased apoptosis. However, both HBEGF upregulation and apoptosis were rescued by exogenous MMP2. We propose that MMP2-mediated shedding of HBEGF, initiated by HSP70, contributes to trophoblast survival at the low O<sub>2</sub> levels encountered during the first trimester, and is essential for successful pregnancy outcomes.

### Introduction

In humans, the placenta is not fully perfused with oxygenated maternal blood until after the tenth week of pregnancy, rendering the implantation site a low O<sub>2</sub> environment (Burton, 2009; Burton et al., 1999; Jauniaux et al., 1991). Atypical of most cells, human trophoblast cells not only survive at low O<sub>2</sub>, but also proliferate more rapidly (Genbacev et al., 1996; Genbacev et al., 1997; Kilburn et al., 2000). The epidermal growth factor (EGF) family member, heparin-

binding EGF-like growth factor (HBEGF) is highly expressed in the uteroplacental compartment during implantation and early placentation (Jessmon et al., 2009). We previously reported that HBEGF prevents death of human trophoblast cells exposed to low O<sub>2</sub> concentrations (Armant et al., 2006). Although HBEGF is upregulated ~100-fold in trophoblast cells after exposure to 2% O<sub>2</sub>, HBEGF mRNA remains unchanged and is abundant (2500 copies/cell) at both O<sub>2</sub> concentrations (Armant et al., 2006). Survival of trophoblast cells at low (2%) O<sub>2</sub> requires metalloproteinase-mediated shedding of membrane-bound proHBEGF and HBEGF downstream signaling (Armant et al., 2006). HBEGF is synthesized as transmembrane proHBEGF, and secreted through shedding from the plasma membrane by proteolytic cleavage, allowing it to activate ERBB receptor tyrosine kinases, including its cognate receptors, EGF receptor/ERBB1 and ERBB4 (Holbro and Hynes, 2004). As O<sub>2</sub> increases with the full perfusion of the intravillous space after 10 weeks of gestation (Burton, 2009; Burton et al., 1999; Jauniaux et al., 1991), HBEGF positively regulates trophoblast motility and invasion (Jessmon et al., 2010; Leach et al., 2004). The hypertensive pregnancy disorder, preeclampsia, in which trophoblast invasion is reduced and apoptosis elevated, is characterized by a reduction in HBEGF and other components of the EGF signaling system (Armant et al., 2015; Jessmon et al., 2009; Leach et al., 2002a). It can, therefore, be hypothesized that HBEGF production could be a factor in trophoblast dysfunction associated with placental insufficiency disorders.

In human trophoblast cells, HBEGF activates p38 (MAPK14), ERK (MAPK1), and JNK (MAPK8) (Jessmon et al., 2010). During hypoxia, HBEGF upregulates its biosynthesis through an autocrine feedback mechanism, and prevents apoptosis through a parallel signaling pathway (Armant et al., 2006; Jessmon et al., 2010). Activation of ERBB receptor tyrosine kinase by HBEGF prevents apoptosis through a mechanism mediated by p38 MAPK, while autocrine upregulation of HBEGF appears to be mediated by any one of the MAPKs, p38, ERK, or JNK,



based on experiments using specific inhibitors (Jessmon et al., 2010). However, it is unclear whether the MAPKs specifically function downstream of HBEGF in its autocrine upregulation, or also operate further upstream in the cascade initiated by hypoxia to regulate proHBEGF shedding.

It is well established that metalloproteinases contribute to invasion and tissue remodeling (Loffek et al., 2011; Stamenkovic, 2003). Successful implantation and trophoblast invasion are closely linked to the expression of matrix metalloproteinases (MMPs) that degrade basement membranes (Librach et al., 1991). The gelatinases (gelatinase A/MMP2; 72-kDa, and gelatinase B/MMP9; 92-kDa), which target major components of basement membranes (e.g., collagen IV), are expressed by trophoblast cells, and therefore, regarded as key to the invasion process (Isaka et al., 2003). MMP2 and MMP9 are differentially expressed in first trimester trophoblast cells, with MMP2 more prominently secreted until 9 weeks (Staun-Ram et al., 2004; Xu et al., 2000). MMP2 is constitutively expressed in trophoblast cells throughout pregnancy, but its activity is diminished in the full-term placenta. MMP9 is mainly expressed by trophoblast cells during the period after Week 9, and also decreases at term. Thus, MMP2 and MMP9 are expressed and functioning throughout the periods of low and then elevated  $O_2$  in the reproductive tract, characterized by high trophoblast proliferation and then elevated invasion, respectively (Jovanovic et al., 2010; Librach et al., 1991). While their role in tissue remodeling is well known (Loffek et al., 2011; Stamenkovic, 2003), emerging evidence reveals that MMPs also participate in shedding of membrane-anchored signaling molecules, which contributes to chemokine and growth factor activation (Burton, 2009; Chow and Fernandez-Patron, 2007; Powell et al., 1999).

Shedding is mediated by membrane-type MMPs and MMPs bound to membrane receptors, including MMP2 and MMP9 (Sternlicht and Werb, 2001). Cheng et al reported that

bradykinin-induced proliferation of rabbit corneal cells is blocked by an inhibitor of both MMP2 and MMP9, as well as an inhibitor of HBEGF, suggesting that an MMP could contribute to the cleavage of proHBEGF (Cheng et al., 2012). MMP2 participates in a proteolytic cascade in  $\alpha$ T3-1 cells that directs both proHBEGF shedding and EGFR transactivation (Roelle et al., 2003). In addition, its rapid release in CMTC9 cells after E2 stimulation is correlated with cleavage of proHBEGF (Torres et al., 2009). We previously found that treatment with a general metalloproteinase inhibitor blocks HBEGF accumulation in human trophoblast cells at low O<sub>2</sub>, causing apoptosis that is rescued with recombinant HBEGF, but not other EGF-like ligands (Armant et al., 2006). Autocrine HBEGF activity in trophoblast cells requires, in addition to metalloproteinase-mediated shedding of HBEGF, binding to either EGFR or ERBB4. Blocking HBEGF signaling prevents its upregulation at 2% O<sub>2</sub>, suggesting that low levels of resident proHBEGF are cleaved through activation of metalloproteinases to initiate its autocrine accumulation downstream of ERBB receptors in a positive feedback loop.

To understand the molecular mechanism of trophoblast survival at low O<sub>2</sub>, the HTR-8/SVneo human trophoblast cell line (Graham et al., 1993) was used. The HTR-8/SVneo cell line is an immortalized cell line (Graham et al., 1998) that was established from human first-trimester cytotrophoblast cells (Graham et al., 1993). HTR-8/SVneo cells express cytokeratin (KRT7), a marker for trophoblast and other epithelial cells, as well as the beta subunit of human chorionic gonadotropin ( $\beta$ -hCG), which is trophoblast-specific (Kilburn et al., 2000). This cell line possesses the ability to invade Matrigel basement membrane without being tumorigenic, and expresses the trophoblast-specific major histocompatibility protein, HLA-G, when induced by Matrigel differentiate (Kilburn et al., 2000). In response to Matrigel, HTR-8/SVneo cells switch integrin expression (Damsky) in association with invasive differentiation, while in response to hypoxia, proliferation increases and extravillous differentiation is inhibited (Kilburn et al., 2000).

To examine the hypothesis that MMPs contribute to the shedding and upregulation of HBEGF at low O<sub>2</sub> concentrations required for trophoblast survival in the first trimester, we used HTR-8/SVneo human trophoblast cells, with confirmatory experiments using first trimester villous explants (Castellucci et al., 1990; Genbacev et al., 1992).

## **Materials and Methods**

### ***Cell Culture and Treatments***

The first trimester human TB cell line, HTR-8/SVneo (Graham et al., 1993), was grown in either 96-well culture plates (approx. 500,000 cells) or T25 tissue culture flasks (approx. 85% confluency) during experiments in sterile DMEM/F-12 with 1 mg/ml BSA at either 20% O<sub>2</sub> or 2% O<sub>2</sub>. Cells were treated by adding to the culture medium 1-10 µg/ml  $\alpha$ -amanitin (Sigma-Aldrich), 250 µM CoCl<sub>2</sub> (Sigma-Aldrich), inhibitors (EDM Chemicals, Inc., Gibbstown, NJ) specific for MMP2 and MMP9 (BiPS; (2R)-[(4-Biphenylsulfonyl)amino]-N-hydroxy-3-phenylpropionamide; 100 nM; MMP-2 (IC<sub>50</sub> = 310 nM) and MMP-9 (IC<sub>50</sub> = 240 nM)) (Tamura et al., 1998), MMP2 only [(2-((isopropoxy)-(1,1'-biphenyl-4-ylsulfonyl)-amino))-N-hydroxyacetamide; 250 nM; IC<sub>50</sub> = 12 nM (at high concentration inhibits MMP-9 and MMP-3 (IC<sub>50</sub> = 0.2 and 4.5 µM, respectively))] (Rossello et al., 2004), or MMP9 only [MMP9 Inhibitor I; 100 nM MMP-9; IC<sub>50</sub> = 5 nM (at high concentration inhibits MMP-1 (IC<sub>50</sub> = 1.05 µM) & MMP-13 (IC<sub>50</sub> = 113 nM))] (White et al., 2006), specific inhibitors for ERK, JNK, and p38 (Jessmon et al., 2010), HSP70 inhibitor (VER-155008, Santa-Cruz Biotech; 0.05-100 µM), and 10 nM recombinant MMP2 (R&D Systems; rMMP2;). For protein analysis, attached cells were extracted using cell lysis buffer (Cell Signaling), and total cellular protein concentrations were determined using Pierce BCA protein assay kit (ThermoFisher Scientific). The HTR-8/SVneo cell line was maintained in DMEM/F12 with 10% donor calf serum at 20% O<sub>2</sub> between passages 30-50, and routinely checked for production of  $\beta$ -hCG, KRT7, and when cultured on Matrigel,

HLA-G (Graham et al., 1993; Kilburn et al., 2000). Serum was replaced with BSA 24 h before all experiments.

### ***Villous Explant Culture***

Placental tissues were obtained with Wayne State University Institutional Review Board approval and patient informed consent from first trimester terminations at a Michigan family planning facility. Within a 2-hr period, fresh tissue was collected, placed on ice in PBS, transported to the laboratory, and villous explant cultures were prepared (Bolnick et al., 2015). The chorionic villi were dissected into pieces of approximately 5 mg wet weight and transferred individually into DMEM/F12 culture medium supplemented with 10% donor calf serum, 100 I.U. penicillin and 100 µg/ml streptomycin in a 24-well culture plate (Costar, Corning, NY). The explants were culture overnight at either 8% or 2% O<sub>2</sub> then treated as described for the cell line.

### ***Antibody Arrays***

Cell lysates (1 mL) were incubated overnight with antibody array membranes, using a human MMP antibody array kit (Abcam, Cat # ab134004). The membranes were washed and incubated with a secondary biotin-conjugated antibody, followed by incubation with horseradish peroxidase conjugated streptavidin, according to the manufacturer's direction. The arrays were developed, using enhanced chemiluminescence, and imaged on the ChemiDoc Imaging System (BioRad). Labeling of each protein in the array was quantified using ImageJ software (NIH <http://rsbweb.nih.gov/ij/>). The mean of six negative controls was subtracted for background correction, and the mean of six positive controls was used to normalize the data and calculate the relative expression levels.

### ***Western Blotting***

Western blots were performed as previously described (Kilburn et al., 2000). Briefly, cellular lysates were diluted in SDS sample buffer containing 5% β-mercaptoethanol, run on

precast 4%–20% Tris-HCl gradient gels (BioRad), and blotted with antibodies against MMP2, MMP9, HIF1A (R&D Systems), HIF2A/EPAS1 (Novus Biologicals) and HSPA6 (Abcam) diluted 1:1000 in TTBS and 5% milk. Densitometry was used to quantify grey levels of protein bands of interest, using image analysis software (SimplePCI, Hamamatsu). Background grey levels, determined in a blank lane, were subtracted to obtain the specific grey level for each band. Band intensities were below saturation, although linearity was not determined.

### ***ELISA***

Cells were cultured and treated in six-well plates. ELISA was conducted using HBEGF, MMP2, HIF1A and HIF2A DuoSet ELISA Development kits (R&D Systems). The optical density of the final reaction product was determined at 450 nm using a programmable multiplate spectrophotometer (Power Wave Workstation; Bio-Tek Instruments) with automatic wavelength correction. Data are presented as nanograms (ng) of HBEGF or MMP2 per microgram ( $\mu$ g) of total protein, determined using standard curves generated with the respective recombinant proteins (R&D Systems).

### ***Immunohistochemistry***

Immunohistochemistry was performed using a DAKO (Carpinteria, CA) Autostainer Universal Staining System, as previously described (Leach et al., 2002a). Rehydrated sections of cultured explants were labeled for 1 h at 25°C with 5  $\mu$ g/ml goat polyclonal antibody against human recombinant HBEGF (R&D Systems) that recognizes both membrane and secreted forms of the protein and 2.5  $\mu$ g/ml antibody against cytokeratin (KRT7) (DAKO) specific for trophoblast. Controls were incubated with 10  $\mu$ g/ml non-immune goat IgG (Jackson ImmunoResearch Laboratories, West Grove, PA). Tissues were then incubated 1 h at 25°C with 0.1  $\mu$ g/ml rabbit anti-goat IgG (Jackson ImmunoResearch). Slides were viewed at 400  $\times$  magnification using a Leica (Wetzlar, Germany) DM IRB inverted microscope and imaged with

spot camera. Trophoblast cells were labeled with monoclonal antibodies HSPA6 (Abcam) diluted 1:400. To visualize and quantify bound primary antibody, an Envision System peroxidase anti-mouse/rabbit kit (DAKO) was used. Staining (grey level) was imaged using a Leica DM IRB epifluorescence microscope, and images were captured using a Hamamatsu Orca digital camera. Images were semi-quantified using SimplePCI (Hamamatsu) imaging software, as previously described (Leach et al., 2012).

### ***qPCR***

RNA from HTR-8/SVneo cells was collected using the miRNeasy kit (Qiagen) that included DNase treatment, according to the manufacturer's protocol. RNA concentration was determined using the NanoDrop spectrophotometer and purity was ascertained with a microfluidic Bioanalyzer (Agilent Technologies - 2100 Electrophoresis Bioanalyzer Instrument). RNA was used in subsequent qPCR (Bustin et al., 2009) analysis. Reverse transcription was performed using the Quantitect Reverse Transcription kit (Qiagen), and qPCR for MMP2, HBEGF and HSPA6 was conducted with the Quantitect SYBR Green PCR kit without UNG (Qiagen), in a final volume of 25  $\mu$ l. GAPDH and SDHA were used as housekeeping genes to normalize the data. Semi-quantitative analysis was performed according to the  $\Delta\Delta C_t$  method (Pfaffl, 2001). Primers for GAPDH, SDHA, HBEGF, MMP2 and HSPA6 were obtained from Qiagen.

### ***LongRNA (LnRNA) Library Prep for Next Generation Sequencing (NGS)***

LnRNA was isolated using the miRNeasy mini kit (Qiagen). The RNA was quantified and its purity assessed with an Agilent 2100 Electrophoresis Microfluidics Analyzer. RNA was converted into an adapter-ligated cDNA library (Figure 2), using the Ovation & Encore Library Preparation Kit (NuGen), according to the manufacturers protocol. Each cDNA sample was bar-coded, and the resulting 12 libraries (three replicate libraries for each of the four O<sub>2</sub> conditions)

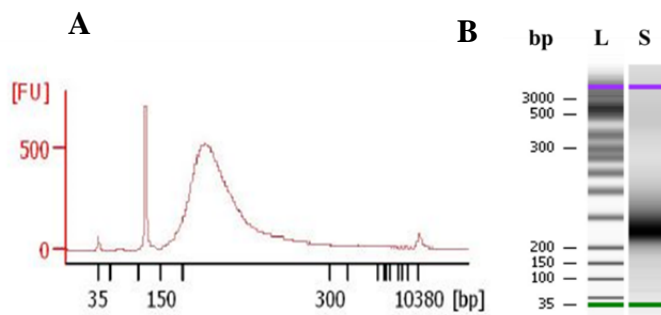


**Figure 2. An example is shown for the size distribution of an individual library using the Agilent Bioanalyzer. A. Peak size (~250 bp) B. Sample (S) size on gel projection, as compared to a base pair (bp) ladder (L).**

were combined for NGS. Paired-end sequencing was performed for 50 cycles using the Illumina HiSeq-2500 sequencer.

### ***Data Alignment & Mapping***

RNA sequencing data was first processed with demultiplexing software (Casava 1.8.2, Illumina). It was then aligned to the human genome build HG19, and to the ribosomal sequences 18s and 28s, using bioinformatics tool Novoalign (Novocraft, 2010). Novoalign determined unique alignments that were used to generate an average of 1000 reads per coding segment per sample. The reads thus generated were converted into bed files and imported to the Genomatix Genome Analyzer (GGA) (Genomatix Software GmbH). The GMS, using RNA-seq analysis, generated data in the form of Reads per Kilobase of exon per Million fragments mapped (RPKM) for 25,000 genes in the database.

### ***Promoter Extraction***

The Genomatix Genome Analyzer (GGA) MatInspector program (Cartharius et al., 2005) was used to extract the promoter regions for the differentially regulated genes. MatInspector utilizes a large library of matrix descriptions for transcription factor binding **sites** to locate matches in DNA sequences. For the purpose of this study it was used to identify hypoxia response elements (HRE) in differentially regulated genes.

### ***Statistics***

All statistics were performed with GraphPad Prism 6 software. One-way ANOVA with

Student–Newman–Keuls *post hoc* comparisons was used to identify changes between controls and treatments. Two-way ANOVA was used for experiments with multiple groups. Significance was defined as  $P < 0.05$ ; all experiments were done three times ( $n=3$ ) and data are expressed as mean  $\pm$  SD. For RNAseq data, adjusted p-values were calculated using Benjamin-Hochberg, and threshold was set at 0.05 to account for false discovery rate.

## Results

### *Upregulation of MMP2 at low O<sub>2</sub>*

Using a human MMP antibody array, we observed that relative expression of MMP2, but not MMP9 or other MMPs, increased 1.7-fold in HTR-8/SVneo trophoblast cells cultured for 4 hrs at 2% O<sub>2</sub> (Figure 3A), as compared to trophoblast cells cultured at 20 % O<sub>2</sub>. The specific increase in expression of MMP2, and not MMP9, was confirmed by western blotting (Figure 3B and Figure 4A &B). Cellular MMP2 was quantified temporally by ELISA in trophoblast cells after shifting to 2% O<sub>2</sub>. The MMP2 concentration abruptly increased 164-fold ( $p<0.0001$ ) after 2 hours of culture at 2% O<sub>2</sub> (Figure 3C). These findings indicate that low O<sub>2</sub> upregulates MMP2 prior to the observed increase in HBEGF, which occurs at 4 hrs (Armant et al., 2006).

### *Role of MMP2 in HBEGF upregulation*

To determine whether MMP2 has a functional role in HBEGF regulation by O<sub>2</sub>, specific inhibitors of MMP2 and MMP9 were supplemented in culture medium during manipulation of O<sub>2</sub> levels. HBEGF failed to accumulate in trophoblast cells cultured at 2% O<sub>2</sub> for 4 h when MMP2 was inhibited (Figure 3D). However, MMP9 inhibition had no effect on the normal accumulation of HBEGF at low O<sub>2</sub>. A third inhibitor that targets both MMP2 and MMP9 (Inh. 2/9) also inhibited HBEGF accumulation. Additionally, TUNEL assays showed increased ( $p<0.0001$ ) trophoblast cell death when both MMP2 and MMP9, or only MMP2, were inhibited (Figure 3E). Inhibition of only MMP9 produced apoptosis levels similar to control. We



conclude that MMP2, but not MMP9, either directly or indirectly, mediates the proteolytic cleavage of proHBEGF, and subsequent survival signaling.

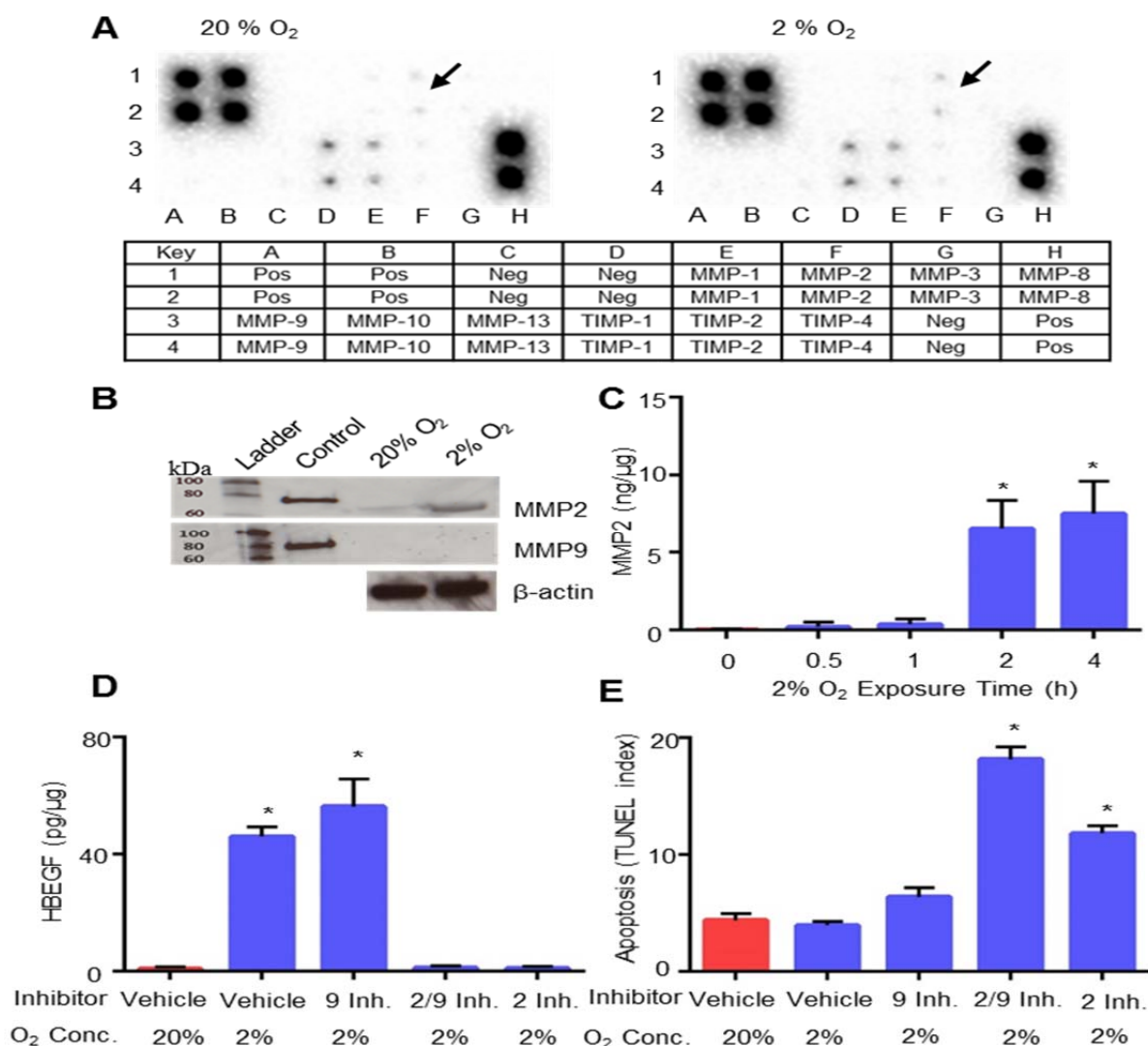


**Figure 3. Upregulation of MMP2 at low O<sub>2</sub>, and its effects on HBEGF and cell survival.** A. Expression arrays for MMP-related proteins incubated with extracts of HTR-8/SVneo cells cultured at 20% (left) or 2% (right) O<sub>2</sub>. Arrows indicate elevated MMP2 at 2% compared to 20% O<sub>2</sub>. The key below indicates the location of duplicate antibody probes for each protein according to the coordinates shown, including both positive (Pos) and Negative (Neg) controls. B. Western blots of molecular weight standards (Ladder), recombinant MMP2 or MMP9 (Control), and extracts of trophoblast cells cultured at 20% or 2% O<sub>2</sub>, as indicated. The upper blot was labeled with anti-MMP2, the middle blot was labeled with anti-MMP9 and lower blot with anti- $\beta$ -actin. C. MMP2 quantified by ELISA in trophoblast cells cultured 0-4 h at 2% O<sub>2</sub>. D. HBEGF quantified by ELISA in trophoblast cells treated during culture for 4 h with the indicated MMP inhibitor or vehicle, and concentration of O<sub>2</sub>. E. Apoptosis was quantified in trophoblast cells cultured as in D using the TUNEL assay. \*  $p < 0.05$ , compared to the control (0 h, vehicle/20% O<sub>2</sub>).

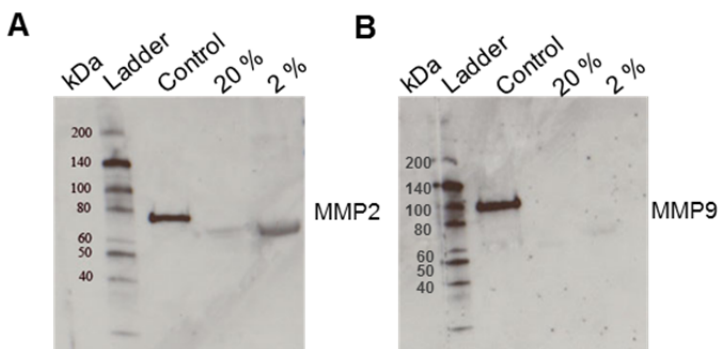


**Figure 4.** Western blots of molecular weight standards (Ladder), recombinant MMP2 or MMP9 (Control), and extracts of trophoblast cells cultured at 20% or 2% O<sub>2</sub>, as indicated. Blot A was labeled with anti-MMP2, blot B was labeled with anti-MMP9

### ***MMP2 mRNA expression***

To determine whether MMP2 is transcriptionally upregulated at low O<sub>2</sub>, its expression was quantified by qPCR, using RNA extracted from HTR-8/SVneo cells cultured at 20 % and 2 % O<sub>2</sub> for 1-4 hrs. Expression values, normalized to GAPDH, were calculated for both MMP2 (Figure 5A) and HBEGF (Figure 5B). MMP2 mRNA, like HBEGF message, did not change ( $p=0.8$ ) at 2% O<sub>2</sub>, suggesting that their proteins are both regulated post-transcriptionally.

### ***Role of transcription in HBEGF upregulation***

Trophoblast cells were cultured at 2% O<sub>2</sub> with or without  $\alpha$ -amanitin, an inhibitor of RNA polymerase-II (Lindell et al., 1970; Stirpe and Fiume, 1967), to examine the role of *de novo* transcription in the upregulation of HBEGF. MMP2 and HBEGF mRNA expression was quantified by qPCR, using RNA extracted from HTR-8/SVneo cells cultured at 20 % and 2 % O<sub>2</sub> for 6h, and with 5  $\mu$ g/ml  $\alpha$ -amanitin for 6h, 8h and 24h at 2 % O<sub>2</sub>. Expression values, normalized to GAPDH and SDHA, were calculated for both MMP2 (Figure 5C) and HBEGF (Figure 5D). The presence of  $\alpha$ -amanitin did not significantly alter the abundance of either MMP2 ( $p=0.4454$ ) or HBEGF ( $p=0.1357$ ) transcripts in trophoblast cells cultured at 2% O<sub>2</sub> for up to 6h. However, a time-dependent decrease in both MMP2 and HBEGF mRNA abundance was observed in  $\alpha$ -amanitin-treated cells at 6-24 h that became significant at 24 h ( $p<0.05$ ), indicative of MMP2 and HBEGF mRNA turnover. Previous work done has shown that culturing

HTR-8/SVneo cells at 2% O<sub>2</sub> for 8h (Armant et al., 2006) and 24h (Kilburn et al., 2000) increases proliferation of trophoblast cells, based on nuclear expression of the cell proliferation marker, Ki-67. This suggests that the decrease in MMP2 and HBEGF mRNA after 24 h of  $\alpha$ -amanitin treatment is not due to increased apoptosis, as the cells are alive and proliferating. Elevation of HBEGF protein after culture at 2% O<sub>2</sub> for 6 h was abrogated in a dose-dependent manner by  $\alpha$ -amanitin, with maximal inhibition attained at 5  $\mu$ g/ml (Figure 5E). Using ELISA, we demonstrated that MMP2 was not only required for HBEGF upregulation (Figure 3D), but that addition of rMMP2 was sufficient to increase ( $p < 0.0001$ ) HBEGF at 20% O<sub>2</sub> to the same extent as trophoblast culture at 2% O<sub>2</sub> (Figure 3F). Furthermore, addition of rMMP2 rescued ( $p < 0.0001$ ) HBEGF biosynthesis in the presence of  $\alpha$ -amanitin at 2% O<sub>2</sub> (Figure 5F), suggesting that *de novo* transcription is required for MMP2 activity leading to the shedding and accumulation of HBEGF.

CoCl<sub>2</sub>, a chemical mimic of hypoxia that stabilizes hypoxia inducible factor (HIF) by inhibiting ubiquitination of HIF (Jiang et al., 1997), was used to examine its effect on HBEGF regulation. At 20% O<sub>2</sub>, CoCl<sub>2</sub> increased ( $p < 0.0001$ ) HBEGF levels. As expected, CoCl<sub>2</sub> induced accumulation of HIF1A and HIF2A, similar to the effect of low O<sub>2</sub>, according to western blotting (Figure 6A, Figure 7A & B). The CoCl<sub>2</sub>-induced accumulation of HIF1A (Figure 6B) and HIF2A (Figure 6C) was quantified by ELISA, establishing a significant increase comparable to low O<sub>2</sub>.  $\alpha$ -Amanitin blocked the CoCl<sub>2</sub>-mediated increase in HBEGF (Figure 6D). The observed effects of  $\alpha$ -amanitin on HBEGF accumulation suggest that transcription of genes, likely regulated by HIF1A or HIF2A, is required to initiate MMP2 accumulation and HBEGF shedding. Additionally, immunohistochemical staining of both HIF1A and HIF2A indicated the localization of both HIF proteins to nucleus (indicated by arrows) as they accumulated after exposure to low O<sub>2</sub> for 0.5 to 1 h (Figure 7C).

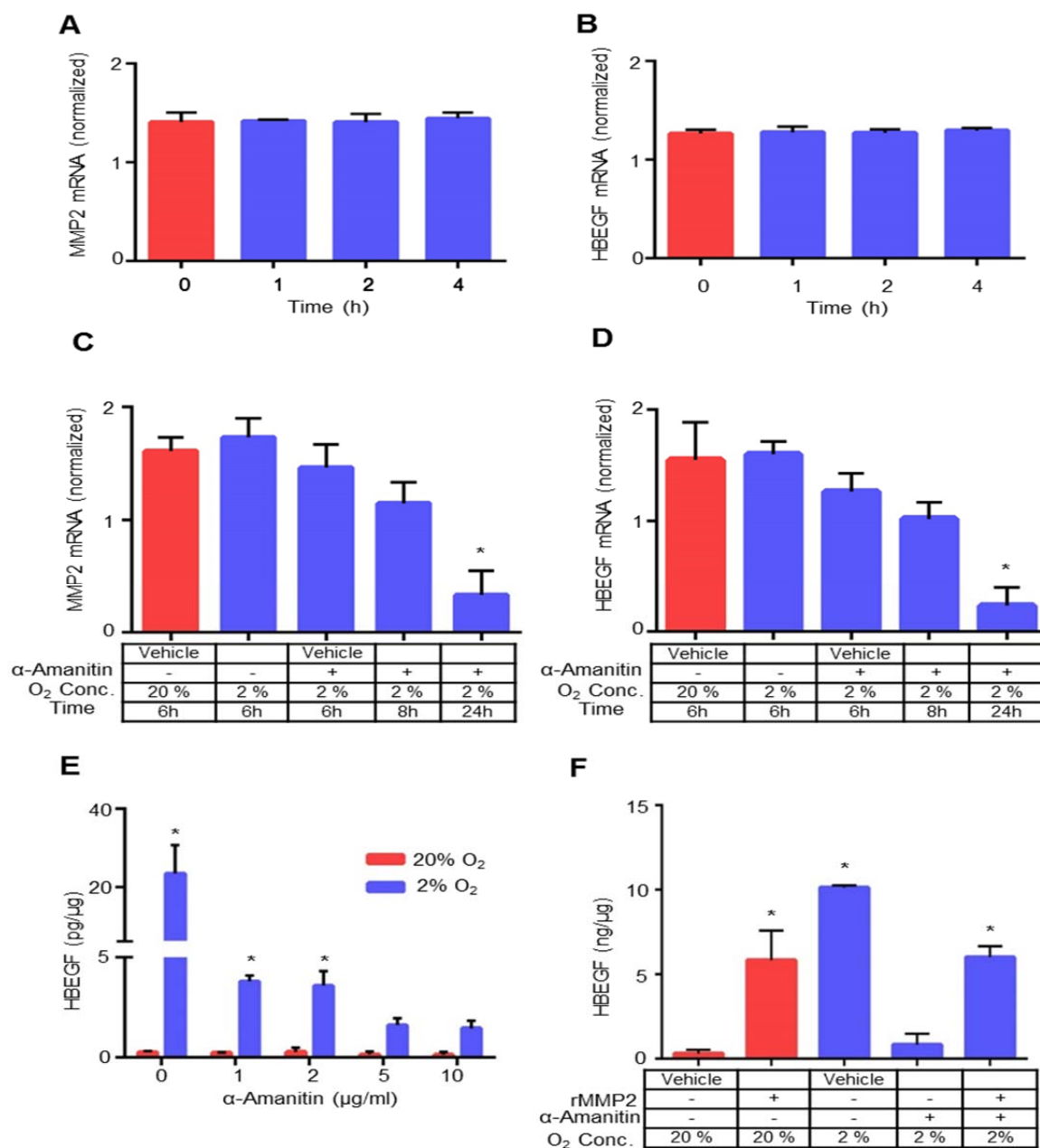


**Figure 5. Expression of MMP2 and HBEGF at 2% O<sub>2</sub> in HTR-8/SVneo cells.** MMP2 (A, C) and HBEGF (B, D) mRNA were measured by qPCR after culture for indicated time at 2% O<sub>2</sub> (A, B) and after culture with  $\alpha$ -amanitin (2  $\mu$ g/ml) at indicated time and O<sub>2</sub> concentration (C, D). HBEGF protein measured by ELISA in extracts of trophoblast cells cultured at the indicated concentrations of  $\alpha$ -amanitin and O<sub>2</sub> (E) and in cellular extracts of trophoblast cells cultured for 4 h at either 20% or 2% O<sub>2</sub> in the presence of recombinant MMP2 (rMMP2) and  $\alpha$ -amanitin, as indicated (F). \*,  $p < 0.05$ , compared to no treatment/vehicle/20% O<sub>2</sub>,  $n = 3$ .

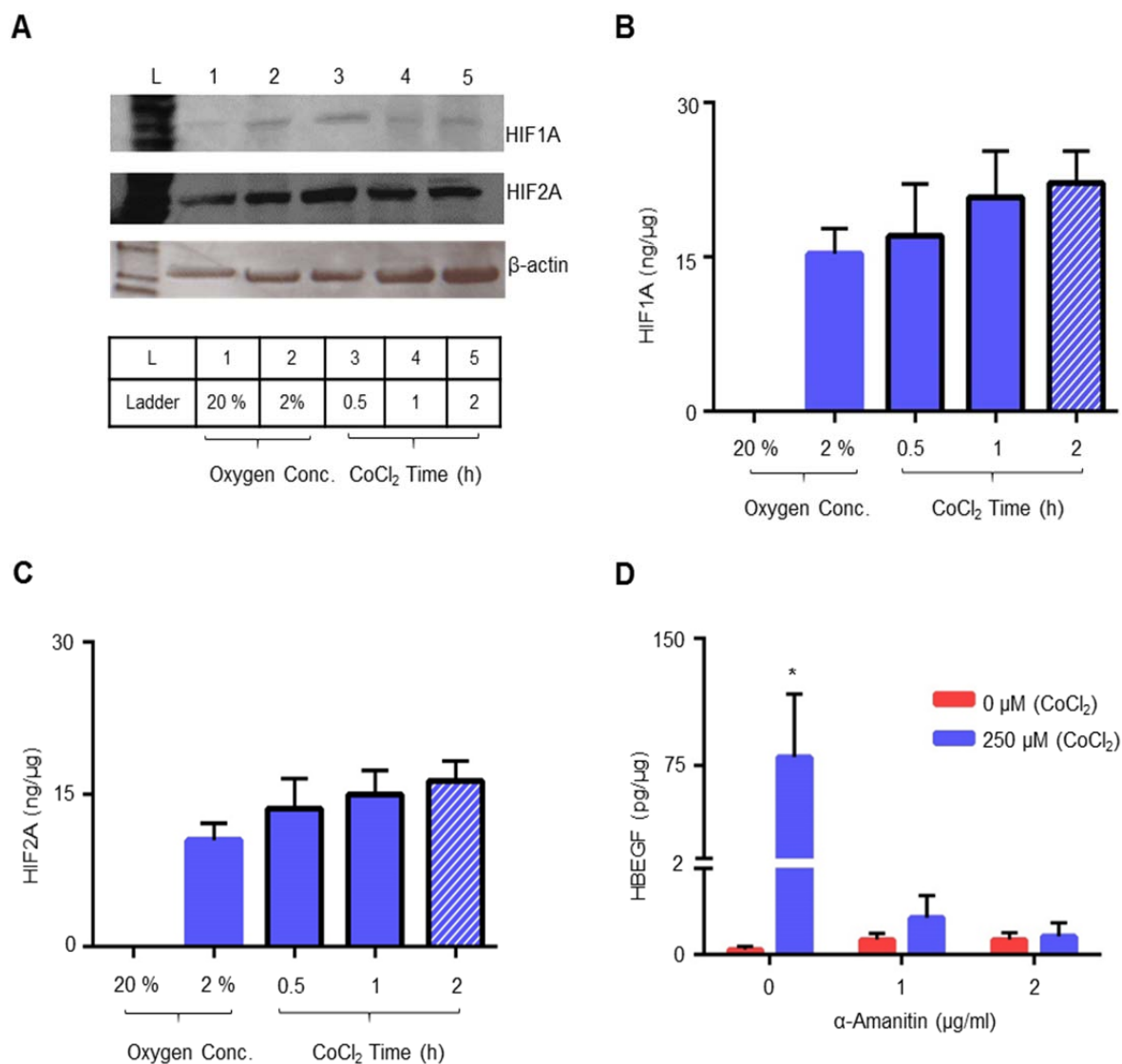


**Figure 6. Expression of HIF proteins and HBEGF in the presence of CoCl<sub>2</sub> in HTR-8/SVneo cells**  
 A. Western blots of HIF1A (~ 93 kDa), HIF2A (~96 kDa) and β-actin (~45kDa) in lysates of cells treated at 20% O<sub>2</sub> or 2% O<sub>2</sub> for 4 h, or at 20% O<sub>2</sub> in the presence of 250 μM CoCl<sub>2</sub> for 0.5 - 2 h, as indicated in the Key below gel images. HIF1A (B) and HIF2A (C) protein measured by ELISA in extracts of trophoblast cells treated at 20% O<sub>2</sub> or 2% O<sub>2</sub> for 4h, or at 20% O<sub>2</sub> in the presence of 250 μM CoCl<sub>2</sub> for 0.5 - 2 h. D. HBEGF protein measured by ELISA in extracts of trophoblast cells cultured at the indicated concentrations of α-amanitin and CoCl<sub>2</sub> at 20% O<sub>2</sub>. \* p < 0.05 compared to no treatment control, n=3.

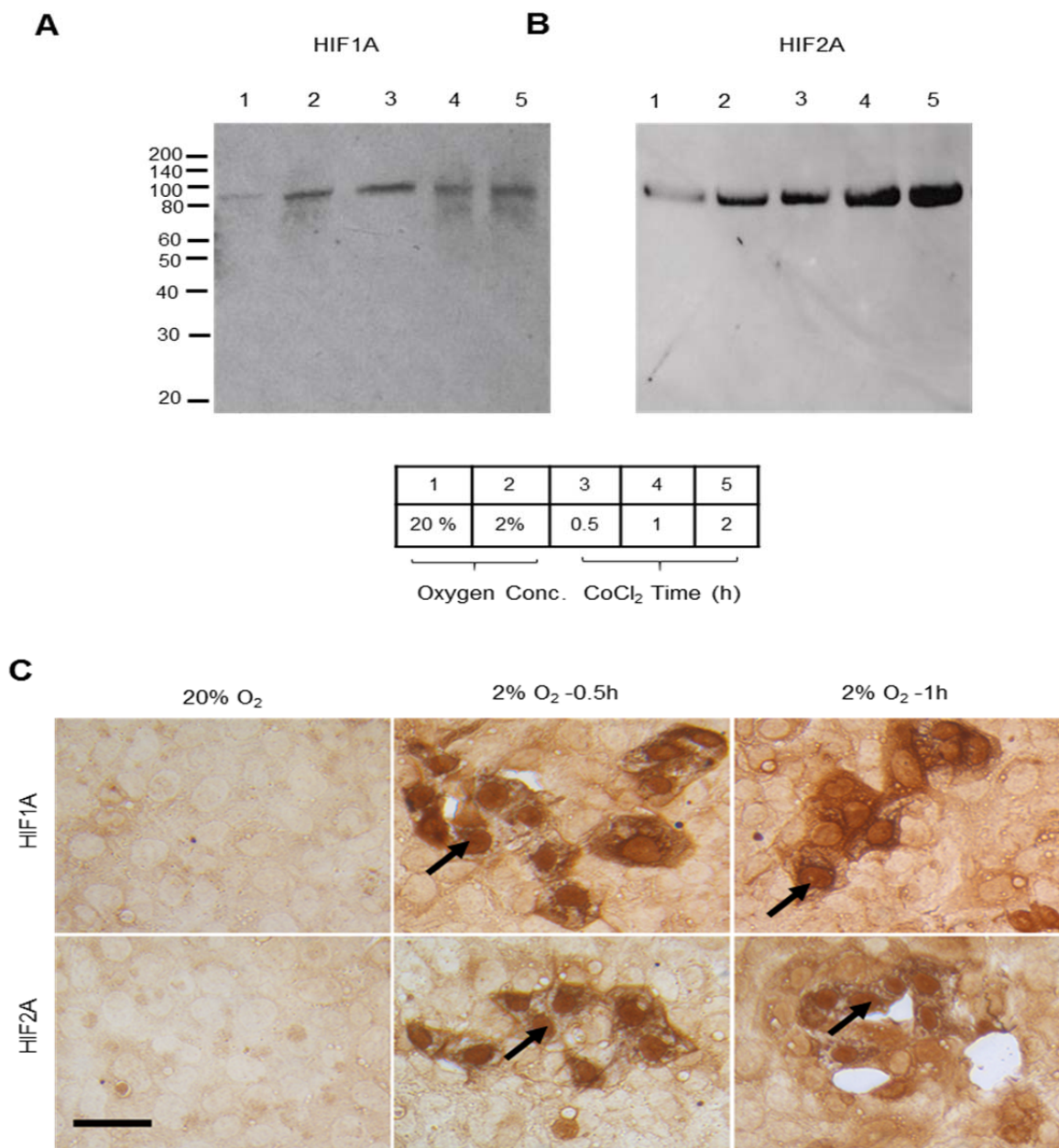


**Figure 7. Expression of HIF1A and HIF2A during altered O<sub>2</sub> concentrations or simulated hypoxia (CoCl<sub>2</sub>) in HTR-8/SVneo cells.** Western blots showing the entire lanes for HIF1A (A, ~ 93 kDa) and HIF2A (B, ~96 kDa) in TB cell lysates prepared after treatment at 20% O<sub>2</sub> or 2% O<sub>2</sub> for 4h, or at 20% O<sub>2</sub> in the presence of 250 μM CoCl<sub>2</sub> for 0.5 - 2 h, as indicated in the Key below gel images. C. TB cells cultured at either 20%, or switched to 2% O<sub>2</sub> for 0.5 or 1 h, as indicated. Cells were fixed and stained for HIF1A (upper panel) and HIF2A (lower panel) using immunohistochemistry. Size bar, 50 μm. Arrows indicate localization of HIF1A and HIF2A in nuclei.

### ***Role of MAPKs in MMP2 upregulation***

We previously showed that upregulation of HBEGF at low O<sub>2</sub> requires MAPK signaling



(Jessmon et al., 2010). MMP2 was quantified by ELISA in extracts of trophoblast cells cultured at 2% O<sub>2</sub> for 4 hours, with or without specific inhibitors of ERK, p38 and JNK, or the corresponding inactive structural analogs (Table 1). Inhibitors of MAPKs had no effect on the increased MMP2 expression at 2% O<sub>2</sub>, suggesting that the upregulation of MMP2 is independent of MAPK, and that MAPK signaling most likely functions exclusively downstream of ERBB activation.

**Table 1. MMP2 upregulation is independent of MAPKs**

% O <sub>2</sub>	Treatment	MMP2 (ng/ml)
20	Vehicle	0.03 ± 0.03
2	Vehicle	7.27 ± 0.74 *
2	U 0126/ERK inhibitor	6.07 ± 0.55 *
2	U0124/ERK Negative control	7.40 ± 0.66 *
2	JNK inhibitor	5.44 ± 1.98 *
2	JNK Negative control	6.53 ± 1.23 *
2	SB203580 P38 inhibitor	6.17 ± 0.87 *
2	SB 202474 P38 Negative control	7.15 ± 0.89 *
2	All 3 inhibitors	5.86 ± 1.51 *
2	All 3 neg. controls	6.34 ± 0.68 *

\* p<0.0001

### *Identification of differentially expressed transcripts*

Transcripts differentially expressed in trophoblast cells at the two O<sub>2</sub> levels were identified, using a non-biased NGS approach. RNA-seq analysis using the GGA revealed a total of 9 upregulated (Table 2) and 120 downregulated genes (Table 3) after 1 hr of exposure to 2% O<sub>2</sub> (Figure 8A). Of the 9 upregulated genes, HSPA6 was the most dramatically upregulated (870-fold) (Table 3), and the only gene that remained elevated at 2 h (Figure 8B) and 4 h (Figure 8C). The increase in HSPA6 expression at 2% O<sub>2</sub> was validated using qPCR (18 fold, p<0.0001) and western blotting (2.3 fold, p<0.05) (Figure 8D, E). Extraction of the promoter region using the GGA MatInspector (Cartharius et al., 2005) program revealed two overlapping HRE's 2.4

kb upstream of the 5'-most HSPA6 transcriptional start site (Figure 9), suggesting that HSPA6 could operate downstream of hypoxia to regulate MMP2 and HBEGF biosynthesis at low O<sub>2</sub>. Interestingly, as expected RNAseq data showed that although HBEGF and HIF1A were not differentially regulated yet their transcripts were present and showed no change in RPKM values after shifting trophoblast cells from 20% to 2% O<sub>2</sub>. Surprisingly, MMP2 was not detected possibly due to low abundance of its transcript, or a problem in the software used to map it to the human genome.

**Table 2. Upregulated transcripts from RNASeq analysis**

Gene Symbol	Gene ID	Log 2 fold change		
		0h vs 1h	0h vs 2h	0h vs 4h
HSPA6	3310	6.771	7.78	6.55
FAP	2191	5.188	--	--
LOC100131607	100131607	5.043	--	--
SNORA5A	654319	4.826	--	--
RPS16P5	647190	4.794	--	--
ZNF319	57567	4.564	--	--
IL8	3576	4.435	--	--
VTRNA1-3	56662	4.039	--	--
CLK1	1195	3.687	--	--

**Table 3. Downregulated transcripts from RNASeq analysis**

Gene Symbol	Gene ID	Log 2 fold change		
		0h vs 1h	0h vs 2h	0h vs 4h
ATG9A	79065	-9.071	-9.071	-9.028
LOC100506361	100506361	-8.257	-8.969	-8.885
WHSC2	7469	-8.225	-8.470	-8.737
CCNF	899	-7.736	-8.450	-8.403
RBPM52	348093	-7.713	-8.306	-8.368
RXRA	6256	-7.617	-8.265	-8.312
PGPEP1	54858	-7.594	-8.234	-8.260
TONSL	4796	-7.569	-8.173	-8.228
RUSC1	23623	-7.518	-8.126	-8.215
SOLH	6650	-7.518	-8.122	-7.867
RPS6KA4	8986	-7.426	-8.015	-7.855
CLEC16A	23274	-7.41	-7.914	-7.831



ZFPL1	7542	-7.365	-7.611	-7.764
CAPG	822	-7.336	-7.595	-7.727
SFSWAP	6433	-7.323	-7.570	-7.687
TMEM184B	25829	-7.293	-7.474	-7.657
BAD	572	-7.262	-7.367	-7.496
SUN2	25777	-6.818	-7.381	-7.534
CDC42EP1	11135	-6.494	-7.293	-7.521
PKMYT1	9088	-6.466	-7.293	-7.465
SCAMP5	192683	-5.818	-7.237	-7.345
WDR6	11180	-5.782	-7.173	-7.147
SMG6	23293	-5.677	-7.033	-6.976
ESPL1	9700	-5.659	-7.020	-6.914
DPYSL2	1808	-5.581	-6.953	-6.879
SEC24D	9871	-5.5	-6.753	-6.791
EPHB4	2050	-5.498	-6.747	-6.704
SEC16A	9919	-5.443	-6.742	-6.685
PLCD3	113026	-5.309	-6.701	-6.648
GLI2	2736	-5.282	-6.688	-6.603
ATXN2L	11273	-5.227	-6.606	-6.518
POLR2A	5430	-5.14	-6.601	-6.488
SLC19A1	6573	-5.13	-6.521	-6.322
RANBP10	57610	-5.095	-6.520	-6.248
SYNPO	11346	-5.043	-6.506	-6.241
SMTN	6525	-5.042	-6.380	-6.188
GYS1	2997	-5	-6.297	-6.148
PTP4A3	11156	-4.964	-6.284	-6.083
RAI1	10743	-4.955	-6.237	-5.994
POM121	9883	-4.935	-6.212	-5.966
PCNXL3	399909	-4.863	-6.146	-5.955
PPDPF	79144	-4.82	-6.113	-5.949
EIF4G1	1981	-4.755	-6.089	-5.933
ZNF646	9726	-4.755	-6.039	-5.911
NUMBL	9253	-4.667	-6.031	-5.837
GPR56	9289	-4.665	-6.026	-5.834
SPSB1	80176	-4.65	-6.435	-5.810
SLC48A1	55652	-4.641	-5.915	-5.745
SHKBP1	92799	-4.616	-5.880	-5.668
ZNF703	80139	-4.585	-5.832	-5.637
ORAI1	84876	-4.582	-5.659	-5.568
TAPBP	6892	-4.58	-5.599	-5.544
RNFT2	84900	-4.547	-5.457	-5.534
SOX13	9580	-4.53	-5.450	-5.490

TMEM131	23505	-4.528	-5.387	-5.482
PLXNB2	23654	-4.511	-5.379	-5.475
CREB3L2	64764	-4.477	-5.163	-5.452
ALG3	10195	-4.426	-5.110	-5.438
MEN1	4221	-4.379	-5.045	-5.333
TTLL4	9654	-4.327	-4.781	-5.305
LLGL1	3996	-4.325	-4.759	-5.302
CTTN	2017	-4.323	-4.755	-5.276
BCL9L	283149	-4.311	-4.673	-5.193
ATN1	1822	-4.286	-4.584	-5.070
MYADM	91663	-4.265	-4.528	-5.040
PHF1	5252	-4.229	-4.506	-4.993
BCAR1	9564	-4.228	-4.432	-4.975
MLXIP	22877	-4.219	-4.383	-4.966
PRRC2B	84726	-4.219	-4.357	-4.962
RNF31	55072	-4.213	-4.304	-4.895
ZNF777	27153	-4.153	-4.233	-4.845
SRRM2	23524	-4.088	-4.232	-4.825
CBX6	23466	-4.084	-4.194	-4.796
RAB1B	81876	-4.069	-4.189	-4.789
COL6A1	1291	-4.035	-4.174	-4.740
WBP2	23558	-4.032	-4.141	-4.707
FOSL2	2355	-3.988	-4.044	-4.704
PRRC2A	7916	-3.983	-4.033	-4.665
TRIM26	7726	-3.962	-4.032	-4.640
COTL1	23406	-3.959	-4.020	-4.522
DBN1	1627	-3.933	-3.989	-4.498
SEPN1	57190	-3.913	-3.964	-4.494
PFKP	5214	-3.907	-3.900	-4.482
RNF220	55182	-3.898	-3.936	-4.438
RAVER1	125950	-3.894	-3.897	-4.422
COL1A1	1277	-3.88	-3.866	-4.249
TMEM109	79073	-3.875	-3.823	-4.239
ACOT7	11332	-3.875	-3.799	-4.226
SDC1	6382	-3.859	-3.781	-4.201
NRSN2	80023	-3.856	-3.754	-4.161
BGN	633	-3.842	-3.700	-4.109
CIZ1	25792	-3.79	-3.677	-4.030
DAG1	1605	-3.789	-3.643	-4.009
NUP214	8021	-3.772	-3.642	-3.918
CYB5R3	1727	-3.771	-3.615	-3.883
NPRL3	8131	-3.762	-3.577	-3.864

COL4A2	1284	-3.748	-3.552	-3.811
SLC7A5	8140	-3.722	-3.482	-3.794
SRCAP	10847	-3.707	-3.460	-3.782
FOSL1	8061	-3.691	-3.443	-3.773
CYP2S1	29785	-3.676	-3.404	-3.762
PLEC	5339	-3.662	-3.405	-3.733
GIT1	28964	-3.657	-3.365	-3.722
NACC1	112939	-3.595	-3.363	-3.710
C20orf112	140688	-3.569	-3.348	-3.672
MAP2K7	5609	-3.487	-3.341	-3.638
C16orf57	79650	-3.475	-3.299	-3.425
ZFP36L1	677	-3.447	-3.234	-3.400
SLC25A23	79085	-3.426	-3.203	-3.395
LDOC1	23641	-3.409	-3.190	-3.235
AP2A1	160	-3.402	-3.180	-3.214
APEX2	27301	-3.357	-3.136	-3.196
PLOD1	5351	-3.312	-3.109	-3.176
EHMT2	10919	-3.268	-3.069	-3.150
SCAMP2	10066	-3.263	-3.037	-3.132
HEATR2	54919	-3.252	-2.956	-3.086
LRRC8A	56262	-3.246	-2.920	-3.079
ZNF574	64763	-3.207	-2.916	-3.006
PTRF	284119	-3.196	-2.892	-2.945
PPARD	5467	-3.026	-2.789	-2.582
MDH2	4191	-2.983	-2.7329	-2.564

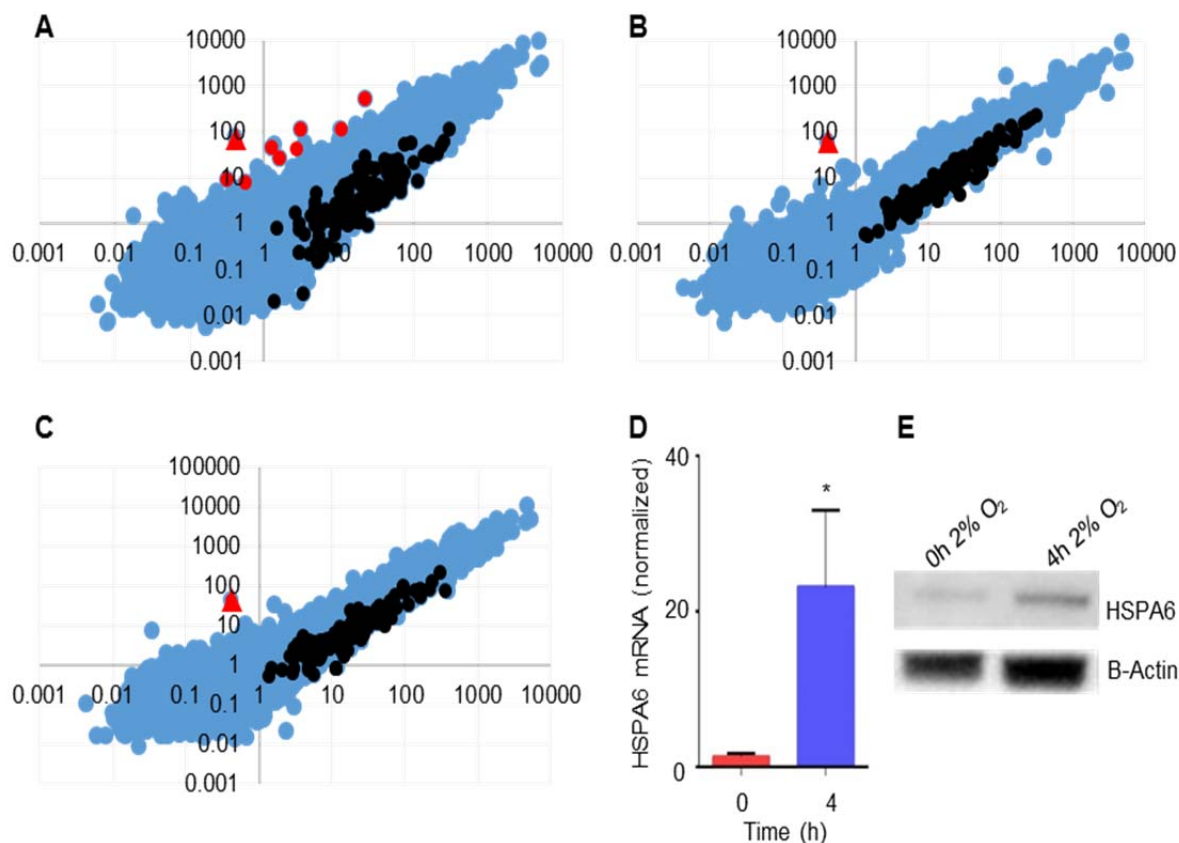


**Figure 8. Transcriptome graph analysis of trophoblast cells exposed to 2% O<sub>2</sub>.** A-C. Abundance of transcripts compared using GGA work station between cells cultured at 2% O<sub>2</sub> for 0 h (x-axis) and 1 h (A, y-axis), 2 h (B, y-axis) or 4 h (C, y-axis). Unchanged transcripts are indicated in blue, upregulated transcripts are red, and downregulated transcripts are black. HSPA6 (red triangle) was the most highly upregulated mRNA, and only transcript upregulated at 2 h and 4 h. D. HSPA6 mRNA was measured by qPCR in trophoblast cells cultured for indicated time at 2% O<sub>2</sub>. E. Western blots of HSPA6 (~70 kDa) and  $\beta$ -actin (~43 kDa) in lysates of trophoblast cells cultured for indicated time at 2% O<sub>2</sub>.

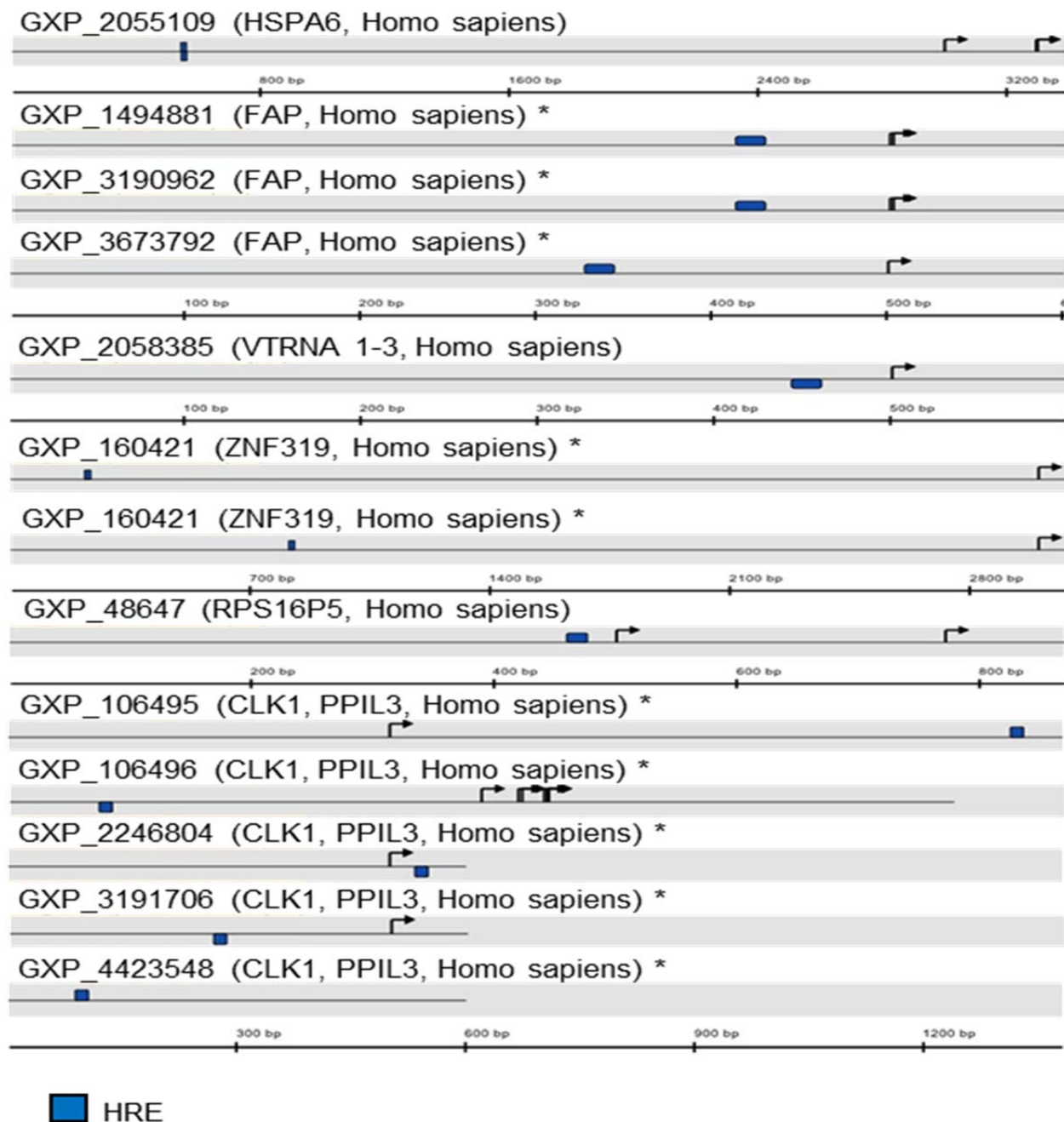


**Figure 9. Transcriptome analysis of trophoblast cells exposed to 2% O<sub>2</sub>.** MatInspector on the GGA work station was used to extract promoter regions of upregulated genes between cells cultured at 2% O<sub>2</sub> for 0 h and 1 h to identify HRE sites (Blue boxes). Splice variants (\*) also shown.

### ***HSP70 function in MMP2 and HBEGF upregulation***

Inhibition of HSP70 with a pharmacological inhibitor, VER 155008 (Schlecht et al., 2013), in trophoblast cells cultured at 2% O<sub>2</sub> caused a dose-dependent decrease in MMP2 (Figure 10A) and HBEGF (Figure 10B). VER 155008 acts by binding to the nucleotide binding site of HSP70 thereby arresting the nucleotide binding domain in a half open conformation. VER 155008 acts as an ATP-competitive inhibitor that prevents allosteric control between the

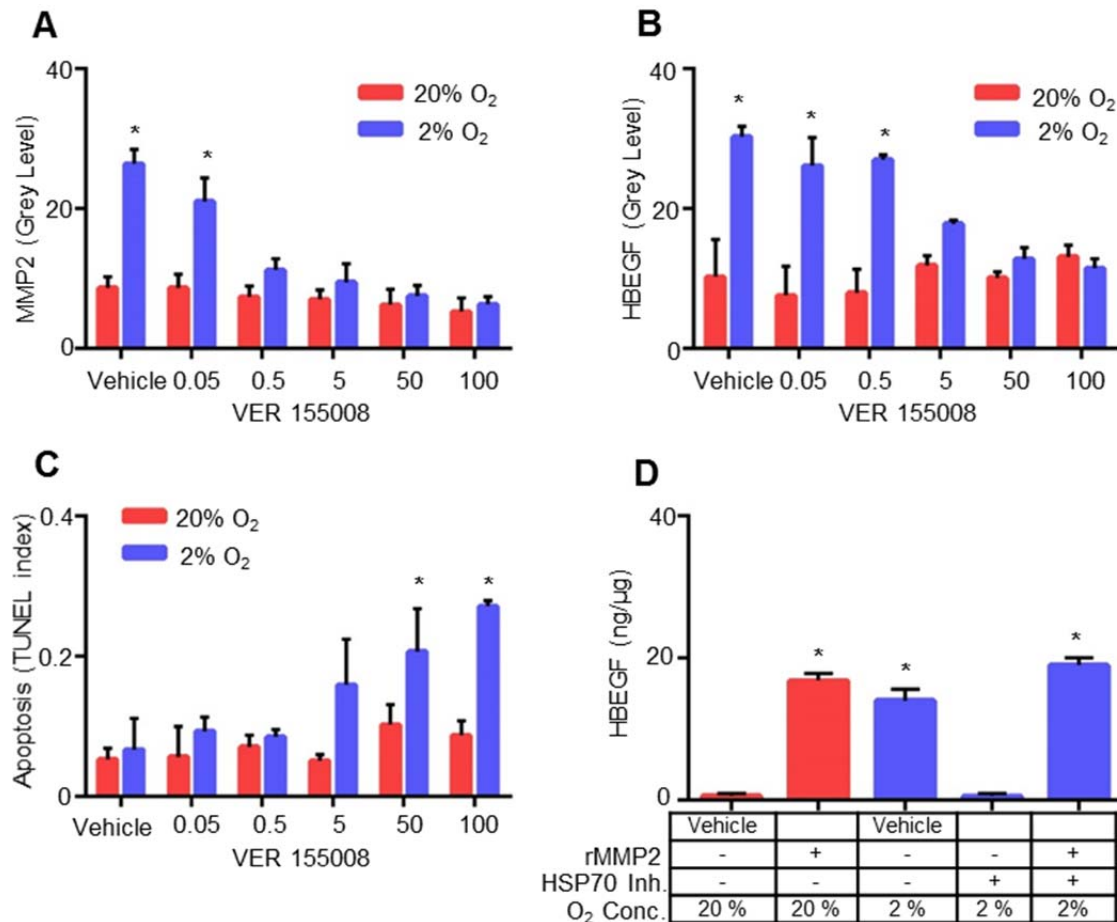


**Figure 10. Regulation of MMP2, HBEGF and cell survival by HSP70.** HSP70 was inhibited using the pharmacological inhibitor VER 155008 during culture of HTR-8/SVneo cells for 4 h at 20% or 2% O<sub>2</sub>. At 2% O<sub>2</sub>, HSP70 inhibition caused a dose-dependent decrease in both MMP2 (A) and HBEGF (B), measured by immunohistochemistry, and concomitantly increased cell death (C), measured by TUNEL. Cells cultured at 20% O<sub>2</sub> were unaffected. D. ELISA for HBEGF in cellular extracts of trophoblast cells cultured for 4 h at either 20% or 2% O<sub>2</sub> in the presence of recombinant MMP2 (rMMP2) and HSP70 inhibitor (VER 155008), as indicated. \*  $p < 0.05$ , compared to vehicle/20% O<sub>2</sub>.

nucleotide binding domain and the substrate binding domain (Schlecht et al., 2013). TUNEL assays showed increased ( $p<0.0001$ ) trophoblast cell death with HSP70 inhibition (Figure 10C), suggesting that survival at 2% O<sub>2</sub>, through upregulation of MMP2 and HBEGF, requires HSPA6 activity. Using ELISA, we demonstrated that MMP2 was not only required for HBEGF upregulation (Figure 3D), but that addition of rMMP2 was sufficient to increase ( $p<0.0001$ ) HBEGF at 20% O<sub>2</sub> to the same extent as trophoblast culture at 2% O<sub>2</sub> (Figure 10D). Furthermore, addition of rMMP2 rescued ( $p<0.0001$ ) HBEGF biosynthesis in the presence of HSP70 inhibitor at 2% O<sub>2</sub> (Figure 10D). These results demonstrate that upregulation of MMP2 requires HSPA6 (HSP70B') activity, while upregulation of HBEGF requires only shedding mediated by MMP2.

#### ***Regulation of MMP2 in first trimester explants***

Using immunohistochemistry and ELISA, it was confirmed that HSP70 inhibitor prevents the upregulation of MMP2 (Figure 11A, B) and HBEGF (Figure 8C, D) in first trimester explants cultured at 2% O<sub>2</sub> similar to the observed expression affects in HTR-8/SVneo (Figure 10). In addition, rMMP2 alone increased ( $p<0.0001$ ) HBEGF at 20% O<sub>2</sub>, and rescued ( $p<0.0001$ ) HBEGF upregulation at 2% O<sub>2</sub> during treatment with HSP70 inhibitor (Figure 11C, D). Cell death assays showed increased ( $p<0.05$ ) cell death during HSP70 inhibition that was rescued ( $p<0.05$ ) by rMMP2 (Figure 11E, F), suggesting that survival at 2% O<sub>2</sub>, through upregulation of MMP2 and HBEGF, requires HSPA6 activity.



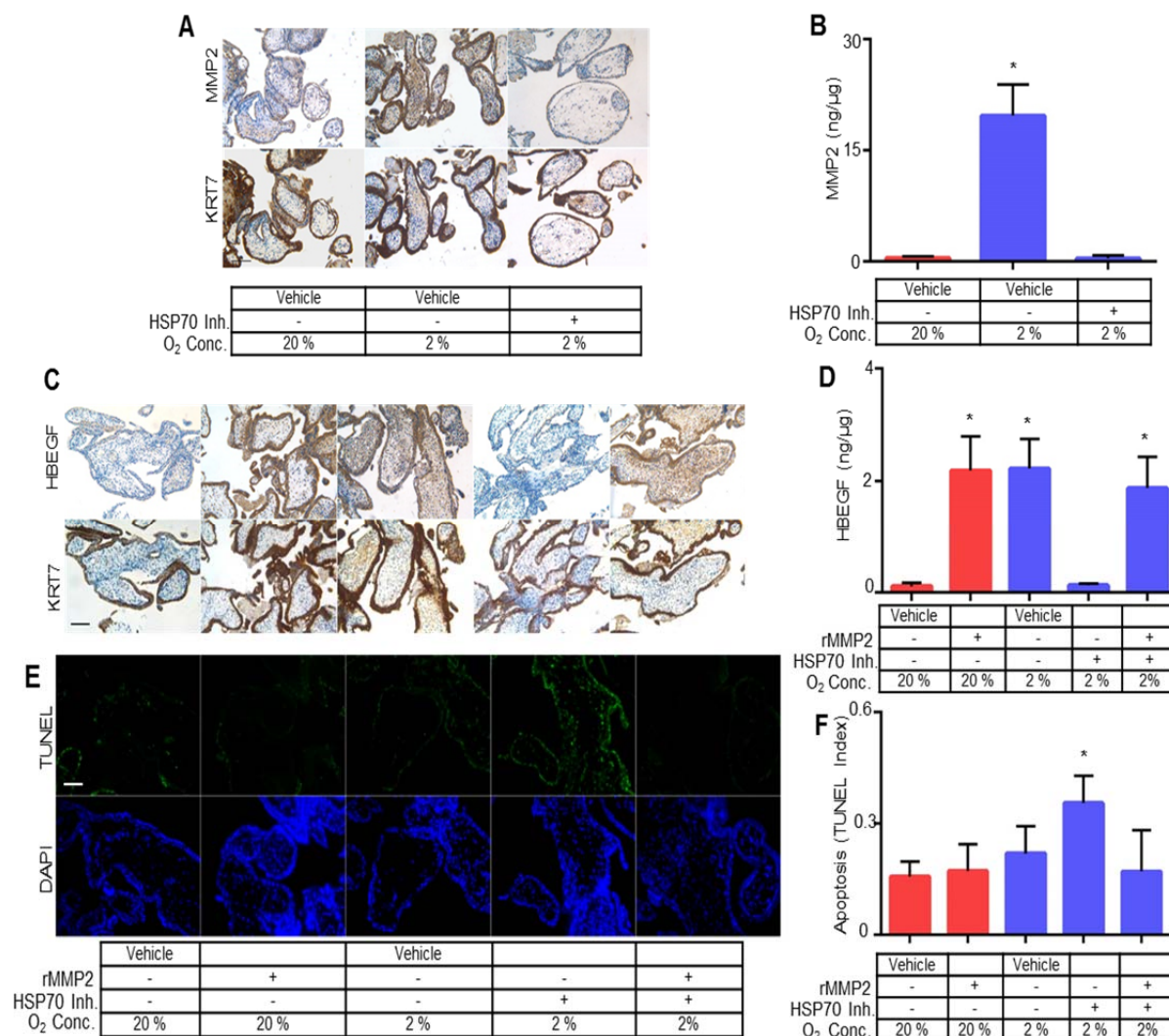


**Figure 11. Regulation of MMP2 in first trimester chorionic villous explants.** First trimester villous explants cultured for 6 h at either 20% or 2% O<sub>2</sub> in the presence of recombinant MMP2 (rMMP2) and VER 155008 (HSP70 inh.), as indicated, were stained for MMP2 & Cytokeratin (KRT7) (A), HBEGF & KRT7 (C) with counterstaining with Hematoxylin. Healthy nuclei counterstained with Hematoxylin appear blue and dual staining with DAPI and TUNEL (E), using immunofluorescence microscopy. Size bars indicating 10 μm are shown in A, C and 100 μm as shown in E. Cell extracts were assayed by ELISA for MMP2 (B) and HBEGF (D), as well as for cell death by TUNEL (F). \*,  $p < 0.0001$  in B and D,  $p < 0.05$  in F, compared to vehicle/20% O<sub>2</sub>,  $n = 3$

## Discussion

The regulation of HBEGF signaling during implantation and placentation is critical for trophoblast survival and invasion (Jessmon et al., 2009; Lim and Dey, 2009). An autocrine, post-transcriptional mechanism induced at low O<sub>2</sub> upregulates HBEGF synthesis and secretion,



providing an important survival factor during early gestation (Armant et al., 2006; Jessmon et al., 2009). The present study provides evidence that a transcriptional event is required to initiate HBEGF shedding downstream of HIF signaling. In seeking a metalloproteinase responsible for HBEGF shedding, a human MMP antibody array, verified by western blot and ELISA, implicated a protease cascade that includes MMP2. A functional role for MMP2 in the accumulation of HBEGF was established using a specific inhibitor. The increase in apoptosis observed by using another specific inhibitor for both MMP2 and MMP9 was greater, but not significantly different than the increase by MMP2 inhibition alone. The increase found with MMP2/9 inhibition could be additive; however, that is unlikely because apoptosis was unaffected by inhibition of MMP9 alone, compared to control. MMP2 mRNA concentration was unaltered by reduced O<sub>2</sub>, suggesting that it was regulated post-transcriptionally. Transcriptomic analysis identified HSPA6, a member of the HSP70 family, as a potential regulator upstream of MMP2. Using an inhibitor of HSP70 and exogenous rMMP2, evidence was obtained supporting a mechanism wherein low O<sub>2</sub> concentrations, as experienced by trophoblast cells during the first 10 weeks of placentation, induce HIF-mediated transcription of HSP70, a chaperone that directly or indirectly facilitates MMP2 accumulation. MMP2, in turn, appears to participate in a protease cascade that sheds HBEGF from the cell surface (Hitchon et al., 2002; Mohammad et al., 2010). The production of sHBEGF initiates autocrine signaling through its cognate receptors, EGFR and ERBB4 which activates its biosynthesis from constitutively-expressed, but latent HBEGF mRNA (Figure 12).

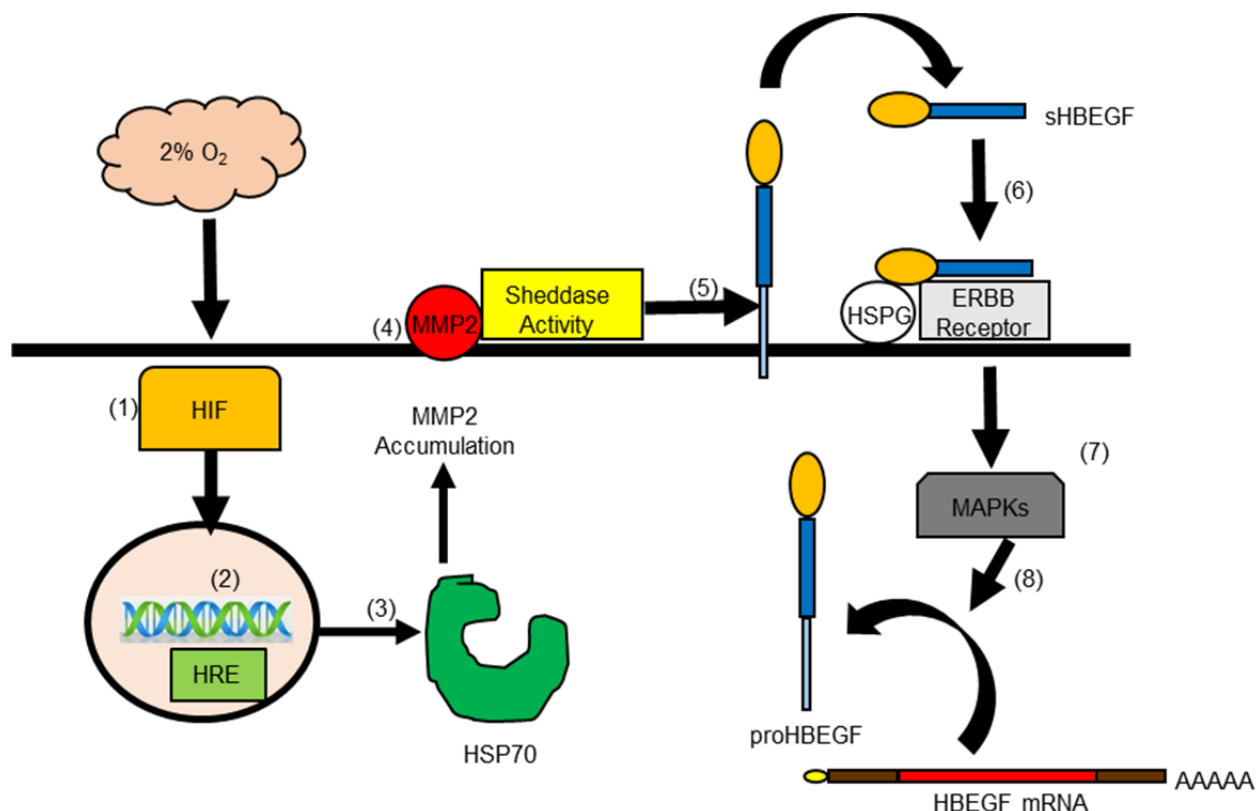


**Figure 12. Proposed Mechanism.** Low (2%) O<sub>2</sub> stabilizes cytoplasmic HIF1A and HIF2A (1) that accumulate and translocate to the nucleus (2) where they dimerize to HIF1B and bind to hypoxia response elements (HRE) in the regulatory regions of target genes, including HSPA6/HSP70B' (3). HSP70 regulates the accumulation of activated MMP2 at the cell surface (4), which is required and sufficient for shedding (5) of the extracellular domain of proHBEGF. The released sHBEGF binds (6) to its receptors, ERBB1 and ERBB4, through its EGF-like domain and to heparan sulfate proteoglycans (HSPG) through its heparin-binding domain. ERBB downstream signaling activates MAPKs (7) required for biosynthesis of proHBEGF from the pool of HBEGF mRNA (8). HBEGF autocrine signaling thereby increases HBEGF secretion to achieve extracellular HBEGF concentrations (>1 nM) sufficient to inhibit apoptosis at 2% O<sub>2</sub>.

Supplementation with HBEGF and other EGF family members such as EGF or TGF $\alpha$  has little effect on proliferation rates, but is highly effective at converting trophoblast cells to an invasive phenotype (Leach et al., 2004). The extensive expression of HBEGF in trophoblast cells, particularly within extravillous populations (Leach et al., 2002a), could be vital for their invasive activities during the establishment of pregnancy and physiological conversion of spiral arteries. Therefore, it has been established that HBEGF regulates trophoblast survival and invasion, two crucial functions that are compromised in pregnancies complicated by

preeclampsia (Brosens et al., 1972; DiFederico et al., 1999). HBEGF and other components of the EGF signaling system are disrupted in placentas of women with preeclampsia (Armant et al., 2015; Leach et al., 2002a). Trophoblast invasion is shallow in preeclampsia, possibly due to a lack of HBEGF-induced cell migration and a rise in apoptosis, exacerbated by reduced cytoprotection. The increased oxidative damage to trophoblast cells (Redman and Sargent, 2005) and the decrease in HBEGF in preeclamptic placentas is consistent with the hypothesis that HBEGF is an important survival factor throughout gestation. In this study we are focused at the role of HBEGF in cell survival to better understand the underlying mechanism.

Jessmon et. al showed that HBEGF activates ERK, p38 and JNK in human trophoblast cells, and treatment with specific inhibitors indicated that hypoxia upregulates HBEGF biosynthesis through any one of the three examined MAPKs (Armant et al., 2006; Jessmon et al., 2010). However, it was unclear whether this MAPK pathway was functional upstream or downstream of HBEGF shedding. Therefore, MMP2 was quantified in human trophoblast cells cultured at 2% O<sub>2</sub> with specific inhibitors of ERK, p38 and JNK. These inhibitors did not influence the upregulation of MMP2 at low O<sub>2</sub>, suggesting that the MAPKs function only downstream of HBEGF signaling through the ERBB1/4 tyrosine kinases in human trophoblast cells, as indicated in Figure 12.

MMP2 was not among the genes that were transcriptionally regulated at low O<sub>2</sub>, but nevertheless appears to participate in a proteolytic cascade that culminates in HBEGF shedding. Studies of early placentation suggest that MMP2 is important in trophoblast invasion (Staun-Ram et al., 2004). Interestingly, very low O<sub>2</sub> (0.1%) increases MMP2 mRNA levels 1.7-fold in trophoblast cells isolated from first trimester placentae (Onogi et al., 2011), which was not found in our study. However, culture at 2% O<sub>2</sub> could differ significantly from 0.1% O<sub>2</sub>, and account for the different outcomes. Using specific inhibitors and rMMP2, we showed that MMP2, but

not HBEGF, is regulated by HSP70. It appears that HSP70 stabilizes either MMP2 or a protein regulating its accumulation at the cell surface for shedding of HBEGF.

Although both MMP2 and HBEGF appear to be regulated by O<sub>2</sub> post-transcriptionally, HBEGF upregulation by low O<sub>2</sub> or CoCl<sub>2</sub> was blocked by  $\alpha$ -amanitin, suggesting the requirement for transcription. HIF proteins are stabilized at low O<sub>2</sub> (Wang and Semenza, 1993), and activate transcription of targeted genes by interaction with specific HREs in the gene promoters (Semenza, 2003), along with transcriptional coactivators to form an initiation complex (Lisy and Peet, 2008). We suspected that either HIF1A or HIF2A could be involved in the response of trophoblast cells to low O<sub>2</sub>, based on their accumulation under the influence of CoCl<sub>2</sub> or 2% O<sub>2</sub>, which was previously reported in JEG3 choriocarcinoma cells (Park et al., 2014). Interestingly, the transcriptome analysis revealed HSPA6/HSP70B' as the most highly upregulated gene at 1-4 h, while no changes occurred in transcripts of metalloproteinases. Extraction of the HSPA6 promoter revealed two overlapping HREs on the sense and anti-sense strands. HREs also appeared in the promoters of the eight other mRNAs that increased 1 h after exposure of trophoblast cells to low O<sub>2</sub>. Interestingly, microarray analysis identifies only 216 genes have HRE sites in the human genome (Ortiz-Barahona et al., 2010). In rabbit chondrocytes and JEG3 cells increased expression of HIF1A under hypoxia (2%) or simulated hypoxia (CoCl<sub>2</sub>) resulted in an increases in HSP70 expression, which is was ablated by HIF1A inhibition or knockdown (Park et al., 2014; Tsuchida et al., 2014). These data suggest that HSP70 transcription is induced by HIF1A signaling.

Induction of heat shock proteins (HSPs) in response to cellular stress has been proposed as a potential strategy of eukaryotic cells to combat lethal conditions (Ananthan et al., 1986; Goff and Goldberg, 1985; Parsell and Sauer, 1989). Within the HSP family, HSP70 functions in the recovery of cells from stress, and in guarding against further insults (Fulda et al., 2010).

HSP70 is a multigene family that includes the stress-inducible members HSPA6 and HSPA1A/HSP70-1 (Schwarz et al., 2003; Tavaría et al., 1996). HSP70 protects stressed cells by recognizing nascent polypeptides, unstructured regions of protein, and exposed hydrophobic stretches of amino acid (Nollen and Morimoto, 2002). The binding of exposed hydrophobic residues in unfolded or partially folded proteins is regulated by ATP-hydrolysis-induced conformational changes in the ATPase domain of HSP70, which is stimulated by co-chaperones (Nollen and Morimoto, 2002). HSP70 is transcribed in response to stress due to activation of heat shock transcription factor (HSF) (Abravaya et al., 1992). Abravaya et al. proposed a model suggesting that physiological stress creates misfolded proteins that compete with HSF for binding to HSP70, resulting in release of transcriptionally active, DNA-binding HSF to induce transcription of heat shock genes. Baird et al. has shown that this HSF-mediated transcription is increased under low O<sub>2</sub> due to direct binding of HIF1A to its HRE on the HSF intron (Baird et al., 2006). These reports are consistent with a mechanism wherein HSP70 transcription is mediated by HSF or HIF1A at low O<sub>2</sub> in trophoblast cells.

HSP70 forms a molecular chaperone complex with HSP90, another highly conserved and essential HSP family member (Pratt et al., 2015; Pratt and Toft, 2003). This molecular chaperone complex is dependent on the hydrolysis of ATP, and ADP/ATP exchange, and is mediated by association with HOP (Hsp70/Hsp90-organising protein)/STIP1 (stress-induced phosphoprotein 1) (Carrigan et al., 2006; Chen and Smith, 1998). The HSP70/HSP90 molecular chaperone complex, optimized by HOP, coordinates interactions that ensure folding and conformational regulation of proteins under stress (Hernandez et al., 2002; Wegele et al., 2004). RNAi knockdown of HOP in pancreatic cancer cells decreases expression of MMP2 (Walsh et al., 2011). Additionally, inhibition or depletion of HSP70 in the breast cancer cell line, MA-MB-231, decreases cell migration and invasion due to a lack of MMP2 activation (Sims et al., 2011).

This suggests that molecular relationships between HSPs, various signaling proteins, and partner proteins mediate the integrity of signal transduction pathways (Nollen and Morimoto, 2002). Our data further supports the role for HSP70 in mediating MMP2 function, which is required in trophoblast cells for HBEGF survival signaling.

The signaling cascade delineated in the present study (Figure 12) could influence multiple physiological processes that play a key role in placentation. There is substantial evidence to support that HBEGF expression is altered in preeclampsia, and that its protein levels are decreased in preeclamptic placentas (Armant et al., 2015; Leach et al., 2002a). MMP2 belongs to a family of extracellular matrix-remodeling enzymes that have been implicated in the regulation of vasculogenesis, which is disrupted in placental insufficiency disorders, such as preeclampsia. There is compelling evidence that MMP2, but not MMP9, increases in women who subsequently develop preeclampsia (Eleuterio et al., 2015; Montagnana et al., 2009; Myers et al., 2005; Narumiya et al., 2001). HSP70 also appears to be altered in adverse pregnancies. In a pilot study, higher levels of HSP70 were reported in patients with early onset of severe PE (Jirecek et al., 2002; Yung et al., 2014). Fukushima et.al reported that serum levels of HSP70 were constant throughout normal pregnancy, but increased significantly in women with preeclampsia (Fukushima et al., 2005; Molvarec et al., 2006) or preterm delivery (Fukushima et al., 2005). Increased circulating HSP70 in preeclamptic patients could be due to systemic inflammation as a result of disease and increased oxidative stress (Ekambaram, 2011; Molvarec et al., 2009). In term preeclamptic placentas, HIF1A and HSP70 are both elevated and, localized prominently in syncytiotrophoblasts and villous endothelial cells (Park et al., 2014). In another study of HSP70 in term placentas, both mRNA and protein increased in women with preeclampsia and intrauterine growth restriction (Liu et al., 2008). However, there has been no information reported on the expression or role of placental HSP70 in the first trimester prior to

this study.

Using an established trophoblast cell line and a villous explant model, we have established a role for HSPA6 (HSP70B'), a HIF-regulated gene, in the regulation of MMP2 required for HBEGF shedding at low O<sub>2</sub>. These findings suggest that trophoblast survival in the low O<sub>2</sub> environment during early pregnancy requires this signaling pathway. Disruption of any component during the first trimester could compromise trophoblast survival and function, leading to placental insufficiency and the resulting obstetrical complications of pregnancy.

### CHAPTER 3 - REGULATION OF HBEGF BY MICRO-RNA FOR SURVIVAL OF DEVELOPING HUMAN TROPHOBLAST CELLS

#### Abstract

The growth factor HBEGF is upregulated post-transcriptionally in the low O<sub>2</sub> environment of the human placenta during the first 10 weeks of pregnancy. We have examined the possible roles of HBEGF turnover and micro-RNA (miRNA) signaling in its regulation by O<sub>2</sub> in human first trimester trophoblast cells. HTR-8/SVneo trophoblast cells were cultured at 2% or 20% O<sub>2</sub> with vehicle, 10 µg/ml cyclohexamide, 1 µg/ml lactocystin, 100 µg/ml MG132, or siRNA to knockdown DGCR8 in the microprocessor. HBEGF, DGCR8, and β-actin were examined by western blotting. HBEGF was quantified by ELISA. Protein turnover studies using cyclohexamide demonstrated faster HBEGF degradation at 20 % O<sub>2</sub> than 2% O<sub>2</sub> mediated by the proteasome. However, proteasome inhibitors were insufficient to initiate HBEGF accumulation at 20% O<sub>2</sub>. Trophoblast cells were transfected with a dual luciferase reporter construct (psiCHECK-2) containing no insert (control), the HBEGF 3' untranslated region (3'UTR), or sub-regions of the 3'UTR. Reporter activity relative to empty vector demonstrated that the intact HBEGF 3' UTR inhibited expression (0.26), while fragments containing only its flanking regions increased reporter activity (3.15; 3.43). RNA was extracted from trophoblast cells cultured at 2% O<sub>2</sub> for 0-4 h for next-generation sequencing to quantify miRNAs. Although, no differential expression of any miRNAs was found in trophoblast cells, nevertheless, HBEGF upregulation at 2% O<sub>2</sub> was blocked when the miRNA-processing protein DGCR8 was silenced, suggesting a role for miRNA. Our findings suggest involvement of flanking regions of the 3'UTR in activating HBEGF protein synthesis in response to 2% O<sub>2</sub>, possibly through a miRNA-mediated mechanism.



## Introduction

The epidermal growth factor (EGF) family member, heparin binding EGF-like growth factor, (HBEGF), is present in the uterus at the time of embryo implantation (Leach et al., 1999; Yoo et al., 1997). In addition, its expression in trophoblast cells of the invading placenta indicates its central role in early implantation and subsequent placentation (Leach et al., 2002a). Since, the placenta is not fully oxygenated until after the 10<sup>th</sup> week of pregnancy, placentation proceeds in a low O<sub>2</sub> (2%) environment. *In vitro* work has demonstrated that HBEGF protein levels are upregulated in human first trimester trophoblast cells at low (2%) O<sub>2</sub> (Armant et al., 2006). Furthermore, HBEGF protects trophoblast cells from apoptosis, and promotes their invasion (Leach et al., 2004; Leach et al., 2008). Preeclampsia, in which trophoblast invasion is reduced and apoptosis elevated, is characterized by *in vivo* reduction of HBEGF expression, as well as disruption of and other regulatory components of EGF signaling system in TB cells (Armant et al., 2015; Leach et al., 2002b). A mechanism for the regulation of HBEGF by O<sub>2</sub> in TB cells is beginning to emerge, based on recent studies of a first trimester TB cell line. Transmembrane HBEGF cleavage in response to low O<sub>2</sub> initiates autocrine signaling that increases HBEGF levels to a concentration that inhibits apoptosis (Armant et al., 2006). The autocrine upregulation of HBEGF requires activation of its cognate receptors (ERBB1 and ERBB4), and downstream signaling through any one of three MAPK pathways initiated by MAPK 1/3, MAPK14 or MAPK8 (Jessmon et al., 2010). Previous work has demonstrated that HBEGF is not transcriptionally regulated by O<sub>2</sub>, although its protein levels increase by over 100-fold at low O<sub>2</sub> (Armant et al., 2006). HBEGF mRNA levels are high and remain unchanged by exposure to low O<sub>2</sub>. It remains to be determined that at what point downstream of HBEGF shedding HBEGF accumulation is regulated by this autocrine mechanism.

Regulation of transcription and translation can be disparate processes, depending on the

gene and cellular context (DiFederico et al., 1999; Koritzinsky et al., 2005). The abundance of specific proteins can be regulated post-translationally by altering their turnover rates (Kristensen et al., 2013). Proteins with fast turnover rates are generally characterized as low abundance (Boisvert et al., 2012; Schwanhausser et al., 2011), intrinsically unstructured (Gsponer et al., 2008; Prakash et al., 2004), or aggregation prone (De Baets et al., 2011; Gsponer and Babu, 2012), and are mostly involved in signal transduction and transcriptional activation (Boisvert et al., 2012; Legewie et al., 2008; Yen et al., 2008). Alternatively, HBEGF downstream signaling could be involved in inhibiting its protein turnover to increase its abundance through its autocrine signaling (Figure 13). Certain proteins can be regulated by either stabilization (Zhao et al., 2008) or destabilization (Baudouin-Legros et al., 2005; Phelps et al., 2006) of their mRNA. A prior study has shown that HBEGF mRNA is stabilized in HeLa cells exposed to a chemotherapeutic agent (Sorensen et al., 2006). Because HBEGF transcript levels are not altered by O<sub>2</sub> fluctuation (Armant et al., 2006), we hypothesized that mRNA translation is a factor contributing to its regulation. There is evidence that microRNAs (miRNA) could directly or indirectly regulate protein expression by increasing translational rates (Baek et al., 2008; Selbach et al., 2008).

MicroRNAs are ~22 nt endogenous small RNA species that primarily target the 3' untranslated region (3'UTR) of mRNA transcripts, and are well known for their roles in suppressing translation or inducing degradation of mRNA (Kim and Nam, 2006; Pillai et al., 2007). DGCR8 is a gene within the "DiGeorge syndrome chromosomal region (DGCR)" at human chromosome 22q11 (Shiohama et al., 2003). DGCR8 combines with Drosha to form a stable microprocessor, or pri-miRNA processing complex (Gregory et al., 2004; Han et al., 2004; Landthaler et al., 2004). MicroRNAs are transcribed as primary miRNA transcripts in the nucleus by RNA polymerase II and are subsequently processed by the microprocessor into

shorter pre-miRNA hairpin precursors. The pre-miRNAs are exported into the cytoplasm and processed into their mature ~22 nt form by dicer (Bartel, 2004). Mature miRNAs are incorporated into RNA-induced silencing complexes (RISCs) or miRNPs (miRNA ribonucleoproteins) where miRNAs target mRNAs by binding with perfect complementarity to a conserved 6-8 nt seed region in the 3'UTR. MicroRNAs have the unique capacity to bind a specific target transcript and, due to imperfect base pairing at nucleotides 10-11, inhibit translation without inducing degradation of the mRNA (Bartel, 2004; Filipowicz et al., 2008; Pillai et al., 2007). A miRNA-mediated mechanism could be responsible for the translational regulation of HBEGF by O<sub>2</sub> concentrations.

Specific miRNAs are expressed in placental tissue (Barad et al., 2004; Maccani and Marsit, 2009; Mouillet et al., 2011) and trophoblast cells (Donker et al., 2007; Spruce et al., 2010). When introduced into carcinosarcoma cell cultures, miRNAs target functional proteins. Mir-152 targets HLA-G in JEG3 cells (Zhu et al., 2010), miR-34a targets Notch1 and Jagged1 in HeLa and JAR cells (Pang et al., 2010), and miR-199b targets SET (protein phosphatase 2A inhibitor) in BeWo and JAR cells (Chao et al., 2010). Donker et al. (Donker et al., 2007) demonstrated in primary trophoblast from term placenta that the miRNP machinery is present in cells cultured for 24-72 h at 20% or 2% O<sub>2</sub>, and silences MED1 (Mediator complex subunit 1) expression through differential regulation of miRNAs (Mouillet et al., 2010). Regulated expression of miRNAs that target HBEGF mRNA could likewise provide evidence that its translational regulation at 2% O<sub>2</sub> is mediated by miRNAs.

In this study we have tested whether the regulation of HBEGF protein is mediated through its turnover rate, or if other post-transcriptional mechanisms are operative. Specifically, we examined reporter expression under control of the 3'UTR of HBEGF, the role of differential miRNA expression in the trophoblast cells exposed to reduced O<sub>2</sub>, and the effect of global

miRNA silencing by DGCR8 knockdown. Our findings suggest a role for miRNA in the upregulation of HBEGF at 2% O<sub>2</sub> rather than its suppression at 20% O<sub>2</sub>. We suggest that the RISC becomes altered to enable translation from constitutively expressed HBEGF message downstream of HBEGF signaling at 2% O<sub>2</sub>.

## **Materials and Methods**

### ***Cell Culture and Treatments***

The first trimester human cytotrophoblast cell line HTR-8/SVneo (Graham et al., 1993) was cultured at either 20% O<sub>2</sub> or 2% O<sub>2</sub> as previously described (Leach et al., 2004; Leach et al., 2008). Cells were cultured for the indicated times in 10 µg/ml cyclohexamide to block *de novo* translation (Sigma-Aldrich), 1 µg/ml lactocystin or 100 µg/ml MG132 to inhibit the proteasome (EMD Biosciences). The HTR-8/SVneo cell line retains important characteristics of primary cultures of human first trimester cytotrophoblast cells (Kilburn et al., 2000), making it a suitable model for this study. This cell line expresses the TB specific marker KRT7. When grown on Matrigel, HTR-8/SVneo cells expresses another TB specific marker HLA-G, and expression of integrin alpha 1 is upregulated, while alpha 6 is downregulated. The expression of KRT7, β-hCG and HLA-G as well as lack of Vimentin is routinely checked and cells are maintained at passages 30-50.

### ***Western Blotting***

Western blots were performed as previously described (Kilburn et al., 2000). Cellular lysates were lysed in SDS sample buffer containing 5% β-mercaptoethanol, run on precast 4%-20% Tris-HCl gradient gels (BioRad), and transferred to nitrocellulose membranes. Monoclonal mouse antibodies against DGCR8 (Proteintech) and GAPDH (Ambion) were diluted in 5% milk dissolved in TTBS to 0.3 µg/ml and 1 µg/ml, respectively. A polyclonal antibody against HBEGF (R&D Systems) was diluted to 0.2 µg/ml in 5 mg/ml BSA in TTBS.

## ***ELISA***

The HBEGF DuoSet ELISA Development kit (R&D systems) was used, as previously described (Armant et al., 2006; Leach et al., 2008). The optical density of the final reaction product was determined at 450 nm, using a programmable multiplate spectrophotometer (Power Wave Workstation; Bio-Tek Instruments) with automatic wavelength correction.

## ***Generation of 3'UTR Luciferase Reporter Vectors***

Regions of the HBEGF 3'UTR were amplified by PCR. Restriction sites for XhoI and NotI were added to forward and reverse primers (IDT DNA), respectively. 3'UTR regions (Figure 14) amplified by the primers and the expected amplicon sizes are listed in Table 4. The PCR amplified 3'UTR regions were cloned into the psiCheck-2 vector (Promega), in which two luciferase genes (Firefly and Renilla) driven by separate promoters are present. HBEGF 3'UTR inserts were cloned into a region immediately following the Renilla luciferase gene, which serves as the reporter, while the Firefly luciferase gene is an internal control. After isolating RNA from trophoblast cells (miRNeasy, Qiagen), cDNA was generated using the Omniscript Reverse Transcription kit (Qiagen). HBEGF 3'UTR fragments were amplified by endpoint PCR, using HotstarTaq Plus Master Mix kit (Qiagen), according to the manufacturer's instructions. In a total reaction volume of 50  $\mu$ l, 0.5  $\mu$ M of each primer and 50 ng of cDNA were combined. PCR products were processed using Wizard SV Gel and PCR Clean-up Kit (Promega). Cleaned amplicons and the PsiCheck2 vector (1  $\mu$ g each) were digested with both XhoI and NotI restriction enzymes (Promega) for 1 h at 37°C in a thermal cycler, followed by a 15 min 70°C inactivation step. Amplified 3'UTR fragments and PsiCheck2 vector were combined and ligated, using Promega's LigaFast Rapid DNA Ligation System. To verify ligation, 1  $\mu$ l of ligated product was amplified by PCR, using primers that bind outside of the PsiCheck2 vector's multiple restriction site, as indicated in Table 4. The primers listed were used in various

combinations to target different regions of HBEGF 3'UTR.

**Table 4. Primer sequence for amplification of HBEGF 3'UTR and vector sequencing.**

Forward Primers	Sequence	Target Site on HBEGF mRNA
HBEGF 3'UTR	AAACTCGAGGGAGGTTATGATGTGGGAAAATGA	844
HBEGF 3'UTR	AAACTCGAGCCTTTGCCACAAAGCTAGGA	1644
HBEGF 3'UTR	AAACTCGAGTTGCCTAGGCGATTTTGTCT	1829
HBEGF 3'UTR	AAACTCGAGAACAGGGAACATTGGAGCTG	2137
PsiCheck-2 vector	AGGACGCTCCAGATGAAATG	
Reverse Primers	Sequence	Target Site on HBEGF mRNA
HBEGF 3'UTR	AAAGCGGCCCGCAGATCCCTTGGTGGTACT	1363
HBEGF 3'UTR	AAAGCGGCCCGCCAGGAAATTGCCAAAGTA	1603
HBEGF 3'UTR	AAAGCGGCCCGCCCAAGTTAACCCCTACATCCTG	1778
HBEGF 3'UTR	AAAGCGGCCCGCATGAACCAGGTTTGGAAATACA	2315
PsiCheck-2 vector	CAAACCCTAACCACCGCTTA	

### ***Bacterial Transformations***

One microliter of the ligation reaction mixture or empty PsiCheck2 vector was placed on ice, combined with 50  $\mu$ l of JM109 bacteria (Promega) and heat shocked. Bacteria were incubated on an LB Agar plate containing AMP-100, X-GAL-80, IPTG-50 (Teknova) overnight at 37°C. Colonies were grown and expanded in 3 ml of LB broth (Becton, Dickinson & Co.) containing 100  $\mu$ g/ml of Ampicillin. Bacterial lysates were prepared and amplified by PCR with primers in Table 1 to select colonies that displayed a correctly-sized insert. Vectors were isolated using the Wizard Plus SV Miniprep kits (Promega), and 100 ng were used for transfection reactions. Vectors were sequenced using the same primers utilized to verify ligation, and aligned to the HBEGF mRNA sequence (PUBMED sequence NM\_0001945.2) using Geneious (Kearse et al., 2012).

### ***Transfection and Luciferase Assay***

HTR-8/SVneo cells were grown to 75 % confluence and cultured for an additional 24 hr in 1 ml serum-free media (DMEM/F-12 with 5 mg/ml BSA) containing 3  $\mu$ l of FuGene-6 and 1

μl of vector (100 ng). The cells were lysed in 500 μl 1X passive lysis buffer (Promega). Lysates (20 μl) was used in each dual luciferase reaction, conducted according to the manufacturer's protocol (Dual Luciferase Reporter Kit, Promega). Negative controls containing untransfected cells were included. Each sample received 100 μl of LARII reagent, and was read after adding 100 μl Stop & Glo reagent (Promega) using a Veritas microplate luminometer (Turner Biosystems). Renilla measurements were normalized to Firefly measurements. Each transfection experiment was repeated at least 3 times.

### ***Library Preparation for NGS***

Trophoblast cells maintained at 20% O<sub>2</sub> were cultured at 2% O<sub>2</sub> for 0-4 hrs and RNA was collected. For RNA-seq, both long RNA and small RNA (sRNA) were isolated with the miRNeasy mini kit (Qiagen). The long RNA fraction was used for transcriptomic analysis in Chapter 2. The sRNA fraction was quantified and its purity assessed, using an Agilent 2100 Electrophoresis Microfluidics Analyzer. A sRNA digital gene expression library was constructed by converting RNA into an adapter-ligated cDNA library, using a ScriptSeq Miner (Epicentre) and following the manufacturer's protocol. Each cDNA sample was bar-coded and the resulting 12 cDNA libraries (3 replicates for each O<sub>2</sub> concentration) were combined for sequencing on Illumina's Genome Analyzer II sequencer at the Wayne State University Applied Genomics Technology Center.

### ***Sequencing Data analysis***

Demultiplexing was performed using configure BclToFastq.pl script (CASAVA-1.8.2; Illumina Inc.) with default parameters for quality and index identification. The sequencing data was aligned to the human genome build (HG19) and to the ribosomal sequences 18S and 28S using Genomatix mapping station (GMS). The GMS generated tsv.files were exported to the Genomatix genome analyzer and subjected to the miRNA expression analysis tool to identify

differentially expressed miRNAs.

### ***DGCR8 Knockdown***

HTR-8/SVneo cells were tested for toxicity due to NeoFX transfection reagent (Ambion), using the Multitox-Fluor Multiplex Cytotoxicity Assay Kit (Promega) to determine an optimal concentration for transfection, which was 0.75  $\mu$ l of NeoFX reagent per well in a 96-well plate, (<10% toxicity after 48 hrs). Cells were transfected in a 96-well plate (5,000 per well) for 48 hr with various concentrations of three siRNAs (s29061, s29062, s29063; Life Technologies) that target DGCR8. Controls included no transfection, treatment with transfection agent only, transfection with a negative control siRNA and a GAPDH siRNA. Cells were fixed with ice-cold methanol for 10 min, permeabilized with 0.1% Triton-X100 for 15 min, stained overnight with primary antibody against DGCR8 (Santa Cruz Biotechnology, Inc.) at 4°C, incubated for 1 hr at room temperature with an anti-mouse/anti-rabbit labeled polymer (DAKO EnVision Dual Link), and visualized with DAB. Based on preliminary experiments, 50 nM siRNA was chosen for DGCR8 knock down.

### ***qPCR***

RNA from HTR-8/SVneo cells was collected using the miRNeasy kit (Qiagen), according to the manufacturer's protocol. RNA concentration was determined using the NanoDrop spectrophotometer and purity was ascertained with a microfluidic Bioanalyzer (Agilent Technologies - 2100 Electrophoresis Bioanalyzer Instrument). RNA was used in subsequent qPCR (Bustin et al., 2009) analysis. Reverse transcription was performed using the Quantitect Reverse Transcription kit (Qiagen), and qPCR for HBEGF was conducted with the Quantitect SYBR Green PCR kit without UNG (Qiagen), in a final volume of 25  $\mu$ l. GAPDH was used as a housekeeping gene to normalize the data. Semi-quantitative analysis was performed according to the  $\Delta\Delta C_t$  method (Pfaffl, 2001). Primers for GAPDH and HBEGF were



obtained from Qiagen.

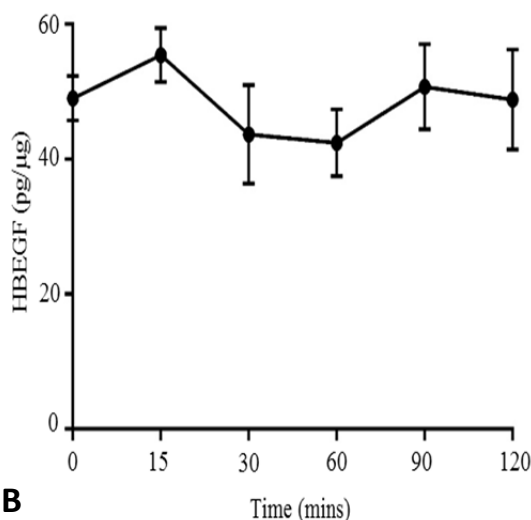
### ***Statistics***

All experiments were repeated at least 3 times and reported as mean  $\pm$  SEM. Statistical significance was determined at  $p < 0.05$  by ANOVA, Student-Newman-Keuls tests and Dunnett t-test using SPSS version 12.0 statistics software (SPSS).

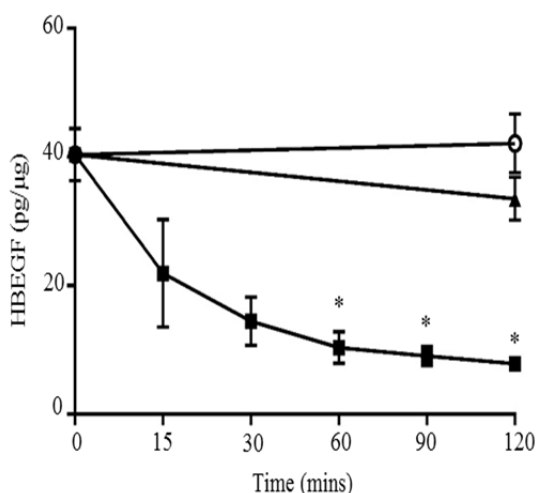
### **Results**

#### ***HBEGF regulation by protein degradation***

The observed increase in HBEGF protein levels at low O<sub>2</sub> could reflect a decrease in protein turnover rate at 2% O<sub>2</sub>. HBEGF protein levels were elevated by culture at 2% O<sub>2</sub> for 6 h and cultured for an additional 2 hours with cyclohexamide to arrest protein synthesis. HBEGF levels remained unchanged (Figure 13 A), indicating a very low turnover rate. In contrast, cells shifted to 20% O<sub>2</sub> after 6 h at 2% O<sub>2</sub> showed a marked destabilization of HBEGF protein, which declined significantly within 15 min (Figure 13 B). HBEGF degradation was abrogated if cells were concomitantly treated with the proteasome inhibitors MG132 or lactocystin after shifting cells to 20% O<sub>2</sub>, suggesting that HBEGF turnover requires the proteasome. However, HBEGF protein did not increase at 20% O<sub>2</sub> when cells were treated with proteasome inhibitors (data not shown), suggesting that stabilization of HBEGF degradation is insufficient for its accumulation at 20% O<sub>2</sub>, and that its accumulation at 2% O<sub>2</sub> requires activation of its translational from mRNA. These finding indicate that destabilization by proteolysis through the proteasome clears HBEGF during reoxygenation.

**A**

**Figure 13. Effect of O<sub>2</sub> concentration on HBEGF stability.** HTR8S/Vneo cells were cultured for 6 h at 2% O<sub>2</sub>, allowing HBEGF protein to accumulate. Afterwards, cells were (A) exposed to cyclohexamide for up to 2 h in the absence or (B) presence of either 1 μg/ml lactocystin (white circle) or 100 μg/ml MG132 (triangle). Cell lysates were collected at the indicated times and HBEGF protein levels quantified by ELISA. \*  $p < 0.05$  according to ANOVA and Student-Newman-Keuls t-tests.

**B**

### ***Regulation by the HBEGF 3'UTR***

The differential regulation of HBEGF synthesis by O<sub>2</sub> in human trophoblast cells could be the result of translational suppression at 20% O<sub>2</sub>, or activation of protein synthesis from its mRNA at 2% O<sub>2</sub> under the direction of its large (1455bp) 3'UTR, a region of mRNA known to be involved in transcript stability (Mignone et al., 2002). To determine whether the 3'UTR of HBEGF can control translation, a PsiCheck-2 luciferase reporter with 3' inserts of the entire HBEGF 3'UTR or its subdomains was prepared and transfected into trophoblast cells cultured at

20% O<sub>2</sub>. The presence of certain portions of the HBEGF 3'UTR altered Renilla Luciferase production, as compared to an empty vector control (Figure 14). A vector containing the full-length 3'UTR (844-2315) significantly ( $p=0.008$ ) repressed reporter activity, as did vectors containing the 5' subdomain (844-1778;  $p=0.031$ ) or 3' subdomain (1644-2315;  $p=0.019$ ). In contrast, the 134 bp region overlapped by the two larger domains did not regulate reporter activity. Vectors containing regions 844-1603, 1644-1778, and 1829-2315 were also not active. Vectors containing either the 5' (844-1363) or 3' (2137-2315) flanking regions of the 3'UTR upregulated Renilla luciferase activity at both 20% O<sub>2</sub> and 2% O<sub>2</sub> ( $p<0.001$  for both). The vectors containing the two flanking regions more significantly upregulated reporter at 20% O<sub>2</sub> as compared to 2% O<sub>2</sub> (t-test,  $p=0.022$  and  $p<0.001$ , respectively). Based on these

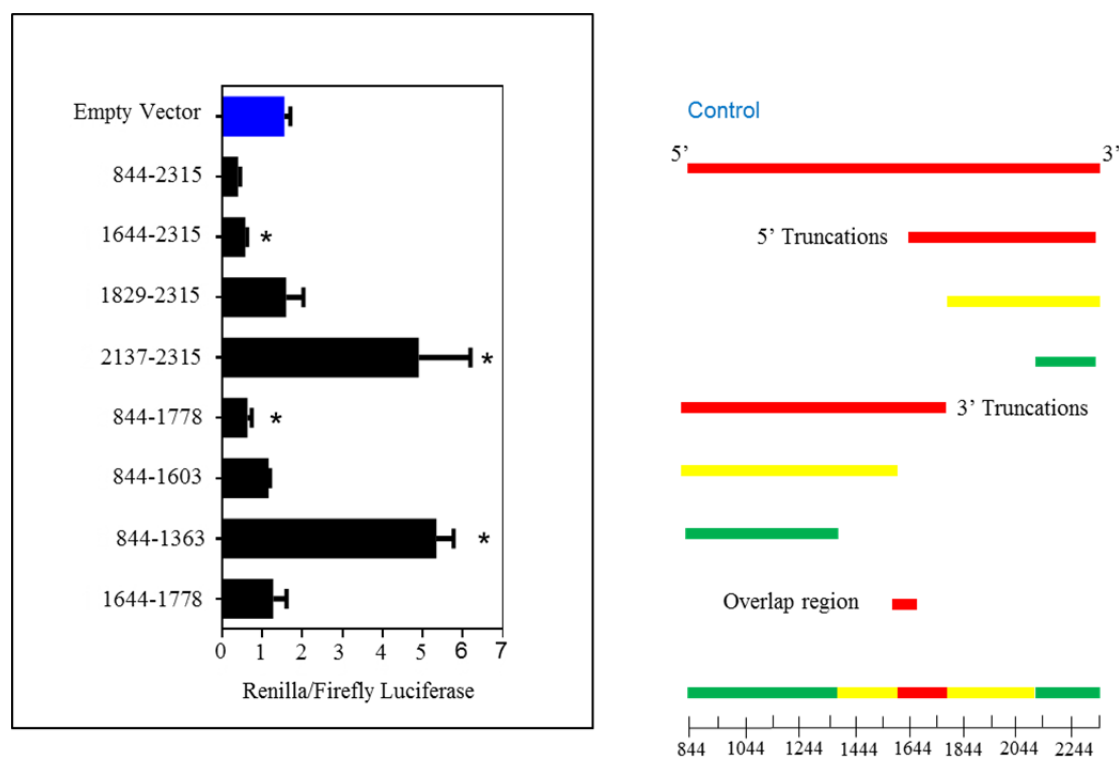


**Figure 14. Translational regulation by HBEGF 3'UTR.** Dual luciferase assays used constructs containing the indicated sequences of the HBEGF mRNA inserted 3' to Renilla luciferase. The left panel shows activities of the Renilla luciferase normalized to a constitutive firefly luciferase. N=3. \*,  $p<0.05$  vs empty vector control (blue bar), ANOVA with Dunnett t-test. Right panel shows the locations of the inserts in colors indicating their effect on translation; yellow, neutral; red, suppression; green, activation. A scale in base pairs is shown below.

observations, it appears that the two flanking domains of the 3'UTR increase translational activity in isolation from the central 3'UTR regions, while the presence of regions from 1363bp-1644bp and 1778bp-1829bp instigated translational suppression. These data are consistent with two opposing activities within the 3'UTR that respectively activate and suppress translation from the HBEGF transcript.

#### *Next generation sequencing to identify differentially expressed miRNAs*

To determine if HBEGF translation is regulated in response to O<sub>2</sub> by differentially expressed miRNAs that interact with its 3'UTR, expression of miRNAs was examined globally by NGS. Trophoblast cells cultured at 20% O<sub>2</sub> were exposed to 2% O<sub>2</sub> for 0, 1, 2 and 4 h, and

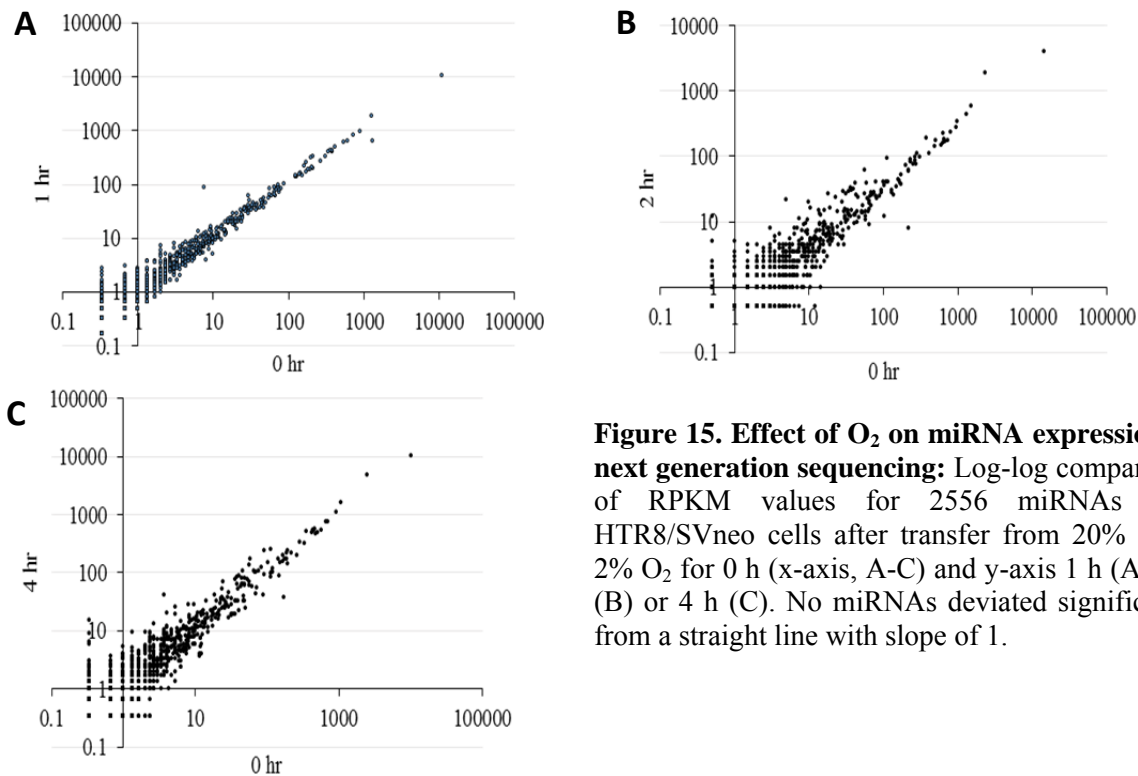


**Figure 15. Effect of O<sub>2</sub> on miRNA expression by next generation sequencing:** Log-log comparisons of RPKM values for 2556 miRNAs in HTR8/SVneo cells after transfer from 20% O<sub>2</sub> to 2% O<sub>2</sub> for 0 h (x-axis, A-C) and y-axis 1 h (A), 2 h (B) or 4 h (C). No miRNAs deviated significantly from a straight line with slope of 1.

barcoded libraries were constructed for NGS. The software analyzed a total of 2556 miRNAs based on the HG19. A log-log plot of RPKM values comparing 0 h to later time points (Figure 15), and statistical analysis by the Genomatix genome analyzer software, revealed that no

miRNAs were differentially expressed. These findings suggest that if a mechanism involving miRNAs regulates HBEGF translation, it does not do so through changes in the expression of the miRNAs.

### ***Global inhibition of miRNA processing***

We further examined the potential role of miRNA in regulating HBEGF, using siRNA to silence DGCR8, which should globally suppress miRNA processing and deplete all miRNA (Landthaler et al., 2004). DGCR8 was knocked down in HTR-8/SVneo cells by transfection for 48 h with siRNA. Controls included no transfection, treatment with transfection reagents only, and transfection with either a negative control siRNA or a GAPDH siRNA. Culture was either continued for 4 h at either 20% O<sub>2</sub>, or shifted to 2% O<sub>2</sub>. Western blots for DGCR8 and toxicity assays were used to optimize conditions for knockdown (Figure 16A, B). DGCR8 was greatly reduced in cells transfected with 50 nM of the targeting siRNA, but not in control treatments. Unexpectedly, HBEGF expression did not increase when DGCR8 was knocked down at 20% O<sub>2</sub> (Figure 16C), suggesting that HBEGF expression was not repressed by miRNA at high O<sub>2</sub>. Repression of translation by miRNA often occurs through degradation of message (Wilczynska and Bushell, 2015). However, HBEGF mRNA was unchanged after DGCR8 knockdown and unaffected by O<sub>2</sub> concentration (Table 5). Surprisingly, the upregulation of HBEGF at 2% O<sub>2</sub> was inhibited in the DGCR8 knockdown compared to controls (Figure 16D). These results were verified by ELISA to quantify HBEGF, which demonstrated levels near 0.01 pg/μg in all treatments at 20% O<sub>2</sub> (Figure 16E). At 2% O<sub>2</sub>, HBEGF levels rose to 5 pg/μg (range 4.2-6.4) in all controls, while cells transfected with 50 nM DGCR8 siRNA contained only 0.88 ± 0.22 pg/μg HBEGF (Figure 16F). These findings indicate that HBEGF expression was not repressed by miRNA at high O<sub>2</sub>, and further suggest that miRNA is required for increased translation of HBEGF at 2% O<sub>2</sub>.

**Table 5. HBEGF mRNA in HTR-8/SVneo cells with or without (Control) exposure to DGCR8 siRNA measured by qPCR\***

20% O <sub>2</sub>		2% O <sub>2</sub>	
Control	DGCR8 siRNA 50nM	Control	DGCR8 siRNA 50nM
1.3 ± 0.26	0.92 ± 0.27	1.07 ± 0.30	1.39 ± 0.39

\*Relative expression of HBEGF mRNA normalized to GAPDH mRNA. Mean ± SE, n = 3.

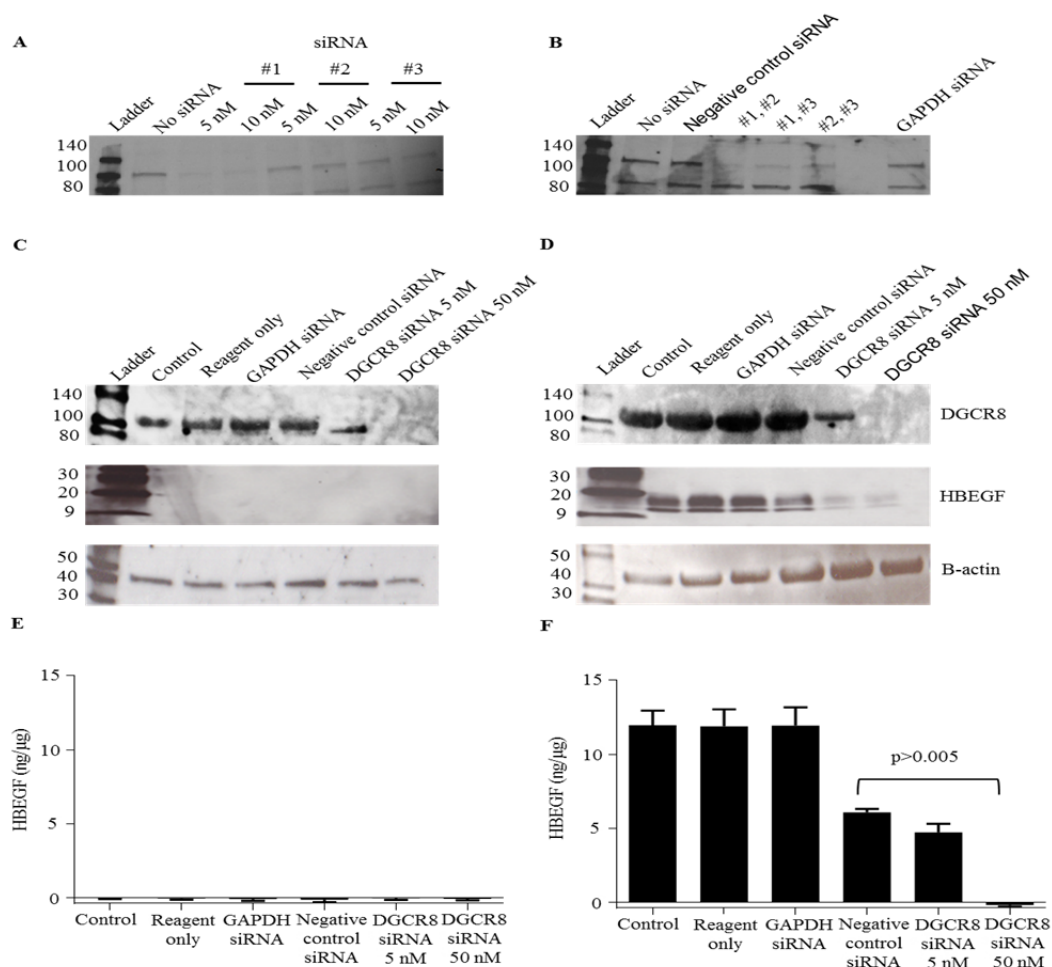


**Figure 16. Effect of DGCR8 Knockdown on regulation of HBEGF by O<sub>2</sub>.** Western blots of DGCR8 in lysates of HTR-8/SVneo cells treated for 48 hr with (A) 5 nM or 10 nM of three different DGCR8 siRNA and (B) different pairings of the three siRNA (5nM). C-F. DGCR8 (~120kDa), HBEGF (~22kDa) and β-actin (~45kDa) were assessed in lysates of HTR-8/SVneo cells (control), cells treated with transfection reagent only, or cells transfected with GAPDH siRNA, 50 nM negative control siRNA, and 5 nM and 50 nM DGCR8 siRNA. After 48 hrs, culture was continued for 4 hrs at 20% O<sub>2</sub> (C, E) or 2% O<sub>2</sub> (D, F). Lysates were assayed by western blot (C, D) or an ELISA for HBEGF (E, F). Untreated trophoblast cells and trophoblast cells containing transfection reagent alone served as Control. \*, p<0.005, compared to Control.

## Discussion

The present study demonstrates the complexity of HBEGF upregulation, and suggests the

potential role of miRNAs. Blocking HBEGF degradation with proteasome inhibitors failed to instigate accumulation of HBEGF in trophoblast cells cultured at 20% O<sub>2</sub>, suggesting that the upregulation of HBEGF at low O<sub>2</sub> is not due solely to decreased HBEGF turnover, but requires increased translation of abundant HBEGF mRNA. HBEGF turnover was indeed strikingly faster at 20% than at 2% O<sub>2</sub>, which could facilitate clearance of the protein during reoxygenation.

Given the lack of transcriptional regulation (Armant et al., 2006), it was hypothesized that HBEGF could be regulated translationally by its large (1461 bp) 3'UTR. Luciferase reporters have been used to assess translational regulation by 3'UTRs (Pang et al., 2009) and provided evidence here that cloned regions of the HBEGF 3'UTR regulate its translation with domain-specific stimulatory or inhibitory activities. Others have examined translational suppression by miRNA with cloned 3'UTR regions by transfecting with an additional vector that contains target miRNA in HEK293 cells (Jiao et al., 2010) and HTR-8/SVneo cells (Mouillet et al., 2010). The methodology that we chose is advantageous because it more closely recapitulates *in vivo* conditions by relying upon endogenous miRNA and translational machinery. Although there was no effect of changing O<sub>2</sub> concentrations, the flanking regions of the 3'UTR (844-1363 and 2317-2315) strongly upregulated luciferase activity, suggesting that these domains could have a role in elevating HBEGF translation at 2% O<sub>2</sub>. In contrast, regions towards the center of the 3'UTR (1363-1603 and 1778-2315) repressed luciferase production, and are likely responsible for the overall repressive effect of the complete 3'UTR sequence. Luciferase assays showed that discrete regions of the 3'UTR are sufficient to differentially regulate HBEGF.

An unbiased NGS approach failed to find miRNAs that are differentially expressed at 20% and 2% O<sub>2</sub>. Therefore, HBEGF was apparently not regulated by changes in the levels of miRNAs that interact with its transcript, but other components of the RISC interacting with miRNAs could be involved. The requirement for miRNA was further examined by blocking

miRNA synthesis in a DGCR8 knockdown experiment, realizing that it could interfere with other unrelated critical cellular processes. Suh et al used Dgcr8 knockout mice to distinguish the effects of miRNA and endogenous siRNA during oocyte maturation and preimplantation development, comparing the effects on development and mRNA expression to oocytes and embryos deficient in Dicer (Suh et al., 2010). During treatment with DGCR8 siRNA, the low expression of HBEGF at 20% O<sub>2</sub> persisted. However, HBEGF protein failed to increase at 2% O<sub>2</sub>, suggesting that miRNA is linked to increased HBEGF translation in either a positive or indirect manner at 2% O<sub>2</sub> rather than through suppression at 20% O<sub>2</sub>. This is consistent with the observation that HBEGF mRNA expression was unchanged by DGCR8 knockdown at either O<sub>2</sub> concentration. Hence, miRNA could be responsible for facilitating the upregulation of HBEGF through changes in other components of the RISC at low O<sub>2</sub> that increase the influence of the flanking regions of the 3'UTR (844-1363 and 2137-2315), or reduce the influence of the repressive central domains. The regulatory activity of the RISC can be affected by structural changes in the 3'UTR, such as shortening. For example, 3' UTR shortening can occur due to cleavage of the alternative poly(A) sites on the 3'UTR of mRNA, and this can lead to changes in protein translation efficiency, mRNA stability, or mRNA localization (Fabian et al., 2010). To see if this structural change was present in HBEGF 3'UTR, we examined the RNAseq data obtained in Chapter 2. However, due to low sequencing depth we found no clear evidence of HBEGF 3'UTR shortening.

Alternatively, miRNAs or other regulatory factors that bind regions outside the 3'UTR (for example, to the 5'UTR) could accelerate translation of HBEGF at 2% O<sub>2</sub>. There is evidence that miR-10a binds to the 5'oligopyrimidine tract motif in the 5'UTR of ribosomal proteins in neural U87 cells and mediates translational upregulation (Orom et al., 2008). MiR-122 targets the 5'non-coding region of the hepatitis C viral genome to positively regulate accumulation of



viral RNA (Jopling et al., 2005) through requisite occupation of two miR-122 binding sites in hepatic cells (Jopling et al., 2008). Hence, miRNA or other regulatory factors that bind regions outside the 3'UTR could integrate with regions in the 3'UTR to induce translation at 2% O<sub>2</sub>.

In the absence of a change in miRNA profile, HBEGF translation could be controlled by other components of the RISC, including regulatory proteins activated downstream of MAPK signaling, which is required for HBEGF upregulation at 2% O<sub>2</sub> (Jessmon et al., 2010). Iwasaki et al. found that loading of sRNA duplexes into the RISC complex requires HSP70/HSP90 chaperones activity (Iwasaki et al., 2010). We find in trophoblast cells that HSP70 transcription is induced at low O<sub>2</sub> (Jain et al., unpublished). Alternatively, there is evidence that the stability of argonaute 2 (AGO2) in the RISC is enhanced by EGFR/ERBB1 through MAPK signaling in cancer cell line MDA-MB-231 (Adams et al., 2009). EGFR induces phosphorylation of Y393 in AGO2 to inhibit miRNA maturation, leading to tumor cell survival (Shen et al., 2013). Using mass spectrometry, multiple phosphorylation sites have been identified in AGO2 from HEK293 cells (Rudel et al., 2011). Phosphorylation of Y529 in the RNA-binding pocket results in inefficient binding of sRNA to the protein, suggesting a mechanism for the alternate binding and release of miRNAs. Additionally, studies in Hela cells demonstrate that phosphorylation of AGO2 by AKT serine/threonine kinase 3 (AKT3) and MK2 at S387 upregulates miRNA-mediated translational repression of endogenous miRNA targets (Horman et al., 2013). Some RNAs can displace miRNAs from their target mRNAs. An example is competing endogenous RNA (ceRNA) (Salmena et al., 2011) or the recently described circular RNA (circRNA) (Hentze and Preiss, 2013), where the RNAs not only manifest themselves in the sequestration of miRNAs, but also act through the direct or indirect binding of RNA-binding proteins.

Genes other than HBEGF are also translationally regulated by O<sub>2</sub>. For example, low O<sub>2</sub> increases ATF4 protein, but doesn't affect its mRNA, in hippocampal neurons (Yukawa et al.,

1999). In addition, chemically-induced endoplasmic reticulum (ER) stress, comparable to effect of low O<sub>2</sub>, shifts ATF4 mRNA from monoribosomes to polyribosomes, indicating that its preexistent mRNA pool is inefficiently translated until cells experience ER stress. This shift to polyribosomes was dependent on the presence of ER-resident eIF2alpha kinase/PERK, suggesting that eukaryotic initiation factor 2A (EIF2A) is phosphorylated prior to translation of ATF4 (Koumenis et al., 2002).

Additional studies are necessary to fully understand the mechanism controlling HBEGF autocrine upregulation. We have presented evidence that the RISC is a key site of regulation; therefore, proteomic analysis of the RISC could identify components that are altered in response to HBEGF downstream signaling. Future studies involving Chip Seq (Park, 2009) could help to elucidate the role of RISC and its components in controlling the HBEGF autocrine loop. Alternatively, motif-binding prediction tools such as Scansite (Obenauer et al., 2003) would help to elucidate the interaction of other molecules with the HEGF 3'UTR that could play a critical role in HBEGF upregulation. The significance of this mechanism *in vivo* is unclear, because this investigation was conducted in a trophoblast cell line. However, we have found that HBEGF is indeed upregulated at low O<sub>2</sub> in villous explants (Chapter 2, Figure 12). The development of an animal model to experimentally investigate the proposed mechanism would be useful to clarify understanding of HBEGF regulation by O<sub>2</sub> *in vivo*.

The present study demonstrates that HBEGF is post-transcriptionally regulated by O<sub>2</sub> through a mechanism involving interactions of miRNAs with its 3'UTR. Luciferase assays identified discrete regions of the 3'UTR that differentially regulate HBEGF translation. A role for miRNA was suggested by knocking down the miRNA-processing protein, DGCR8. Although no differentially expressed miRNAs were found, it can be speculated that miRNAs are required for translation of HBEGF, but not for its repression at low O<sub>2</sub>. The regulation of

HBEGF through a targeted mechanism that increases its translation rate, putatively involving miRNA and the RISC, appears to be uncommon based on a paucity of similar reports in the literature. The elucidation of this complex regulatory mechanism could provide important insights into trophoblast survival during early placentation, and its disruption in pregnancies with developmental pathologies.

## CHAPTER 4 - FETAL GENOME PROFILING AT FIVE WEEKS OF GESTATION AFTER NONINVASIVE ISOLATION OF TROPHOBLAST CELLS FROM THE ENDOCERVICAL CANAL

### Abstract

Single gene mutations account for over 6000 diseases, 10% of all pediatric hospital admissions, and 20% of infant deaths. Down syndrome and other aneuploidies occur in over 0.2% of births worldwide and are on the rise due to advanced reproductive age. Birth defects of genetic origin can be diagnosed *in utero* after invasive extraction of fetal tissues, while noninvasive testing with circulating cell-free fetal DNA is limited by a low fetal DNA fraction. Both modalities are unavailable until the end of the first trimester. We have isolated intact trophoblast cells from Papanicolaou smears collected non-invasively at 5-19 weeks of gestation for next-generation sequencing of fetal DNA. Matched maternal, placental and fetal samples (n=20), were profiled by multiplex targeted DNA sequencing of 59 short tandem repeat and 94 single nucleotide polymorphism sites across all 24 chromosomes. The data revealed a fetal DNA fractions of 85-99.9% with 100% correct fetal haplotyping. This noninvasive platform is capable of providing comprehensive fetal genomic profiling as early as 5 weeks of gestation.

### Introduction

Current models for studying placental biology include *ex vivo* models like explant culture (Genbacev et al., 1992) and *in vivo* models involving cell lines (Orendi et al., 2011). Although these models mimic the physiology of trophoblast cells, yet they are a mixed population of cells. Based on the research over decades, the current notion is that the disruption of function of extra-villous trophoblast (EVT) cells leads to placental insufficiency and the root cause lying in the first trimester of pregnancy. Both the *ex vivo* and *in vivo* models not only fail to represent a pure EVT population but are only based end point analysis. Therefore, there is a need of a platform to assess the EVT cells in ongoing pregnancies to better understand their pathophysiology and their

role in the progression of disease. Trophoblast retrieval and isolation from the cervix (TRIC) is an innovative and transformative technology to safely assess these cells (Bolnick et al., 2014). Fetal cells isolated by TRIC can provide the conceptual foundation to develop a reliable approach for interrogation of the pathophysiological status of pregnancy *in vivo* that will enhance research on the human placenta, and the ability to diagnosis perinatal disease. Although it appears that cells obtained by TRIC are indeed of fetal origin based on lineage marker expression and Y chromosome detection by fluorescent in situ hybridization (FISH) when a male fetus is present (Bolnick et al., 2014), we rigorously tested this assumption by comparing the genotypes of maternal-fetal cell pairs from twenty pregnancies examined by TRIC in the study presented here.

Prenatal testing for genetic disorders is currently performed invasively with a limited, but definite, risk using amniocentesis (earliest at 12 weeks) or chorionic villous sampling (CVS) (earliest at 9 weeks) (Mujezinovic and Alfirevic, 2007; Wapner, 2005). In addition, preimplantation genetic screening is available as an adjunct to *in vitro* fertilization (Sermon et al., 2004). In the past five decades, tremendous efforts have been made to develop reliable, noninvasive, early and safe prenatal testing techniques, using intact fetal erythrocytes, cell-free fetal DNA, and endocervical fetal cells (Chitty and Bianchi, 2013; Gil et al., 2015; Rodeck et al., 1995). These approaches have identified chromosomal abnormalities, sex-linked diseases, and RHD genotype in fetuses. In addition, prenatal screening of cell-free fetal DNA in maternal blood (earliest at 8 weeks) has been implemented clinically with some restrictions. The technology relies on fetal DNA fragments that accumulate and rapidly turn over in maternal blood, with analysis by massively parallel sequencing to distinguish fetal from maternal haplotypes (Gil et al., 2015; Wapner, 2005; Wong and Lo, 2016). However, the small fetal

fraction (4-10% at 10 weeks of gestation) and fragmentation of degrading DNA (146 bp) in the circulation limit its reliability for probing a broad range of significant genetic anomalies (Wang et al., 2013; Wong and Lo, 2016). The fetal fraction of DNA rises steadily with gestational age, but must exceed 4% for accurate and reliable assessment of specific trisomies (Wang et al., 2013). It is particularly challenging with a low fetal fraction to detect a fetal haplotype that is over-represented in the maternal fraction of DNA, such as a male fetus at risk for an X-linked disorder (Wong and Lo, 2016). Digital polymerase chain reaction (PCR) assays can detect autosomal recessive sickle cell anemia (Barrett et al., 2012) and X-linked hemophilia (Tsui et al., 2011), but rely on exact quantification of the fetal fraction, which can be problematic in the first trimester due to the overwhelming amount of co-purifying maternal DNA. The American College of Obstetricians and Gynecologists recommends that positive cell-free DNA results should be verified by the invasive tests, CVS and amniocentesis, which are considered diagnostic (2015).

A simple, reliable, and safe approach to fully interrogate the intact fetal genome early in the first trimester of pregnancy at single nucleotide resolution currently does not exist. To address and close this gap, we developed a straightforward alternative that uses a Papanicolaou (Pap) smear to capture intact fetal cells in numbers sufficient for next generation sequencing as early as 5 weeks of gestation. Fetal cells with a placenta (trophoblast) -like cellular phenotype are naturally shed from the conceptus into the reproductive tract by a poorly understood mechanism (Adinolfi and Sherlock, 1997; Imudia et al., 2010; Shettles, 1971). Until now their presence offered little benefit for noninvasive testing due to low cell recovery, and a 2000-fold excess of maternal cells and DNA in endocervical specimens (Imudia et al., 2009). We first reported that fetal cells can be purified to near homogeneity by TRIC (average 99%), using Pap

smears safely collected during early pregnancy with a nylon cytobrush from the lower segment of the endocervical canal (Bolnick et al., 2014). Importantly, in contrast to cell free fetal DNA (Wang et al., 2013), we showed that provision of fetal cells by TRIC is unaffected by gestational age between 5 and 20 weeks of gestation, or by maternal obesity (Fritz et al., 2015b), thus providing a robust source of fetal DNA during a period of pregnancy when it is most useful clinically.

Here, we report the development of a DNA isolation and genotyping protocol that provides a high fetal fraction from cervical fetal cells obtained by TRIC during ongoing pregnancies at 5-19 weeks of gestation (Figure 16). Fetal DNA was assessed in twenty specimens using multiplex targeted sequencing to distinguish it from maternal DNA, based on profiling of 153 short tandem repeat (STR) and single nucleotide polymorphism (SNP) sites across the entire genome.

## **Materials and Methods**

### ***Patient selection***

The institutional review board of Wayne State University approved this study, and each participating patient provided informed written consent. Pregnant women between 5-19 weeks of gestation and undergoing pregnancy termination were recruited. The patients were counseled for collection of endocervical specimens and placenta at the Safe and Sound for Women Clinic in Las Vegas, NV and the Northland Family Planning Centers of Michigan.

### ***Isolation of endocervical fetal trophoblast cells***

Endocervical sampling was performed as described previously (Imudia et al., 2009). Endocervical cells were immediately fixed post the Pap smear procedure, using a ThinPrep kit (Hologic, Marlborough, MA) to preserve cells, proteins, and nucleic acids. Trophoblast cells

were isolated from each specimen using TRIC (Bolnick et al., 2014). Briefly, cells were centrifuged and re-suspended in 10 mL phosphate buffered saline (PBS), washing them three times. After a final resuspension in 1.5 mL PBS, anti-HLA-G-coated magnetic nanoparticles were added and incubated overnight at 4°C with mixing. The non-bound (maternal) cells were collected after magnetic immobilization of HLA-G-positive cells, which were recovered after three washings in PBS. The HLA-G-positive (fetal) cells were assessed by immunofluorescence microscopy for expression of  $\beta$ -hCG, and the percentage of labeled cells was determined.

#### ***Fluorescence in situ hybridization (FISH)***

Isolated fetal cells were mounted on slides and probed for X and Y chromosomes by FISH at the Detroit Medical Center Cytogenetics Laboratory, using the DYZ1 satellite III on the Y chromosome, and the DXZ1 alpha satellite on the X chromosome as fluorescently-labeled probes (Abbott Molecular). Nuclei were counterstained with DAPI and scored for each chromosome to quantify cells that were XX or XY.

#### ***Targeted sequencing***

DNA was obtained from fetal and maternal cells isolated by TRIC and tissue from the corresponding placenta. Targeted sequencing was performed using pregnancies with both male and female fetuses (N=20).

#### ***Nuclear isolation and DNA extraction***

Targeted sequencing was performed for 94 SNPs and 56 STRs listed in Table 6 after digestion of exogenous DNA. Fetal and maternal cells obtained by TRIC were dropped on slides and allowed to dry. Prior to DNA extraction, the slides were immersed in pepsin solution (0.01g in 100 ml 0.1N HCl) for 11 mins, followed by a PBS wash for 5 mins to remove cell membranes and contaminating maternal DNA fragments. Exogenous or circulating DNA was further



eliminated from the glass-bound nuclei by adding 10  $\mu$ L of washed, immobilized DNase (DNase I, immobilized on matrix F7M, MoBiTec, Goettingen, Germany) onto the pepsin-treated slides,

**Table 6: List of SNP's and STR's targeted by FORENSEQ.**

Sr.No	SNP name	Sr.No	SNP name	Sr.No	STR name	Sr.No	STR name
01	rs1490413	48	rs1498553	01	D1S1656	48	DYS438
02	rs560681	49	rs901398	02	TPOX	49	DYS612
03	rs1294331	50	rs10488710	03	D2S441	50	DYS390
04	rs10495407	51	rs2076848	04	D2S1338	51	DYS643
05	rs891700	52	rs2107612	05	D3S1358	52	DYS533
06	rs1413212	53	rs2269355	06	D4S2408	53	Y- GATA- H4
07	rs876724	54	rs2920816	07	FGA	54	DYS385a-b
08	rs1109037	55	rs2111980	08	D5S818	55	DYS460
09	rs993934	56	rs10773760	09	CSF1PO	56	DYS549
10	rs12997453	57	rs1335873	10	D6S1043	57	DYS392
11	rs907100	58	rs1886510	11	D7S820	58	DYS448
12	rs1357617	59	rs1058083	12	D8S1179	59	DYF387S1
13	rs4364205	60	rs354439	13	D9S1122		
14	rs2399332	61	rs1454361	14	D10S1248		
15	rs1355366	62	rs722290	15	TH01		
16	rs6444724	63	rs873196	16	vWA		
17	rs2046361	64	rs4530059	17	D12S391		
18	rs279844	65	rs1821380	18	D13S317		
19	rs6811238	66	rs8037429	19	PentaE		
20	rs1979255	67	rs1528460	20	D16S539		
21	rs717302	68	rs729172	21	D17S1301		
22	rs159606	69	rs2342747	22	D18S51		
23	rs13182883	70	rs430046	23	D19S433		
24	rs251934	71	rs1382387	24	D20S482		
25	rs338882	72	rs9905977	25	D21S11		
26	rs13218440	73	rs740910	26	PentaD		
27	rs1336071	74	rs938283	27	D22S1045		
28	rs214955	75	rs8078417	28	DXS10135		
29	rs727811	76	rs1493232	29	DXS8378		
30	rs6955448	77	rs9951171	30	AMELX		
31	rs917118	78	rs1736442	31	DXS7132		
32	rs321198	79	rs1024116	32	DXS10074		
33	rs737681	80	rs719366	33	DXS10103		
34	rs763869	81	rs576261	34	HPRTB		
35	rs10092491	82	rs1031825	35	DXS7423		
36	rs2056277	83	rs445251	36	DYS505		
37	rs4606077	84	rs1005533	37	DYS570		
38	rs1015250	85	rs1523537	38	DYS576		
39	rs7041158	86	rs722098	39	DYS522		
40	rs1463729	87	rs2830795	40	DYS481		
41	rs1360288	88	rs2831700	41	DYS19		
42	rs10776839	89	rs914165	42	DYS391		
43	rs826472	90	rs221956	43	DYS635		
44	rs735155	91	rs733164	44	DYS437		
45	rs3780962	92	rs987640	45	DYS439		
46	rs740598	93	rs2040411	46	DYS389I		
47	rs964681	94	rs1028528	47	DYS389II		

and incubating for 3-5 mins at room temperature. The slides were washed with PBS to remove the beads and terminate DNA digestion. The nuclei were lysed by incubation overnight at 65°C with 0.5  $\mu$ L/cell of Arcturus PicoPure DNA lysis buffer (Applied Biosystems), and then inactivated at 95°C for 30 min.

Placental villi (20-25 mg) were dissected and suspended in 100  $\mu$ L PBS. Ten  $\mu$ L of immobilized DNase was added and shaken for 10 min at room temperature to ensure efficient extracellular maternal and fetal DNA digestion. DNase beads were removed by washing in PBS. DNA was extracted from the tissue, using the Qiagen DNeasy Blood & Tissue Kit.

All DNA was purified using the Qiagen MinElute PCR purification kit, eluted in a final volume of 20  $\mu$ L, and quantified using the PicoGreen assay.

#### ***Library preparation for ForenSeq***

DNA libraries were prepared with the ForenSeq DNA Signature Prep Kit (Illumina), using primer mix A, as instructed by the manufacturer. Individual samples were quantified by Qubit, and analyzed using Agilent high-sensitivity DNA chips prior to library normalization. The percentage of libraries between 200-1000 bp was calculated based on the library traces, and was mixed accordingly at the genomic core facility at the University of Illinois. A pool size of 200bp-1 kb was selected, and the size-selected negative controls were mixed into the pool. The samples were sequenced on a MiSeq FGX system including positive and negative controls (Illumina).

#### ***ForenSeq data analysis***

ForenSeq with primer mix A analyzes 94 SNP loci and 59 STR loci on all human chromosomes (Figure 17c, Table 6). The ForenSeq Universal Analysis software provides a run quality report and detailed genotype. From this report, data was extracted and allele percentages

determined, using the read depth of each STR or SNP. For STR data, the two dominant alleles with highest relative peaks were used for further analysis.

To determine the purity of fetal DNA, the level of contamination with maternal DNA was calculated from the SNP data. For each sample triad (fetal, maternal, placental), the homo- or heterozygosity of each SNP was determined, first in the placenta, then comparing to fetal, and the percentage deviation of the fetal DNA was calculated. Deviations from homo- or heterozygosity were also calculated in the SNP profile of maternal DNA to determine a threshold of technical and/or biological variation. Maternal and placental SNP profiles were then compared, and the non-informative SNPs (i.e., identical maternal and placental alleles) were filtered out. For the informative SNPs, the deviations obtained from the maternal sample were subtracted from the fetal sample and multiplied by two (to account for two maternal alleles contributing to the fetal sample), yielding the percentage of maternal contamination.

To investigate whether the fetal genotype could be accurately determined in the absence of reference DNA, autosomal STR's were used. The dominant alleles with highest relative peaks were summed, to establish the median and range, which discriminated the pure (<15% contamination) from impure samples. Pure samples had median STR alleles >85%, while impure samples had median STR alleles <80%. To establish a cutoff for discriminating pure from impure samples, 82.5% was chosen. The determined threshold for autosomal STR alleles then provided 100% correct calls for the fetal haplotype.

For SNP analysis, a threshold of 10% allowed a maximal maternal contamination of approximately 20%. Therefore, a homozygous SNP was only analyzed in fetal samples when the variant allele represented either 0-10% or 90-100% of the read depth, while heterozygous SNPs were only analyzed when the variant allele read depth was between 40 and 60%.

## Results

### *Isolation and characterization of fetal cells*

Using TRIC (Bolnick et al., 2014), maternal and fetal cells were isolated from endocervical specimens (n=20), as illustrated in Figure 17a, at gestational ages ranging from 5 to 19 weeks ( $8.3 \pm 3.6$  weeks; Table 7). Matched maternal cells, and placental tissues were used as references for analysis. An average of 282 trophoblast cells (range, 170-410) were separated from maternal cells that were in excess of 200,000 cells. Purity of fetal cells was assessed by staining for expression of the trophoblast-specific protein, human chorionic gonadotropin  $\beta$  subunit ( $\beta$ -hCG). On average, 89.2% ( $\pm 5.0\%$ ) of the isolated fetal cells stained positive for  $\beta$ -hCG, which was completely absent in maternal cells (Table 7, Figure 17a, lower panel). The gender of the isolated cells was determined by fluorescence *in situ* hybridization (FISH) for the X and Y chromosomes. In pregnancies with a male fetus, the fetal cells showed positive probe binding for both X and Y chromosomes, as expected, while the maternal cells were positive only for the X chromosome (Figure 17a, lower panel). Fetal and maternal DNA was obtained from 234 ( $\pm 75$ ) and 335 ( $\pm 104$ ) cells, respectively, using endocervical specimens (n=20) and small pieces of placental tissue. (Table 7). For fetal cells, nuclear isolation combined with DNase treatment after TRIC (Figure 17, Material and Methods) was necessary to ensure high quality fetal DNA samples (Figure 18).

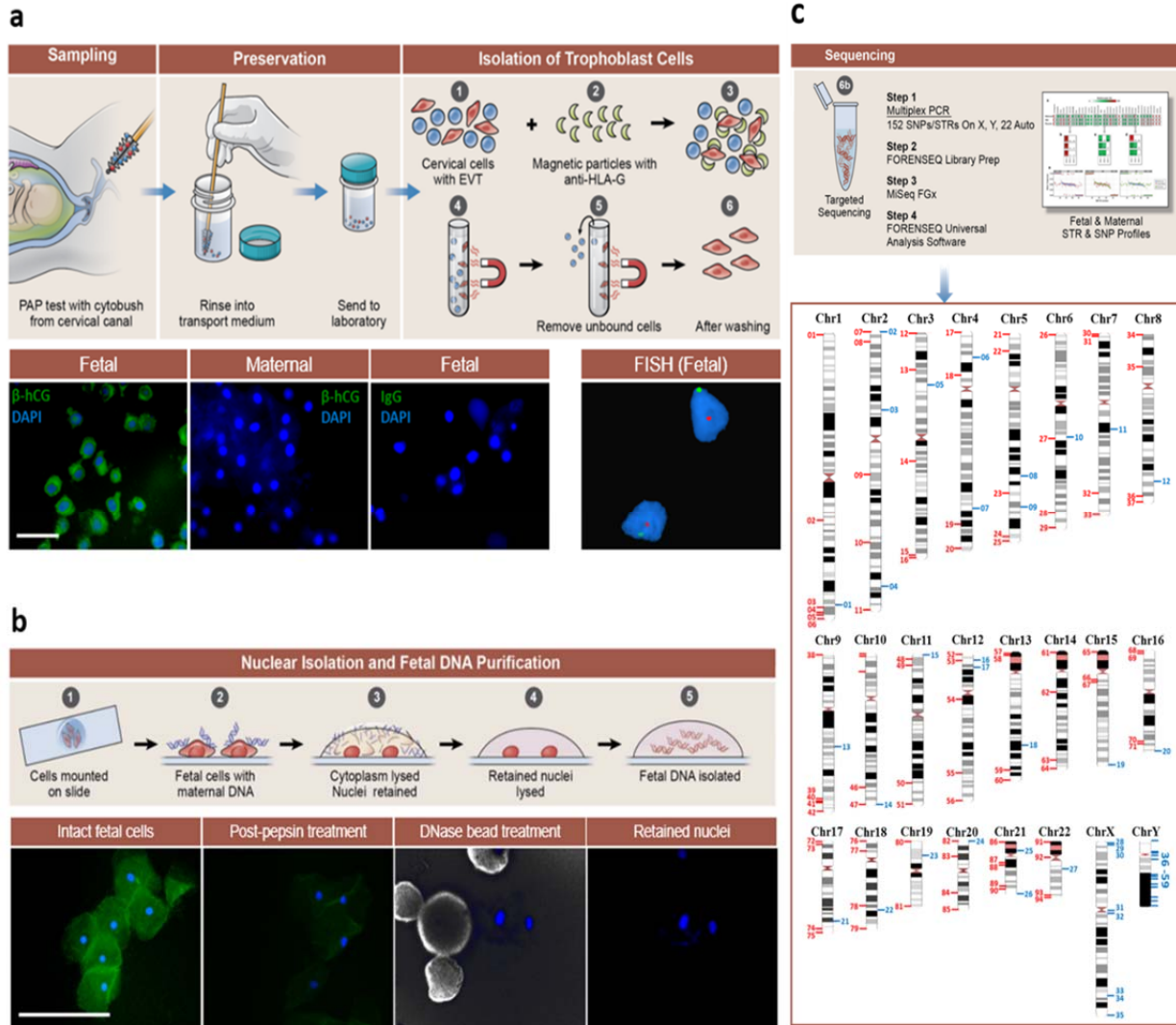


**Figure 17. Trophoblast isolation, assessment of cell purity, and fetal DNA isolation for sequencing.** **a**, Endocervical specimen collection and immuno-magnetic separation of trophoblast cells, using anti-HLA-G coated magnetic nanoparticles [1-6]. Below, trophoblast purity assessment by immunofluorescence staining for  $\beta$ -hCG (green), maternal and IgG were negative (first three panels), and screening for gender by fluorescent in situ hybridization (FISH) for the X and Y chromosomes (right panel, male sample). **b**, Top panel illustrates nuclear DNA isolation from the fetal cells [1]. Maternal DNA is blue, fetal cells and DNA are red [2]. Fetal nuclei remain adherent to slides after limited cell proteolysis [3]. Nuclei are lysed [4], providing fetal DNA [5]. The lower panels show immunofluorescence microscopic images of fetal cells during procedure. F-actin in green (FITC-phalloidin), and nuclei in blue (DAPI). Pepsin digestion removed F-actin. DNase immobilized on beads degraded residual maternal DNA. Nuclei were used for fetal DNA purification. **c**, Top panel illustrates the steps for targeted sequencing using the Forenseq platform [1-4]. The lower panel shows the locations of the 59 STR (blue) and 94 SNP (red) sites targeted across the human genome. Size bars, 100  $\mu$ m

**Table 7. Overview of samples and results for targeted sequencing approach**

Sample ID	Gestational Age	Tropho-blast cell purity (% $\beta$ -hCG)	Fetal Gender	Autosomal STR alleles in TRIC		% Fetal Fraction (% maternal fraction)	# of Informative SNP's		
				Media n	Range		In sample triads (%)	In Fetal cells after threshold (# total SNP's detected)	Incorrectly called in Fetal cells
<u>S<sub>A</sub></u>	5 wks	86	Male	94.8	85.6 - 100	97.6 (2.4)	41 (43.6)	41 (93)	0
<u>S<sub>B</sub></u>	5 wks	89	Female	85.5	75.1 - 100	92.2 (7.8)	44 (44.7)	31 (77)	0
<u>S<sub>C</sub></u>	5 wks	91	Female	89.1	73.5 - 100	87.2 (12.8)	51 (54.3)	39 (82)	0
<u>S<sub>D</sub></u>	6 wks	85	Female	91.9	80.8 - 98.7	95.2 (4.8)	42 (44.7)	40 (89)	0
<u>S<sub>E</sub></u>	6 wks	92	Male	86.4	85.7 - 96.9	85.6 (14.4)	30 (40.4)	25 (62)	0
<u>S<sub>F</sub></u>	6 wks	93	Male	88.1	73.2 - 99.4	75.6 (24.4)	49 (52.1)	11 (55)	0
<u>S<sub>G</sub></u>	6 wks	89	Male	93.3	84.9 - 100	93.9 (6.1)	48 (51.1)	45 (91)	0
<u>S<sub>H</sub></u>	6 wks	86	Female	92.7	77.8 - 98.5	98.6 (1.4)	51 (54.3)	47 (89)	0
<u>S<sub>I</sub></u>	6 wks	89	Male	95	88.9 - 100	100 (0.0)	38 (40.4)	35 (90)	0
<u>S<sub>J</sub></u>	7 wks	92	Female	89	77.7 - 96.6	82.1 (17.9)	41 (43.6)	19 (68)	0
<u>S<sub>K</sub></u>	8 wks	80	Female	89	72.3 - 100	82.4 (17.6)	42 (44.7)	22 (74)	0
<u>S<sub>L</sub></u>	8 wks	96	Female	92	79.6 - 99.4	97.2 (2.8)	40 (42.6)	38 (87)	0
<u>S<sub>M</sub></u>	8 wks	96	Female	90.2	78.3 - 100	90.8 (9.2)	47 (50)	44 (91)	0
<u>S<sub>N</sub></u>	8.4 wks	92	Female	93.3	76.5 - 99.2	92.8 (7.2)	45 (47.9)	42 (90)	0
<u>S<sub>O</sub></u>	9 wks	85	Male	93.6	79.8 - 100	92.9 (7.1)	52 (55.3)	46 (90)	0
<u>S<sub>P</sub></u>	9 wks	94	Male	91.9	81.9 - 100	100 (0.0)	38 (40.4)	37 (92)	0
<u>S<sub>Q</sub></u>	11 wks	85	Female	91.9	73.8 - 97.6	95.9 (4.1)	41 (43.6)	39 (89)	0
<u>S<sub>R</sub></u>	13 wks	91	Male	87.4	77.7 - 100	91.9 (8.1)	57 (60.6)	41 (77)	0
<u>S<sub>S</sub></u>	14 wks	90	Male	91.7	81.8 - 100	92.6 (7.4)	44 (46.8)	44 (93)	0
<u>S<sub>T</sub></u>	19 wks	80	Female	93.2	85.3 - 99.5	98.7 (1.3)	48 (51.5)	48 (92)	0

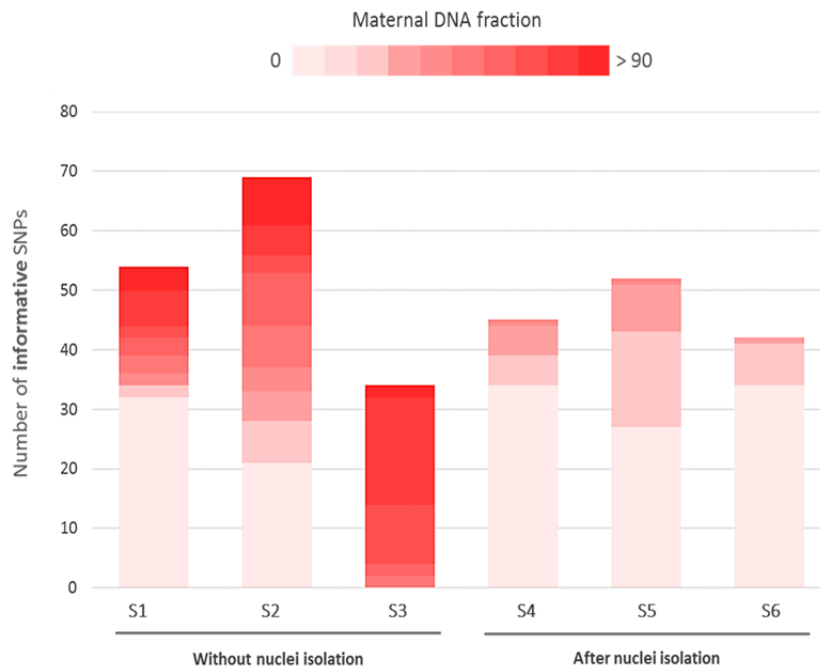


**Figure 18. Comparison of fetal fractions obtained with/without nuclear isolation.** The stack bar graph for the distribution of co-purifying maternal DNA (calculated as percentages and represented in gradient shades) in TRIC cells among informative SNPs. Samples S1-3, sequenced without fetal cell nuclear isolation show high proportion of maternal SNP's. Samples S4-6 were subjected to nuclear isolation before sequencing and show decreased detection of maternal SNP's.

### ***Targeted multiplex next generation sequencing***

We determined whether fetal DNA obtained by TRIC possessed the fidelity for reliable detection of single nucleotide mutations, as well as small DNA insertions and deletions. To do this, we utilized the ForenSeq platform to genotype and distinguish the fetus and mother, using small quantities of DNA (Churchill et al., 2016; Kidd et al., 2006; Sanchez et al., 2006) to target 59 STRs (27 autosomal, 7 X, and 24 Y haplotype markers) and 94 SNPs on all 22 autosomes (Figure 17c; Table 6). On average  $1.9 \pm 0.9$  ng DNA ( $n=20$ ) from fetal cells and DNA from matched placental and maternal cells was sequenced. All 153 loci (Table 6) were sequenced at a mean sequencing depth of  $5268 \pm 1714$  per STR and  $760 \pm 218$  per SNP. The fetal nuclear isolation strategy developed here generated a high-resolution STR profiles, detailing multiple shared and discriminatory alleles between mother and fetus. Detailed analysis revealed concordance between allelic profiles of fetal DNA obtained by TRIC and reference placental DNA, which were both distinct from maternal DNA, and provided 100% correct fetal gender identification in all samples compared to fetal reference DNA (Figure 19a and Table 7).

We observed that all 94 SNP's were detected in the fetal samples, and matched the placental reference DNA haplotypes (Figure 19c). Discriminatory SNP analysis, comparing the maternal haplotype to the reference placental DNA and fetal haplotype (Figure 19 b, d, Methods), revealed an average fetal DNA fraction of  $92.2 \pm 6.5\%$ , indicative of low levels of maternal DNA in the fetal samples (Table 7). Additionally, all of the maternal and fetal haplotype pairs lacked forbidden combinations (AA/BB) at any allele (Figure 19b), consistent with unique individuals, related as parent and offspring. Forbidden combinations were checked to ensure that in each of the samples at least one allele was derived from the mother thereby demonstrating that the fetus is related to the mother.



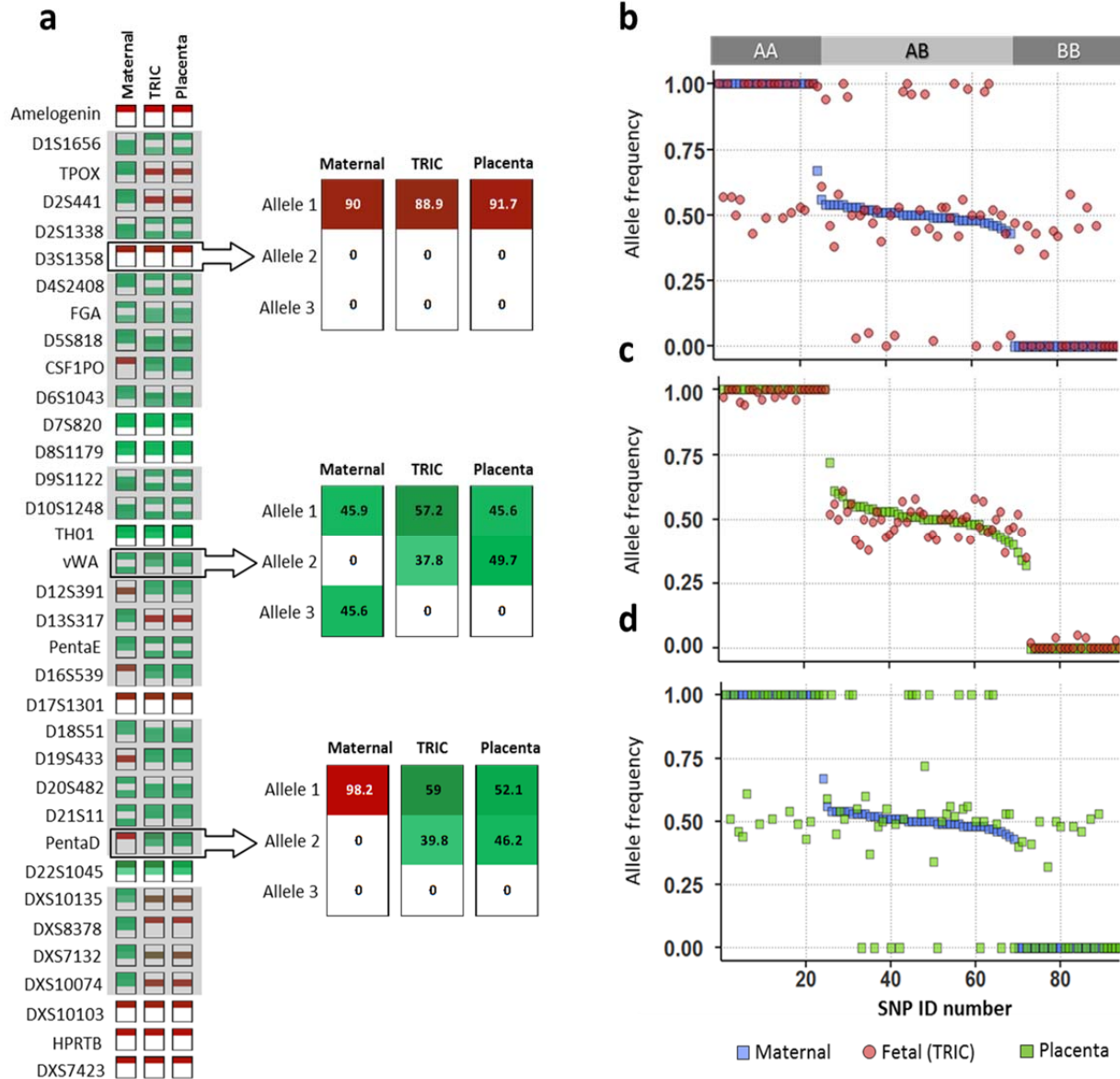


**Figure 19. Targeted sequencing of fetal cells obtained by TRIC. a. d a**, Graphical representation of STR profiles of DNA triads composed of maternal cells (Maternal), fetal cells (TRIC) and placental tissue (Placenta) from sample  $S_N$  (Table 2.0). For each DNA sample, the two dominant alleles with highest relative peaks for a given STR were determined and compared. The adjacent mini-plots show distribution of shared STR's (upper mini-plot) and discriminatory STR's (middle and lower mini-plots). **b-d**, Comparisons of allelic frequencies for the sequenced 94 SNPs in sample  $S_D$  (Table 2.0); **b**, fetal and maternal cells, **c**, fetal cells and placenta, **d**, maternal cells and placenta.

#### Accuracy of Haplotype Determinations

Using a threshold filter derived from reference placental DNA to account for variant reads due to maternal DNA that co-purified with fetal DNA (Methods), homozygous SNPs were



only called when the variant allele reads were within 0-10% or 90-100%, while heterozygous SNPs were only called between 40 and 60% (Methods). We observed that even after the threshold was applied, we were able to call  $89\% \pm 12\%$  of all the 94 SNP's in fetal samples (Table 7). The haplotype of any SNP that passed the filter always matched the placental reference DNA and was, therefore, correctly determined. The number of SNPs recovered after filtering correlated with the amount of co-purifying maternal DNA present. Stratifying the twenty samples, we found that the presence of less than 5% maternal DNA ( $n=8$ ) resulted in  $95.4 \pm 2.5\%$  recovery of the SNPs available pre-filtering; for 6.1% to 9.2% maternal DNA ( $n=7$ ), average recovery was  $92.5 \pm 7.3\%$  of SNPs; whereas higher contamination (12.8% to 24.4%,  $n=5$ ) reduced recovery of SNPs to  $62.5 \pm 15\%$ .

The data were further analyzed to determine when the purity of the fetal fraction was sufficient to call the correct fetal haplotypes in the absence of reference (e.g., placental) DNA. An internal quality control was established using the median summed autosomal STR allele percentage (Methods). A median summed autosomal STR allele percentage greater than 82.5% (achieved in 15 of the 20 samples) was required to consider a sample adequately pure for precise single nucleotide resolution. In general, any given SNP in any samples that passed the filter was correctly called.

## Discussion

Genetic disorders pose a significant risk for the newborn. After forty-five years of exploring the diagnostic utility of fetal trophoblast cells residing in the female reproductive tract (Imudia et al., 2010; Shettles, 1971), we report in this study that the entire fetal genome can be analyzed with a noninvasive and standardized procedure, beginning at three weeks post conception (five weeks after the previous menses). The TRIC protocol, followed by nuclear

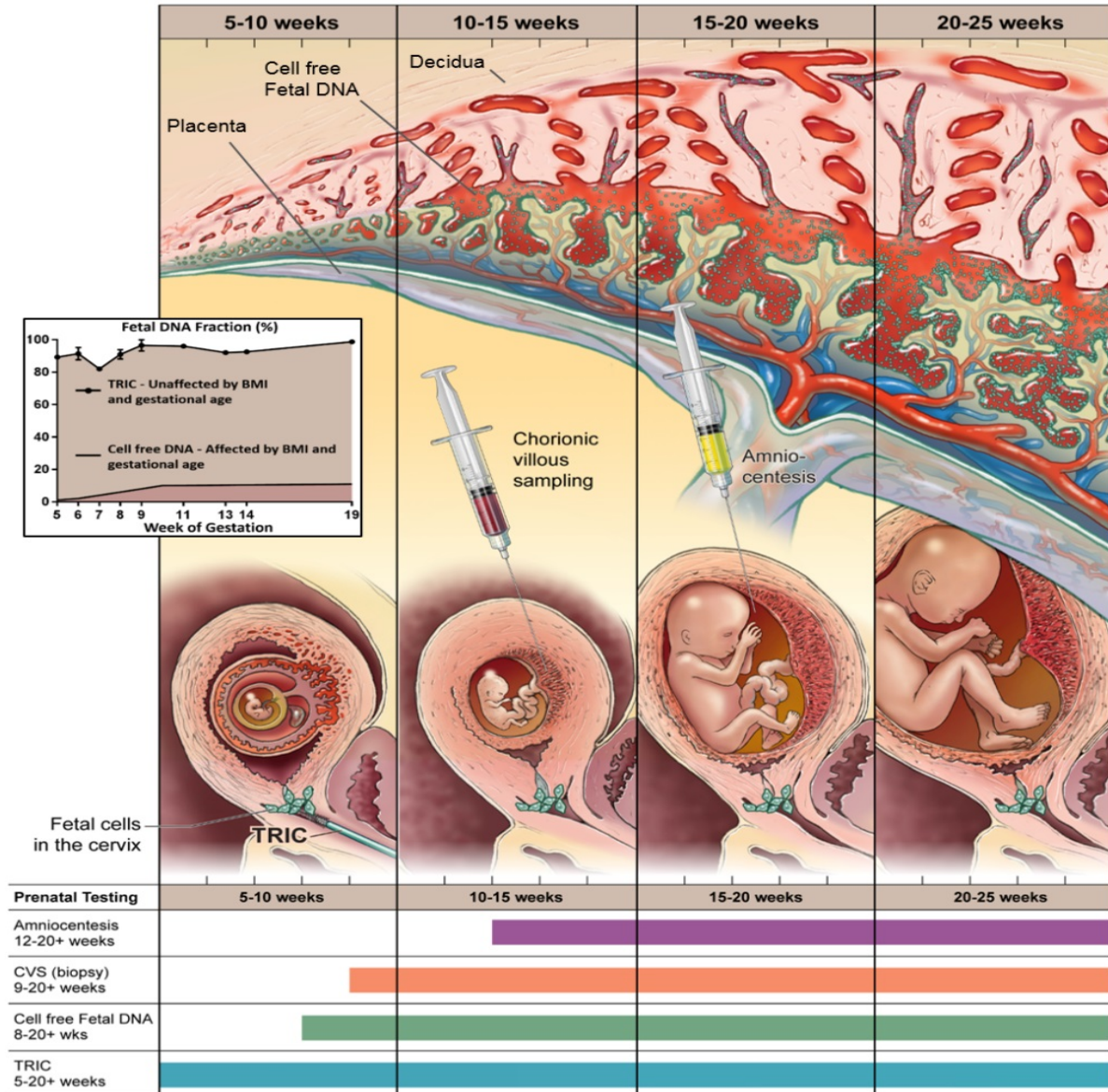


**Figure 20. Approaches to obtain fetal DNA for prenatal testing in ongoing pregnancies in comparison to trophoblast retrieval and isolation from the cervix (TRIC).** Sources of fetal DNA throughout early pregnancy are illustrated at the maternal-fetal interface. Amniocentesis is available beginning at 12-15 weeks of gestational age (GA) and is invasive, but provides intact fetal cells from amniotic fluid for DNA isolation. Chorionic villous sampling (CVS), available at 9-10 weeks of GA, provides fetal DNA from intact cells of a placental biopsy obtained invasively. Fetal cells are extremely rare in maternal blood. However, fragments of fetal DNA released from degrading placental cells accumulate in maternal blood with increasing GA as cell-free fetal DNA. This cell free fetal DNA can be obtained non-invasively from maternal blood, beginning at 8-10 weeks of GA and can be analyzed using multiple parallel sequencing combined with extensive computational analysis to distinguish it from cell-free maternal DNA. Hundreds of intact trophoblast cells can be safely retrieved non-invasively in Pap smears using a cytobrush. TRIC captures trophoblast cells migrating into the reproductive tract that accumulate in the endocervical canal beginning at 5 weeks of GA without negative effects early GA or maternal obesity found with cell free DNA. (Table 7)

isolation, provided access to the full, unfragmented fetal genome for analysis earlier in gestation than any procedure currently in practice (Figure 20).

Previous studies have suggested genetic testing protocols using fetal cells captured from the cervix by size selection and laser micro dissection (Bussani et al., 2007; Bussani et al., 2002; Katz-Jaffe et al., 2005; Mantzaris and Cram, 2015; Pfeifer et al., 2016). A critical obstacle was the inability to generate pure, well-characterized fetal cell populations. The lack of sufficient quantities of fetal DNA for reliable molecular analysis limited DNA characterization and reproducibility. As a result, those approaches have never been adapted for clinical use.

To overcome these limitations, we have developed a rapid isolation protocol that provides fetal cells and DNA within one day, using immunomagnetic isolation of fetal cells (Bolnick et al., 2014). Although trophoblast HLA-G expression decreases in women with placental disorders, such as preeclampsia (Goldman-Wohl et al., 2000), fetal cell yield is not significantly hindered in those pregnancies (Fritz et al., 2015b), which reduces dropouts due to lack of DNA. Initial experiments that isolated DNA from fetal cell extracts (Figure 17) failed to reliably provide a high fetal DNA fraction that was adequate for clinical analysis, suggesting co-purification of maternal DNA fragments bound to the fetal cells. This complication has likely hindered comprehensive analysis of the fetal genome by other groups working with specimens collected from the reproductive tract. Nuclear isolation eliminated the maternal DNA, resulting in unprecedented fetal DNA purity from transcervical specimens. An average fetal fraction of 91.5% was obtained before 10 weeks of gestation, with a fetal fraction up to 99.9% as early as 6 weeks of gestation.

Next generation sequencing is a powerful tool for both global analysis of the genome and targeted sequencing of selected loci. Whole genome and exome sequencing have the advantage

of identifying chromosome structural anomalies, as well as *de novo* mutations. However, those approaches require larger quantities of DNA for complete coverage and adequate read depth (>30x) in order to obtain single nucleotide resolution. The small fraction of fetal DNA available in cell-free DNA limits its usefulness to chromosome copy number variance testing as a noninvasive perinatal screen. However, approximately 90% of congenital defects are not caused by aneuploidies (Christianson and Modell, 2004). By accessing intact fetal cells with entire genomes, the TRIC protocol reliably provides comprehensive fetal genetic analysis as demonstrated here using targeted sequencing.

Targeted sequencing without whole genome amplification is currently the method of choice for diagnostic screening of specific genomic regions and gene mutations. It requires less DNA, provides greater depth (>300x), and is therefore a reliable, low cost approach. Additionally, data is easier to analyze compared to whole genome sequencing due to the limited number of loci involved. It avoids as well the potential of uncovering maternal disorders, including cancers that can be detected with the current NGS shotgun sequencing approaches (Bianchi et al., 2015).

With as few as 125 cells, the exact fetal genotype was determined reliably by targeted multiplex sequencing of 157 loci across all chromosomes. However, the limit at which cycle saturation would cause a bias is not currently known. SNPs are naturally occurring single nucleotide variations in the genome that, from a technical standpoint, are comparable to pathogenic point mutations. Similarly, STRs mimic small insertions and deletions in the genome that distinguish some clinically-relevant mutations. Targeted sequencing of SNPs has been extended on a large scale for aneuploidy analysis of cell free fetal DNA (Wong and Lo, 2016). The ability to detect both SNPs and STRs is evidence that prenatal genotyping by TRIC is

capable of detecting any genetically-transmitted disease.

Achievement a high fetal fraction through TRIC and nuclear isolation solves a critical problem in the detection of gene mutations in the first trimester of pregnancy. Here, we provide proof that recessive, autosomal, single nucleotide polymorphisms in a male fetus can be easily detected without the need of paternal haplotyping, based on our analysis. The approach used in this study can be effortlessly adjusted to test for any genetic variation or disorder. If discriminatory SNPs or STRs are included in the targeted sequencing strategy, contaminating maternal DNA can be quantified and subtracted to determine the fetal haplotype. Therefore, genotyping is straightforward and can be adjusted to established commercial pipelines. With advances in targeted multiplex sequencing approaches, Nicolaides et al. have successfully used 19,488 parallel reactions to detect aneuploidies in cell free DNA (Nicolaides et al., 2013), which should be feasible using fetal cells from the cervix to screen aneuploidies, as well as multiple genetic disorders.

TRIC can potentially fill an important gap in current noninvasive prenatal testing with the precision of current invasive technology, but unhampered by limitations due to a large maternal DNA fraction, rapid fetal DNA catabolism, early gestational age or maternal obesity. Due to its simplicity, TRIC will in the future enable prenatal genetic analysis in a diagnostic clinical setting without the necessity of complex bioinformatics for interpretation of massively parallel sequencing. Isolation of fetal cells by TRIC holds not only promise for prenatal genetic testing, but also provides a novel approach to investigate trophoblast cells in ongoing pregnancies (Imudia et al., 2010), exploring their biology and relationship to the various placental insufficiency syndromes that jeopardize fetal and maternal health.

## **CHAPTER 5 - TRANSCRIPTOMIC PROFILING FOR CHARACTERIZATION OF CELLS ISOLATED BY TRIC**

### **Abstract**

The survival and differentiation of extravillous trophoblast (EVT) cells at the beginning of pregnancy is crucial, and deficiencies are linked to diseases of uteroplacental insufficiency, including early pregnancy loss, fetal growth restriction and preeclampsia. It is anticipated that EVT gene expression in the first trimester is altered prior to the onset of overt disease in the third trimester. Fetal cells that express EVT lineage proteins can be obtained from ongoing pregnancies by Trophoblast Retrieval and Isolation from the Cervix (TRIC), and provide a novel platform for examining gene expression. Transcriptomic analysis using next-generation sequencing (NGS) offers as an unbiased approach to identify differentially expressed transcripts in these fetal cells during the first trimester from normal and pathologic pregnancies. RNA isolated from the fetal cells was quantified and assessed for quality to establish its stability during TRIC. NGS identified 409 genes differentially expressed between the fetal cells and maternal cells from the same cervical specimens. However, no significant differences in gene expression were noted between replicate RNA aliquots, or between fetal cells from different patients. Bioinformatics, including gene ontology pathway analysis and BioPython library demonstrated that 21 genes were EVT specific. This study suggests that not only can RNA of adequate quality be isolated from cells obtained by TRIC, but it can be used to reliably interrogate the transcriptome. TRIC and NGS could provide for the first time molecular profiles that reveal early pathophysiological events postulated to occur in EVT cells at the inception of pregnancies that develop uteroplacental insufficiencies and cause major obstetric disorders.

### **Introduction**

The placenta is a multifunctional organ that not only provides a fetal-maternal interface,



but is also the site of exchange of nutrients, oxygen, metabolites and other molecules between the mother and the fetus (Dilworth and Sibley, 2013). The placenta is important for the survival of the fetus, as well as health of the mother. They are composite organs consisting of a trophoblast compartment that enables nutrient and gas exchange between the fetal and maternal blood circulations, and mesodermal lineages that form the umbilical cord and the fetal portion of the placental vasculature (Chaddha et al., 2004). The trophoblast compartment consists of a population of villous cytotrophoblast cells that fuse into syncytiotrophoblast or proliferate along the fetal-maternal interface to form cell columns and undergo a well-defined differentiation into invasive extravillous trophoblast (EVT) cells. The syncytiotrophoblast layer is responsible for all nutrient and gas exchange between the maternal and fetal blood circulations (Knofler and Pollheimer, 2013). EVT cells discharge through the maternal mucosal fluids after invading the uterine wall, where they are deployed to facilitate spiral artery remodeling and immune modulation at the fetal-maternal interface.

Trophoblast Retrieval and Isolation from the Cervix (TRIC) is a novel experimental platform (Bolnick et al., 2014) that provides a novel approach to non-invasively acquire fetal cells hypothesized to be EVT that are central for proper placentation. TRIC uses the EVT lineage protein, HLA-G, to efficiently separate maternal cells from fetal cells in endocervical specimens. The isolated cells are positive for  $\beta$ -hCG (>98%), while the depleted maternal cells do not express this trophoblast product (Bolnick et al., 2014; Fritz et al., 2015a). Cells isolated by TRIC are clearly fetal in origin, based on the presence of a Y chromosome when the fetus is male (Bolnick et al., 2014), and comparison of haplotypes between maternal and fetal cells isolated during TRIC (Chapter 4). Two other trophoblast marker proteins, cytokeratin 7 (KRT7) and placental lactogen (CSH1) are uniformly expressed in the isolated fetal cell fraction

(Bolnick et al., 2014). The phenotype of the isolated fetal cells was investigated using ICC, demonstrating that they express several EVT markers (ITGA1, CDH5, PECAM1, MMP9, HLA-G), but lack villous trophoblast markers (ITGA6, CH1, PSG1) (Bolnick et al., 2014).

Uteroplacental insufficiency, defined as inadequate perfusion of the placenta, is a pathology associated with several perinatal disorders, including early pregnancy loss (EPL), intrauterine growth restriction (IUGR) and preeclampsia (PE) (Hossain and Paidas, 2007; Papageorgiou et al., 2004). There is compelling evidence that uteroplacental insufficiency originates with the failure of EVT cells to properly differentiate, invade intravascularly, and convert the uterine spiral arteries to low resistance, high volume conduits of maternal blood into the intervillous space (Chaddha et al., 2004). These events transpire during the first trimester, well before clinical symptoms of IUGR or PE occur. However, direct evidence that the EVT cells are altered in the first trimester prior to development of those disorders is lacking. Fritz et al examined a set of proteins associated with uteroplacental insufficiency in fetal cells obtained by TRIC between 5 and 10 weeks of gestational age (GA) and found significant differences in six of the seven proteins between control pregnancies and those ending in EPL (Fritz et al., 2015a), suggesting that the molecular profiles of the EVT-like fetal cells reflect pregnancy status.

It is hypothesized that fetal cells obtained from the cervix by TRIC have a similar phenotype and physiology to EVT cells residing in the basal plate and placental bed. Understanding the relationship between EVT cells in the placenta and cervix will establish the developmental significance of the cells, and their utility as an experimental paradigm to investigate placental pathophysiology. As an initial assessment, the transcriptome of fetal cells obtained by TRIC will be compared to that of the maternal epithelial cells from the cervix to



establish their unique RNA profile and to determine if the differentially expressed genes are indicative of an EVT phenotype. Because EVT invasion and conversion of the maternal spiral arteries occurs in the first and early second trimesters, it is hypothesized that comparison of fetal cells obtained by TRIC from pregnancies that develop severe placental insufficiency causing EPL with fetal cells isolated from pregnancies with healthy term deliveries will generate a unique set of differentially expressed genes associated with deficient trophoblast development, and could help identify novel disease biomarkers with very high sensitivity and specificity for future preclinical testing. These studies will provide a clearer view of the utility of fetal cells obtained by TRIC from ongoing pregnancies for investigating early placentation and pathological etiologies, and the potential of TRIC as a platform for perinatal interrogation of the placenta to predict maternal risk of placenta-based disease.

## **Materials and Methods**

### ***Sample Collection***

Pregnant patients (N=50) were recruited at 5-20 weeks GA with informed consent and approval of the institutional review board of Wayne State University. EVT cells were obtained with a ThinPrep kit (Hossain and Paidas, 2007) and immediately fixed during the PAP smear procedure, preserving proteins and nucleic acids, including RNA. Prior to fetal cell isolation, all cells were pelleted to remove ThinPrep fixative and then cross-linked with 10 ml of 2% paraformaldehyde for 10 min. This was followed by washing the cells 3 times with 10 ml of PBS by centrifugation and resuspension. Fetal cells were then purified by immunomagnetic isolation with anti-HLA-G, according to the TRIC protocol (Bolnick et al., 2014). Recovery after immunomagnetic isolation averages  $746 \pm 59$  (Bolnick et al., 2014)

### ***RNA Extraction***

Fetal RNA was isolated after de-crosslinking, using a Qiagen FFPE RNA kit, incubating at 56°C for 15 min and 80°C for 15 min and incubating with 1500 Kunitz DNase for 15 min prior to RNA extraction. Isolated RNA was quantified with the RNA Pico Kit (Agilent Technologies), and its purity assessed using an Agilent 2100 Electrophoresis Microfluidics Analyzer. The amount of RNA per cell recovered is reported in Figure 21C (Results).

### ***Library Preparation***

Eleven patients were selected for RNAseq after outcomes were determined from patient medical records. A control cohort of pregnancies with uncomplicated term deliveries (n=9) and adverse pregnancy cohort (n=2) were identified and selected for library preparation. RNA libraries were prepared from both fetal and maternal cells isolated by TRIC using the ScriptSeq v2 RNA-Seq Library Preparation Kit (Epicenter) and 500 pg of fragmented RNA. Uniquely barcoded adaptors were ligated to the RNA, followed by PCR amplification and library purification. Each uniquely barcoded sample was quantified and its quality assessed, using the High Sensitivity DNA Chip (Agilent Technologies). The cDNA was combined from barcoded individual libraries before multiplex sequencing, eliminating any sequencing lane effects. Paired-end sequencing was performed for 50 cycles using the Illumina HiSeq-2500 sequencer.

### ***Data Alignment & Mapping***

RNA sequencing data was first processed with demultiplexing software (Casava 1.8.2, Illumina). It was then aligned to the human genome build GRCh37.p7/hg19, using TopHat2 ver 2.0.13 (Kim et al., 2013), and to the ribosomal sequences 18S and 28S, using the bioinformatics tool Novoalign (Novocraft, 2010). Novoalign determined unique alignments that were used to generate 1000 reads per coding segment per sample. The reads thus generated were converted

into bed.files and imported to the Genomatix Genome Analyzer (GGA) (Genomatix Software GmbH). The GGA, using RNA-seq analysis, generated data in the form of Reads Per Kilobase of exon per Million fragments mapped (RPKM) for 25,000 genes in the database. A set of differentially expressed genes (DEGs) were identified with bioconductor package DESeq2 (Anders and Huber, 2010). A gene was considered significantly altered if the adjusted p-value was  $< 0.05$ . p-values were calculated by the DeSeq2 program. DEGs were subjected to Ingenuity Pathway Analysis (IPA) to identify the top functional interaction networks and key central regulatory genes. The most significant network in which the differentially expressed genes were enriched was selected and illustrated.

### ***qPCR***

The quality of the fragmented RNA was validated by semi-quantitative qPCR for HBEGF, MMP2 and 18sRNA, using SYBR green and a CFX384 BioRad thermal cycler (Life Technologies). NGS data was validated using qPCR with primers (IDT) for genes listed in Table 8. RNA for each of the samples used in NGS was converted to cDNA, using 4  $\mu$ l iSCRIPT (BioRad) and pre-amplified for x cycles in a multiplexed reaction using all primers and SsoAdvanced PreAmp Supermix (BioRad). Samples were then target-amplified with individual primers. After each of the samples was target-amplified, qPCR was quantified by delta (Bustin et al., 2009) analysis.

**Table 8: Genes used for qPCR validation**

Gene name	Forward Primer	Reverse Primer	
HLA-G	GTG TGG TAC TTT GTC TTG AGG A	AGA GTA GCA GGA AGA GGG TT	Trophoblast marker
KRT7	GGT CAG CTT GAG GCA CTG	ACC ACA AAC TCA TTC TCA GCA	Trophoblast marker
CDH5	AAG AAC TGG CCC TTG TGA C	CAG CCT TTC TAC CAC TTC CAG	Invasion/migration marker
MMP9	CGT CGA AAT GGG CGT CT	ACA TCG TCA TCC AGT TTG GTG	Invasion/migration marker
ITGA6	TTG GAC TCA GGG AAA GCT ATT G	GAT CTC CAC TGA GGC AGT TAT G	Epithelial marker
CDH1	CTG AGG ATG GTG TAA GCG ATG	GTC TGT CAT GGA AGG TGC TC	Epithelial marker
CD38	TCC GAA GAT GTG GAC TTG C	TCT CCA TCC TCT CTT CAC CA	Trophoblast specific genes upregulated in fetal cells when compared to maternal cells.
CSF1	TCT TTC AAC TGT TCC TGG TCT AC	TGT CGG AGT ACT GTA GCC A	
DDX39A	CAC CGA AGA ACA CAG ACA CC	TCA ACG GAC AGG TGA CG	
RBM15	TCT TCT TGT TCT CAT ACC TAA CTC C	AGT TCT CCC AGC AGT TCC T	
TLR1	AGA CAT TCC TAA AGG TAG AAG CTG	GAA GAA ATC AGG ATA ACA AAG GCA	
AMBP	GTA TCT GTT TTC TCA TAA GCT CCA G	GAC AGG ATG ACA GTG AGC AC	Trophoblast specific genes downregulated in fetal cells when compared to maternal cells.
FGF23	TAT CTT CTG CTC ATC ACA CCT G	GCC AGG AAC AGC TAC CAC	
KCNQ5	CTT CCT TGC CAT CCT CTA TAT CG	AGT GTT TTC TAC CAT CCC TGA G	
NUNDT9	TTC TGT AAG GAG TTG GA GCT TC	AAG GAA AGA CTG TGG AGA ATG G	
TRPC7	CAT CAA AGT AAG ACA GCC AGA GT	TGC TCA ACA TGC TAA TAG CCA	
C3	TGT TAA ATG GCT GAT CCT GGA G	GCC ATG TCT TTC TCG TTG TTG	Genes upregulated in fetal EPL cells when compared to fetal normal
CCND1	GTT CCA CTT GAG CTT GTT CAC	GCT GTG CAT CTA CAC CGA	
FGF2	GCC AGG AAC AGC TAC CAC	TAT CTT CTG CTC ATC ACA CCT G	
HSP90B1	AAG GAC TAC TGC ACC AGA ATG	TGT TTC CGA AGA CGT TCC AC	
PRDX6	TGT GAC AGC TCG TGT GGT GT	GTC AGC TGG AGA GAG ATG AC	
SUMO2	CCT GCA CAG TTG GAA ATG GAG G	AGT AGA CAC CTC CCG TCG TCT GCT	Genes downregulated in fetal EPL cells when compared to fetal normal
DUSP1	ACC ATC TTC CAT GCT TAC CAC	AAC TTG GCA CTG CAT TTT GG	
FOS	ACA CTC CAA GCG GAG ACA GA	CTG AGC TGC CAG GAT GAA CT	
IL1B	TGG CCT TGG GCC TCA AGG A	CTA CAC TCT CCA GCT GTA GAG	
IL8	TGT CTG GAC CCC AAG GAA	CAT CTT CAC TGA TTC TTG GAT ACC	
JUNB	CGG ATG TGC ACT AAA ATG GAA C	GGT TTC AGG AGT TTG TAG TCG T	
NFKBIA	CAG GAG ACG TGA AGA TGC TG	AGT TGA GAA TGA AGG TGG ATG A	
SOC3	CAA GGA CGG AGA CTT CGA TTC	GGA AAC TTG CTG TGG GTG A	

## Results

### *TRIC provides stable RNA from isolated cells*

To assess RNA stability during TRIC, the HTR-8/SVneo cell line was treated similarly to cervical specimens collected in the ThinPrep fixative. Both fresh cells and cells fixed in ThinPrep produced intact RNA, however, after a series of PBS washes or incubations to mimic the TRIC protocol at both 4°C and room temperature degradation of RNA was apparent (Figure 21A), possibly due to introduction of endogenous RNases.

Formaldehyde covalently binds proteins and nucleic acids by reacting with primary amino groups, and prevents loss of highly soluble nucleic acids by inactivating endogenous RNases. Aldehyde crosslinkers are reversible by heat and salt treatment (Niranjanakumari et al., 2002). TRIC was modified to incorporate formaldehyde crosslinking prior to removal of cells from the ThinPrep fixative to preserve RNA integrity. Fetal and maternal RNA was extracted after de-crosslinking, which resulted in fragmented RNA (Figure 21B). RNA extracted from ThinPrep-fixed cells prior to TRIC (crude) and maternal or fetal cells separated by TRIC using the crosslinking and de-crosslinking protocols produced equal amount of RNA/cell (Figure 21C). This finding suggests that the formaldehyde cross-linking prevents RNA degradation. qPCR for several known mRNAs in the isolated maternal and fetal cells produced Ct values comparable to RNA isolated from the crude cells (Figure 21D), suggesting that fragmentation following de-crosslinking does not impact the over-all quality of the RNA extracted after TRIC for use in mRNA quantification. The fragmented RNA is ideal for downstream NGS (Head et al., 2014).

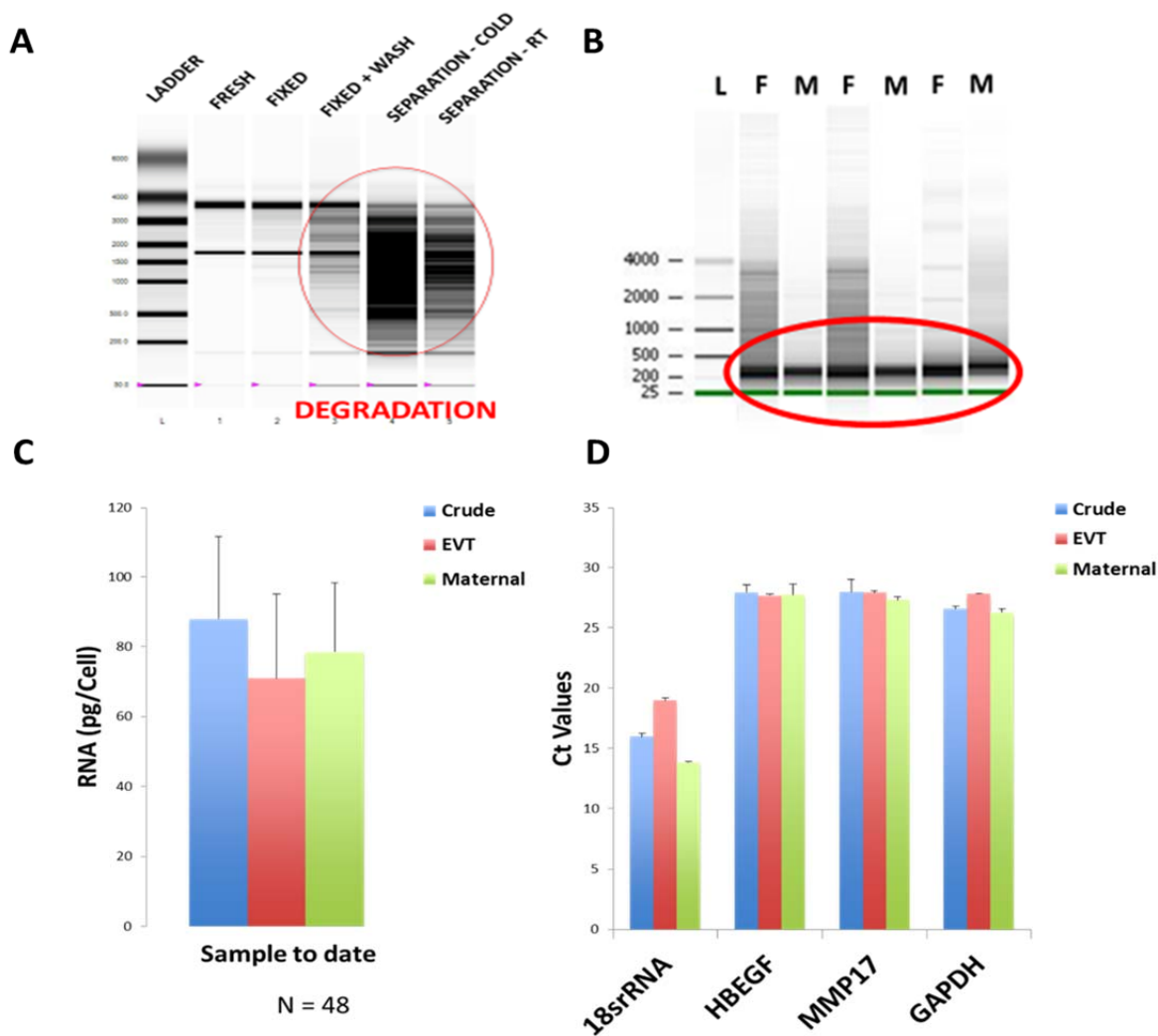


**Figure 21. Assessment of RNA quality and integrity.** A and B. Gel Images (Agilent 2100 Bioanalyzer) of total RNA. A. RNA extracted from HTR-S/Vneo cells was immediately examined (Fresh), or fixed with ThinPrep (Fixed), washed in PBS (Fixed + Wash) and processed by the TRIC protocol (Separation) at either 4°C (Cold) or room temperature (RT). High-quality samples (Fresh and Fixed) produced two distinct bands corresponding to the 18S and 28S ribosomal RNAs. Smearing in the other lanes was indicative of RNA degradation. B. RNA extracted from fetal (F) and maternal (M) cells isolated using the formaldehyde crosslinking protocol showed smearing and strong bands at ~200 bp, indicative of fragmentation. C. RNA recoveries, quantified by Agilent Bioanalyzer, were determined from crude cells in ThinPrep fixative and maternal and fetal cells separated by TRIC using the formaldehyde crosslinking protocol (N = 48 cervical specimens). D. cDNA made from equal amounts of RNA in C was assayed by qPCR with primers for the indicated RNAs

### *Transcriptomic analysis of cells isolated by TRIC from normal term pregnancies*

Total RNA was prepared after TRIC, using the formaldehyde crosslinking and decrosslinking protocol from cervical samples obtained from patients with normal full term

deliveries (n=9, Table 9). The transcriptome was analyzed by RNA sequencing and bioinformatics to identify genes differentially expressed between the isolated fetal and maternal cells. A total of 428 differentially expressed transcripts were obtained. Analysis of transcripts by DESEQ2 for 2.0-fold up or down regulation, generated 209 up and 219 downregulated transcripts (Figure 22A). Each of the differentially regulated transcripts appeared in MA (Figure 22A) and volcano (Figure 22B) plots, demonstrating at least a 2-fold change and a p-value of  $<0.05$ , respectively as determined by the DESeq2 program.

**Table 9. Patient and specimen characteristics**

Characteristics	Control	EPL1	EPL2
Number, <i>n</i> (% of total)	9 (81)	1 (9.5)	1 (9.5)
Maternal age in years, <i>median (IQR)</i>	26 (22-28)	26	29
Ethnicity			
Caucasian, <i>n</i> (%)	0 (0)	0 (0)	1 (100)
African, <i>n</i> (%)	9 (100)	1 (100)	0 (0)
Asian, <i>n</i> (%)	0 (0)	0 (0)	0 (0)
Hispanic, <i>n</i> (%)	0 (0)	0 (0)	0 (0)
Unknown, <i>n</i> (%)	0 (0)	0 (0)	0 (0)
Gestational age at the time of sampling in weeks, <i>median (IQR)</i>	8 (7.6-11.6)	5	7.5
Gravidity, <i>median (IQR)</i>	2 (1 - 2)	3	1
Parity			
Nulliparous, <i>n</i> (%)	7 (78)	0 (0)	0 (0)
Parous, <i>n</i> (%)	1 (11)	0 (0)	0 (0)
Unknown, <i>n</i> (%)	1 (11)	1	1
Delivery mode			
Normal Spontaneous Vaginal Delivery (NSVD), <i>n</i> (%)	7 (78)	0 (0)	0 (0)
Cesarean section (CS), <i>n</i> (%)	2 (22)	0 (0)	0 (0)
Unknown, <i>n</i> (%)	0 (0)	1 (100)	1 (100)
Recovered fetal cells			
Purity (percentage of $\beta$ -hCG positive cells), <i>median (IQR)</i>	100 (98-100)	90%	97%

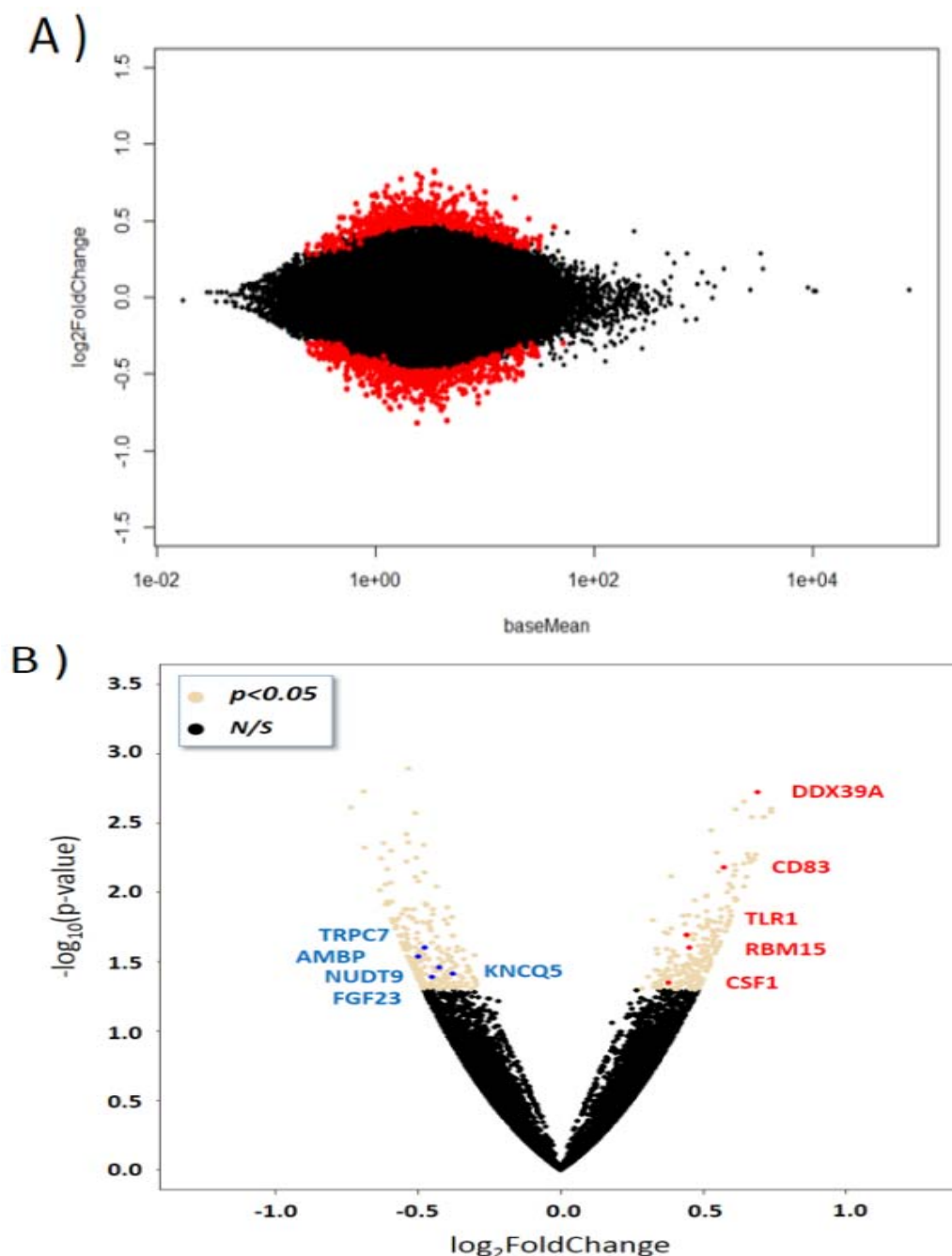


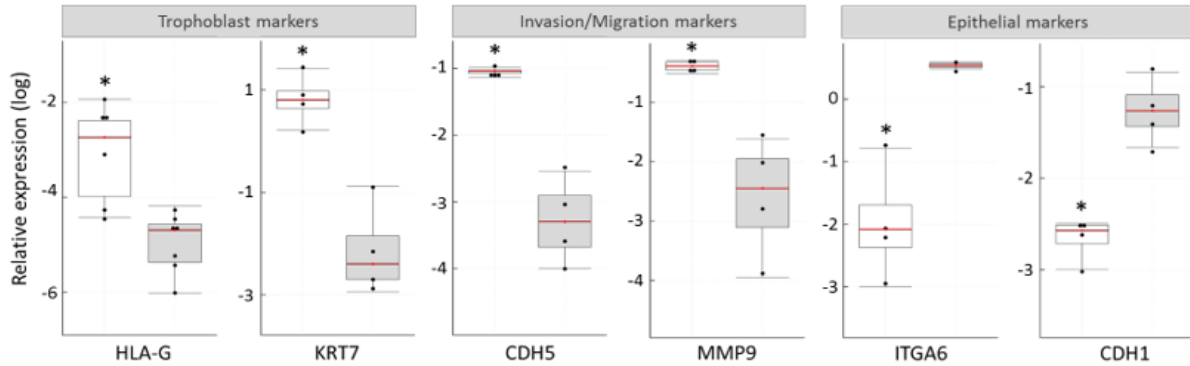
**Figure 22.** Two visualizations of the comparative transcript expression profiles between fetal and maternal cells A) A) Scatterplot (MA plot) of the log<sub>2</sub>-fold change in genes expressed in fetal cells compared to maternal cells generated by DESeq2 on the y-axis, versus baseMean of normalized counts on the x-axis. The differentially expressed genes (DEGs) (p-values < 0.05) were indicated by bold red dots. The black dots reflect genes with no significant change. B) Volcano plot of RNA-seq data represented by log<sub>2</sub>-fold change (x-axis), versus -log<sub>10</sub> p-value. The light colored dots represent DEGs (p-value < 0.05) in fetal compared to maternal cells. Among DEGs, 5 up-regulated (red) and 5 down-regulated (blue) genes were selected for further validation by PCR (see Fig. 23B and C).



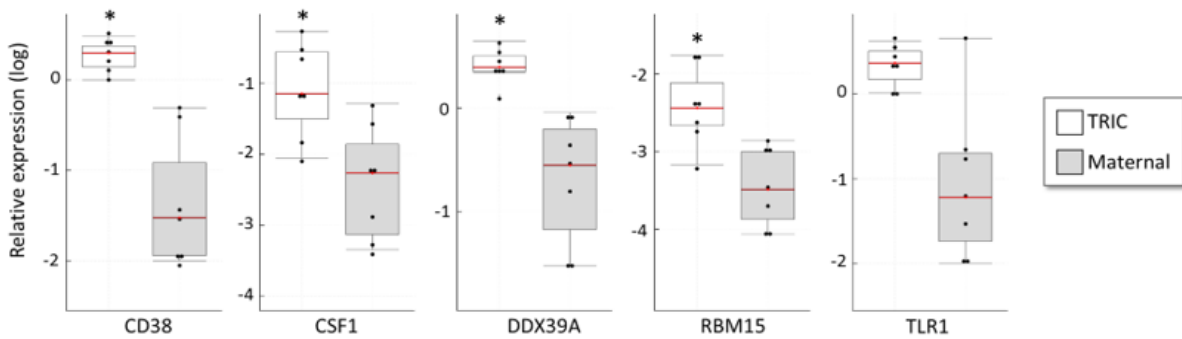
### ***Characterization of cells isolated by TRIC***

To characterize the two isolated cell populations (fetal, maternal) the expressions of 8 genes known as markers for trophoblast, epithelial, and invasion/migration were selected and were examined by real-time qPCR in RNA from all 9 samples. Comparison between cervical fetal and maternal cells showed expression of trophoblast markers in high abundance in the fetal cells (Figure 23A). HLA-G and KRT7 were highly expressed compared to the maternal cells. HLA-G was most highly expressed in fetal cells, which were isolated using anti-HLA-G immune-separation. CDH5 and MMP9, which are invasion/migration markers were expressed more in fetal cells than maternal cells. E-Cadherin (CDH1) and integrin alpha 6 (ITGA6), both epithelial markers, were found in maternal cells, but were very low in the fetal cells, as expected of the most penetrating EVT (Zhou et al., 1997). Of the differentially regulated genes, ten were selected based on their association with trophoblast based on a literature search, using BioPython (Cock et al., 2009). Indeed, transcripts that were upregulated in the fetal cells based on NGS showed significantly higher mRNA expression by qPCR in fetal RNA compared to maternal RNA (Figure 23B). Similarly, transcripts that were downregulated in the fetal cells according to RNAseq showed lower mRNA expression in fetal RNA than maternal RNA (Figure 23C), validating the NGS data and further confirming that the fetal cells are in fact of trophoblastic origin.

A)



B)



C)

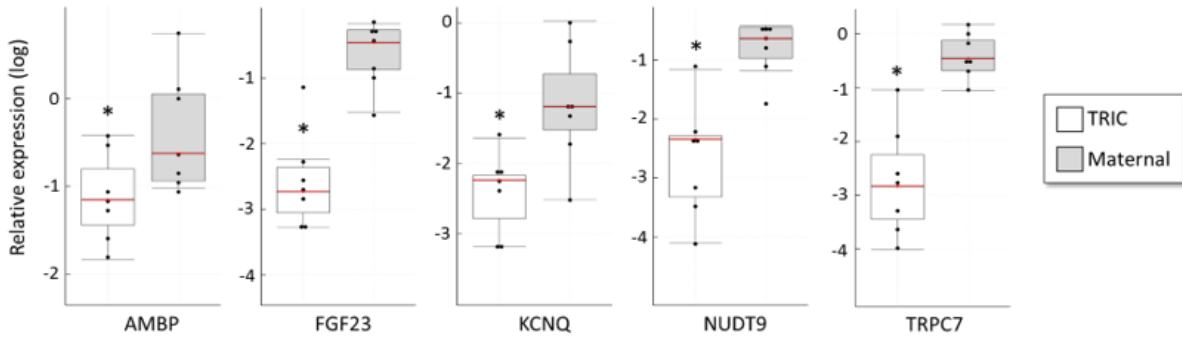


**Figure 23. Validation of RNAseq by qPCR.** A. To characterize the isolated fetal and maternal cell populations), the expression of 6 genes known as markers for trophoblast, epithelial, and invasion/migration were selected and examined by qPCR for the 9 control pregnancies. The expression values are presented as whisker-box plots. Transcript levels of 5 up-regulated (B) and 5 down-regulated (C) genes in the fetal transcriptome identified by RNA-Seq were also validated by real-time qPCR. \*  $p < 0.05$ ; The boxes represent the 25th to 75th percentiles, and horizontal red lines within the boxes indicate the medians. The whiskers are drawn to indicate  $1.5 \times$  Inter Quartile Range (3rd quartile – 1st quartile).

*Gene Ontology Consortium, analysis for fetal and maternal DEGs in normal pregnancies*

For gene ontology (GO) analysis, the differentially expressed transcripts ( $p < 0.05$ )

between the fetal and maternal cells were analyzed using Ingenuity pathway analysis (IPA). For this analysis, biological processes were analyzed. IPA generated the top protein-protein interaction network with a score of 32 comprising of 27 differentially expressed genes that were involved in invasion and migration differentiation and proliferation (Figure 24). The prominence of these pathways suggests that the fetal cells isolated by TRIC have an EVT phenotype.

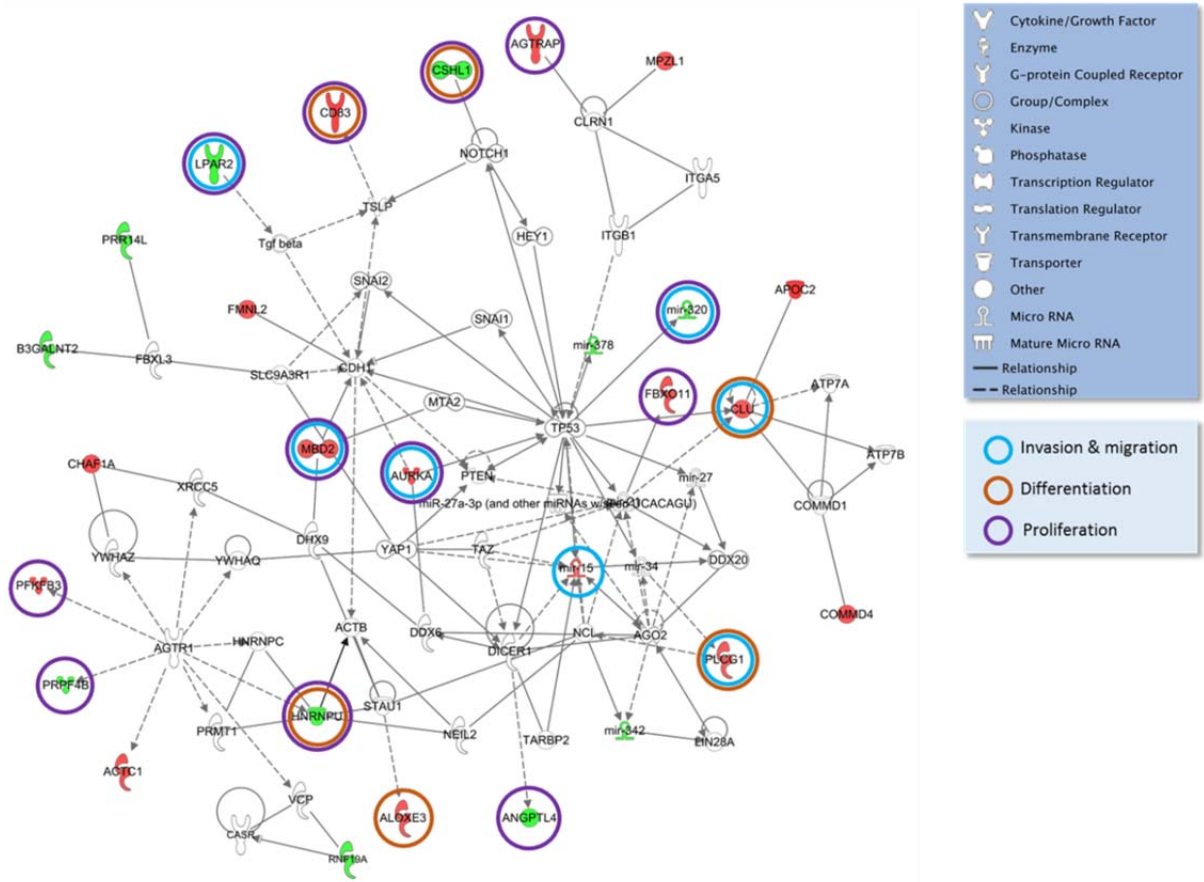


**Figure 24. Protein-protein interaction network.** Among the potential regulatory networks identified by Ingenuity pathway analysis for the genes differentially expressed between fetal and maternal cells ( $p < 0.05$ ), the top protein-protein interaction network is shown. It contains the key regulatory genes involved in invasion and migration, differentiation and proliferation. Green symbols indicate genes downregulated, and red symbols indicate genes upregulated in the in our study.

### *Transcriptomic analysis and validation of cells isolated by TRIC in Early pregnancy loss*

After the pregnancy outcomes were known, 2 cases of early pregnancy loss (EPL) were identified and compared by NGS to 2 selected control pregnancies (EPL, 5 and 7.5 weeks, Table

9). Libraries were prepared for both the fetal and maternal cell populations from the EPL samples and sequenced. Analysis of the sequencing data identified 348 genes differentially expressed between the fetal cells from control and EPL pregnancies. Out of the 348 differentially expressed genes, 69 were upregulated and 279 were downregulated, each with a  $p$ -value  $<0.05$  (Figure 25, Tables 10 & 11). Of the differentially expressed transcripts, both up and downregulated genes were randomly selected for validation by qPCR. Transcripts that were upregulated in RNAseq data had a higher mRNA expression level in the qPCR analysis (Figure 26A), and those that were downregulated had a higher expression in the normal group (Figure 26B). However, because there were only two EPL samples, statistical analysis should be interpreted cautiously. Nevertheless, both the NGS and qPCR data show a similar pattern.

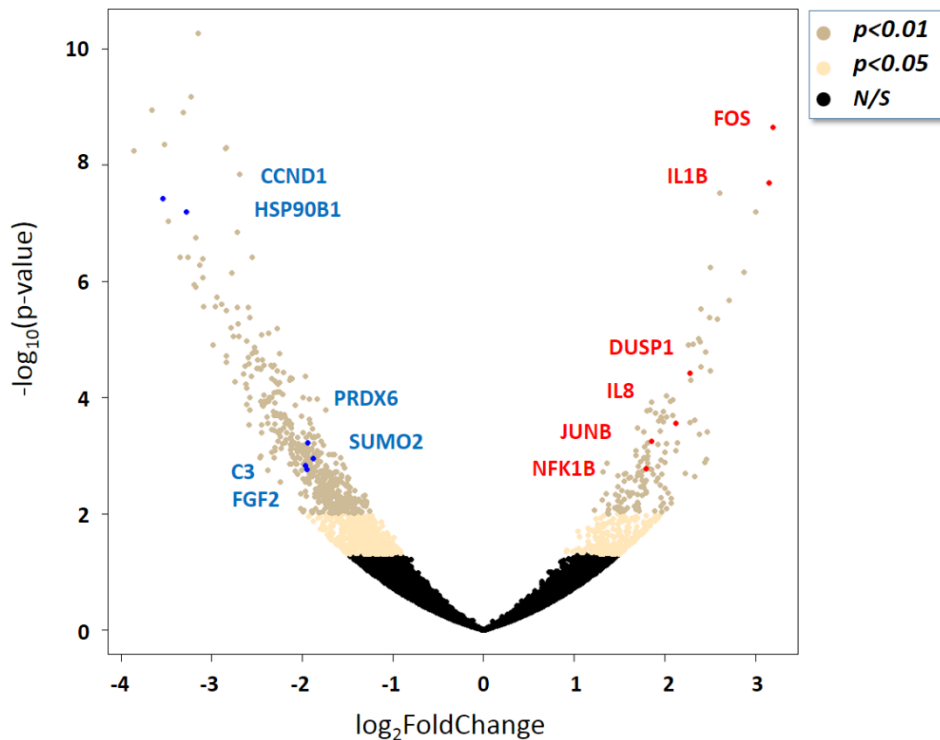


**Figure 25. Volcano plot presentation of transcripts in EPL versus control fetal cells.** The light dots represent significantly up- and down-regulated genes at two significant levels ( $p < 0.05$  and  $p < 0.01$ ) shown in the legend to the right. Of all differentially expressed genes, 6 down-regulated (blue dots) and 7 up-regulated (red dots) were chosen for qPCR validation.

**Table 10. Upregulated fetal genes in EPL compared to normal pregnancy**

Gene id	log2fold change	Symbol	Gene id	log2fold change	Symbol
2353	3.189	FOS	5209	1.799	PFKFB3
3553	3.147	IL1B	4792	1.79	NFKBIA
8794	2.999	TNFRSF10C	366	1.784	AQP9
6688	2.868	SPI1	54210	1.784	TREM1
3577	2.712	CXCR1	2214	1.771	FCGR3A
2215	2.606	FCGR3B	6648	1.767	SOD2
23135	2.581	KDM6B	5329	1.747	PLAUR
1958	2.504	EGR1	23645	1.737	PPP1R15A
5008	2.502	OSM	3985	1.729	LIMK2
4046	2.489	LSP1	5341	1.702	PLEK
50486	2.455	G0S2	57580	1.685	PREX1
1439	2.401	CSF2RB	2180	1.683	ACSL1
8843	2.392	HCAR3	64744	1.669	SMAP2
4688	2.372	NCF2	7133	1.619	TNFRSF1B
7832	2.314	BTG2	6515	1.597	SLC2A3
55911	2.287	APOBR	3579	1.574	CXCR2
1843	2.276	DUSP1	6402	1.551	SELL
3936	2.26	LCP1	3059	1.484	HCLS1
3576	2.116	IL8	3937	1.477	LCP2
338442	2.092	HCAR2	2495	1.357	FTH1
4332	2.058	MNDA	7439	1.316	BEST1
5552	2.023	SRGN			
3851	2.023	KRT4			
1230	1.981	CCR1			
8291	1.98	DYSF			
3133	1.964	HLA-E			
3106	1.96	HLA-B			
7128	1.955	TNFAIP3			
1441	1.932	CSF3R			
2212	1.905	FCGR2A			
7408	1.868	VASP			
7538	1.849	ZFP36			
3726	1.848	JUNB			
10135	1.845	NAMPT			
4542	1.808	MYO1F			
9021	1.806	SOCS3			
5997	1.806	RGS2			
9516	1.803	LITAF			

**Table11. Downregulated fetal genes in EPL compared to normal pregnancy**

Gene id	log2fold change	Symbol
6206	-3.665	RPS12
595	-3.539	CCND1
6181	-3.311	RPLP2
7184	-3.284	HSP90B1
10963	-3.186	STIP1
302	-3.183	ANXA2
1915	-3.155	EEF1A1
6124	-3.13	RPL4
9349	-3.102	RPL23
6205	-3.102	RPS11
3182	-2.992	HNRNPAB
6188	-2.94	RPS3
7531	-2.886	YWHAE
811	-2.846	CALR
4904	-2.844	YBX1
5315	-2.84	PKM
304	-2.84	ANXA2P2
6125	-2.788	RPL5
594839	-2.781	SNORA33
10594	-2.764	PRPF8
7052	-2.723	TGM2
6135	-2.718	RPL11
6185	-2.708	RPN2
821	-2.703	CANX
1938	-2.691	EEF2
654364	-2.647	NME1-NME2
6204	-2.63	RPS10
3015	-2.617	H2AFZ
64710	-2.615	NUCKS1
22948	-2.608	CCT5
6128	-2.601	RPL6
6167	-2.599	RPL37
60674	-2.588	GAS5
3945	-2.561	LDHB
6191	-2.547	RPS4X
2597	-2.546	GAPDH
308	-2.54	ANXA5
3688	-2.513	ITGB1
6143	-2.502	RPL19

Gene id	log2fold change	Symbol
3799	-2.493	KIF5B
3308	-2.484	HSPA4
7416	-2.462	VDAC1
1982	-2.461	EIF4G2
10959	-2.445	TMED2
6222	-2.436	RPS18
54443	-2.426	ANLN
5885	-2.422	RAD21
6152	-2.417	RPL24
7027	-2.417	TFDP1
2280	-2.414	FKBP1A
3939	-2.383	LDHA
3326	-2.382	HSP90AB1
6176	-2.372	RPLP1
6232	-2.362	RPS27
1.01E+08	-2.349	RPS10-NUDT3
6160	-2.339	RPL31
3843	-2.337	IPO5
5757	-2.329	PTMA
3313	-2.323	HSPA9
7169	-2.315	TPM2
22974	-2.31	TPX2
6194	-2.309	RPS6
23193	-2.309	GANAB
11167	-2.299	FSTL1
6210	-2.296	RPS15A
23521	-2.294	RPL13A
3608	-2.294	ILF2
908	-2.285	CCT6A
2923	-2.279	PDIA3
93621	-2.278	MRFAP1
284119	-2.275	PTRF
6129	-2.269	RPL7
9761	-2.253	MLEC
351	-2.25	APP
1937	-2.25	EEF1G
5901	-2.245	RAN
7431	-2.245	VIM
22836	-2.242	RHOBTB3

Gene id	log2fold change	Symbol
8754	-2.226	ADAM9
629	-2.224	CFB
813	-2.218	CALU
2288	-2.21	FKBP4
619564	-2.206	SNORD72
5718	-2.191	PSMD12
372	-2.19	ARCN1
10112	-2.188	KIF20A
6155	-2.185	RPL27
4628	-2.172	MYH10
29789	-2.165	OLA1
6169	-2.151	RPL38
47	-2.151	ACLY
5478	-2.147	PPIA
51406	-2.14	NOL7
6122	-2.136	RPL3
6130	-2.128	RPL7A
125144	-2.126	C17orf76-AS1
3181	-2.124	HNRNPA2B1
2201	-2.123	FBN2
4430	-2.122	MYO1B
10606	-2.12	PAICS
10562	-2.117	OLFM4
6233	-2.111	RPS27A
6175	-2.106	RPLP0
8872	-2.104	CDC123
10197	-2.098	PSME3
5688	-2.094	PSMA7
6217	-2.09	RPS16
488	-2.081	ATP2A2
6780	-2.067	STAU1
1662	-2.065	DDX10
826	-2.054	CAPNS1
56910	-2.052	STARD7
7520	-2.013	XRCC5
5707	-2.01	PSMD1
3998	-2.007	LMAN1
3875	-1.994	KRT18
9052	-1.993	GPRC5A
51400	-1.992	PPME1

Gene id	log2fold change	Symbol
124801	-1.992	LSM12
7913	-1.991	DEK
11222	-1.987	MRPL3
4288	-1.978	MKI67
2195	-1.977	FAT1
3069	-1.971	HDLBP
1.01E+08	-1.971	SEN3-EIF4A1
6590	-1.971	SLPI
84154	-1.967	RPF2
718	-1.967	C3
857	-1.967	CAV1
23435	-1.962	TARDBP
2547	-1.959	XRCC6
58517	-1.958	RBM25
1973	-1.958	EIF4A1
6790	-1.958	AURKA
6189	-1.953	RPS3A
2247	-1.947	FGF2
9588	-1.944	PRDX6
5591	-1.936	PRKDC
1282	-1.934	COL4A1
6134	-1.93	RPL10
10568	-1.928	SLC34A2
476	-1.924	ATP1A1
6133	-1.924	RPL9
140609	-1.922	NEK7
6289	-1.921	SAA2
7529	-1.92	YWHAB
805	-1.916	CALM2
6171	-1.915	RPL41
1786	-1.914	DNMT1
5962	-1.914	RDX
7178	-1.911	TPT1
2131	-1.911	EXT1
7812	-1.907	CSDE1
23215	-1.907	PRRC2C
23028	-1.904	KDM1A
9805	-1.898	SCRN1
80014	-1.897	WWC2
6228	-1.895	RPS23

Gene id	log2fold change	Symbol
967	-1.893	CD63
3915	-1.89	LAMC1
3187	-1.886	HNRNPH1
6599	-1.886	SMARCC1
6613	-1.879	SUMO2
9221	-1.878	NOLC1
51747	-1.874	LUC7L3
9897	-1.873	KIAA0196
9669	-1.866	EIF5B
6136	-1.865	RPL12
6229	-1.865	RPS24
1173	-1.862	AP2M1
9055	-1.855	PRC1
1984	-1.849	EIF5A
4436	-1.847	MSH2
3184	-1.844	HNRNPD
79026	-1.843	AHNAK
6202	-1.839	RPS8
11014	-1.838	KDELR2
54407	-1.837	SLC38A2
26585	-1.835	GREM1
7057	-1.832	THBS1
2935	-1.83	GSPT1
1315	-1.826	COPB1
1E+08	-1.808	MTRNR2L8
1457	-1.807	CSNK2A1
9045	-1.804	RPL14
1431	-1.802	CS
7266	-1.8	DNAJC7
4673	-1.798	NAP1L1
4057	-1.796	LTF
7414	-1.795	VCL
10521	-1.793	DDX17
94025	-1.791	MUC16
2335	-1.791	FN1
10769	-1.779	PLK2
7082	-1.775	TJP1
27316	-1.773	RBMX
11217	-1.771	AKAP2
9126	-1.771	SMC3

Gene id	log2fold change	Symbol
689	-1.77	BTF3
8886	-1.768	DDX18
10399	-1.767	GNB2L1
2058	-1.765	EPRS
51495	-1.765	PTPLAD1
114908	-1.764	TMEM123
10250	-1.762	SRRM1
9793	-1.76	CKAP5
23603	-1.756	CORO1C
8615	-1.751	USO1
10199	-1.75	MPHOSPH10
5411	-1.748	PNN
6147	-1.746	RPL23A
2746	-1.74	GLUD1
23367	-1.739	LARP1
23524	-1.737	SRRM2
4670	-1.736	HNRNPM
51474	-1.734	LIMA1
9987	-1.726	HNRNPDL
10128	-1.723	LRPPRC
26135	-1.72	SERBP1
5955	-1.713	RCN2
2956	-1.71	MSH6
27101	-1.709	CACYBP
6154	-1.707	RPL26
3192	-1.699	HNRNPU
445815	-1.696	PALM2-AKAP2
214	-1.694	ALCAM
8394	-1.694	PIP5K1A
3376	-1.691	IARS
23020	-1.681	SNRNP200
4144	-1.679	MAT2A
3178	-1.676	HNRNPA1
1965	-1.67	EIF2S1
6059	-1.669	ABCE1
26509	-1.668	MYOF
1303	-1.668	COL12A1
1933	-1.668	EEF1B2
9804	-1.654	TOMM20
7430	-1.649	EZR



Gene id	log2fold change	Symbol
55706	-1.642	NDC1
10276	-1.64	NET1
2040	-1.635	STOM
9879	-1.635	DDX46
667	-1.634	DST
6421	-1.628	SFPQ
6385	-1.626	SDC4
6201	-1.624	RPS7
7037	-1.619	TFRC
4076	-1.615	CAPRIN1
4735	-1.591	2-Sep
3655	-1.577	ITGA6
1213	-1.576	CLTC
3646	-1.575	EIF3E

Gene id	log2fold change	Symbol
22872	-1.574	SEC31A
7874	-1.573	USP7
7415	-1.553	VCP
1778	-1.53	DYNC1H1
10490	-1.527	VTI1B
9908	-1.522	G3BP2
8500	-1.512	PPFIA1
6709	-1.501	SPTAN1
1981	-1.5	EIF4G1
1495	-1.488	CTNNA1
51280	-1.482	GOLM1
79832	-1.477	QSER1
6651	-1.472	SON

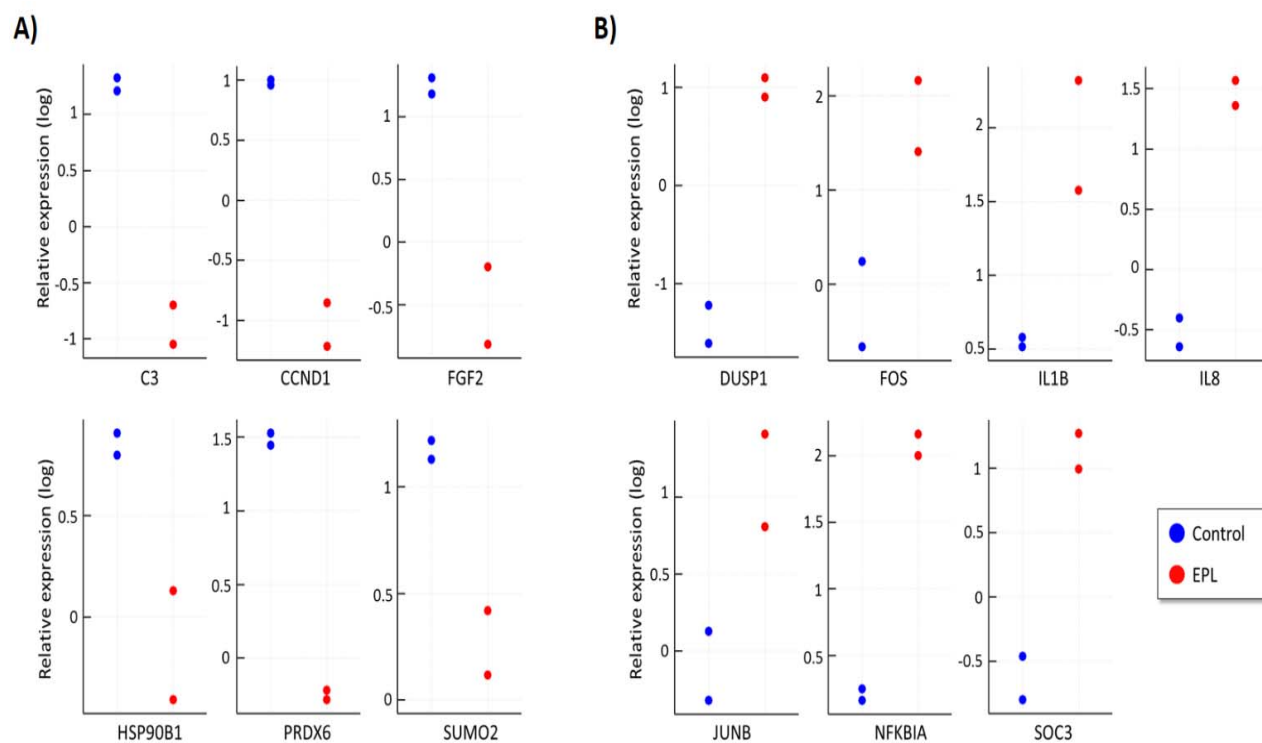


**Figure 26: Real-time qPCR validation of selected differentially expressed genes.** Shown are 6 down-regulated (A) and 7 up-regulated (B) genes in EPL (n=2) compared to control (n=2) pregnancies for fetal cells. The trends match that predicted by RNAseq results for each of the genes.

### *Gene Ontology Consortium analysis for DEGs in EPL*

For gene ontology (GO) analysis the differentially expressed transcripts between the fetal

cells from EPL and fetal normal pregnancies were analyzed using Genomatix pathway analysis. The analysis generated pathways such as apoptosis (Figure 27A), inflammation (Figure 27B) and placental disease (Figure 27C) that are expected to be involved in placental insufficiency and EPL. This result supports our hypothesis that cells isolated by TRIC are EVT like fetal cells that accurately reflect pathologies of pregnancy associated with placental EVT deficiencies. Due to the small number of subjects (n=2) for the EPL group, Genomatix was used for initial analysis.

## Discussion

Uteroplacental insufficiency is at least in part caused by defects affecting all EVT cells independently of their location at either the implantation site or cervix. Recent published findings (Fritz et al., 2015a) reveal a strong correlation early in gestation between cervical EVT expression patterns of several proteins suspected of involvement in uteroplacental insufficiency and adverse pregnancy outcomes such as EPL (Fritz et al., 2015a). The exact origin and biology of EVT-like cells residing in the cervix, and their relationship to the human placenta and pregnancy outcomes, are widely unknown. Based the information gathered so far, it can be hypothesized that, as the placenta grows, EVT cells are naturally shed into the cervical canal, and their overall phenotype is comparable to the EVT cells residing in the placenta. Any differences found in their RNA expression profiles could reflect the influences of the respective local environments. Previously, investigators have tried to harness the cervical cells, but have failed to get a pure population. In this study, for the first time using TRIC it has been possible to study the transcriptomic signature of EVT like fetal cells that were obtained in a noninvasive fashion as early as 5 week of gestation and utilize them as an experimental paradigm to investigate placental pathophysiology.

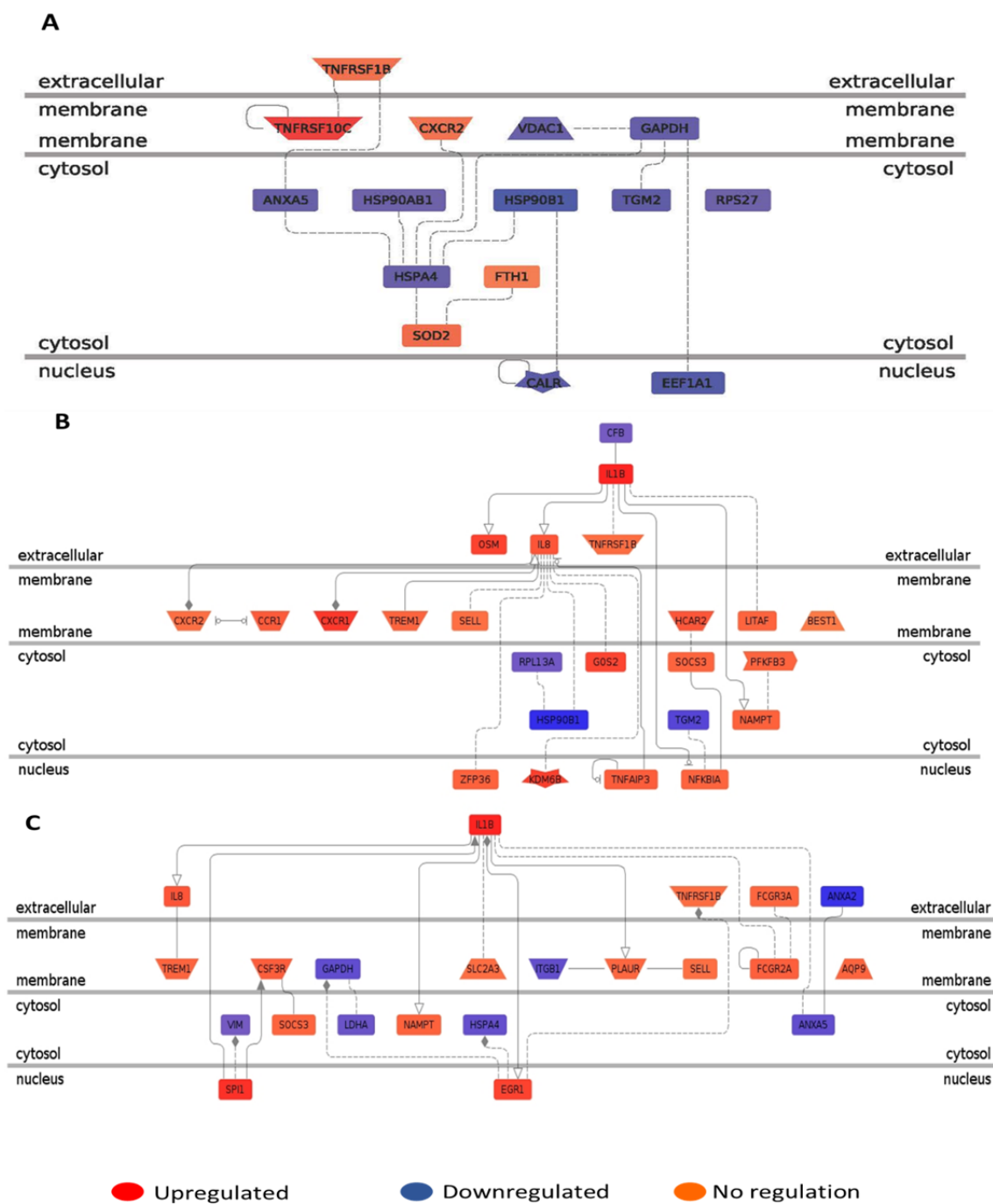


**Figure 27. Pathway Analysis for EPL.** Potential regulatory networks identified by Genomatix pathway analysis for genes differentially expressed between fetal EPL and control pregnancies. A. Apoptosis. B. Inflammation. C. Placental disease. Upregulated genes represented in red, downregulated in blue, and no regulation in orange, according to the key at bottom of figure.

TRIC provides ample RNA from isolated EVT cells for extensive transcriptomic analysis. Statistical analysis of TRIC/RNAseq data revealed 428 genes differed significantly (Figure 22) between cervical EVT and maternal cells of which trophoblast specific genes were validated using RT-PCR. mRNA expression of cervical EVT cells showed not only higher expression trophoblast markers such as HLA-G and KRT7 but also a higher expression of invasion/migration markers like CDH5 and MMP9. Additionally, lower expression of epithelial markers like CDH1 and ITGA6 was also seen in these EVT like fetal cells.

Expression of trophoblast specific markers, trophoblast invasion/migration markers and epithelial markers suggests an epithelial -mesenchymal transition (EMT). During implantation and subsequent placentation cells of the trophoblast that are known to be precursors of cytotrophoblast undergo EMT that induces trophoblast invasion and anchoring of the villi into maternal decidua to promote nutrient and gas exchange (Aplin et al., 1998; Bischof et al., 2006; Vicovac and Aplin, 1996). EMT results in the loss of junction and polarity of epithelial cells results in a reorganization of their cytoskeleton, reprogramming of gene expression and initiation of increased motility and invasive phenotype (Thiery et al., 2009; Thiery and Sleeman, 2006). Interestingly, bioinformatics analysis on the differentially regulated genes between the maternal and EVT like fetal cells generated pathways involved in invasion, migration and proliferation as the top scored (Figure 24). Based on the mRNA expression of cells isolated by TRIC it can therefore be hypothesized that the isolated cells are indeed EVT like and could have undergone EMT.

Overall, this data indicated the expected phenotypic similarities of the two trophoblast populations, and suggested that cervical EVT were mostly fully differentiated EVT. Based on these findings, we conclude that cDNA libraries can be constructed from RNA isolated cervical

EVT cells and reproducibly sequenced by NGS. Furthermore, libraries produced from different cell types show expected differences. Significant differences were measured in gene expression between first trimester samples with early pregnancy loss and normal term deliveries (Figure 25). A comparison of the EVT like fetal cells from normal term deliveries and those from early pregnancy loss generated a total of 348 differentially expressed genes. Of these some of the genes upregulated in the EPL group such as FOS (Sitras et al., 2009), IL1B (Hefler et al., 2001), IL8 (Shimoya et al., 1999) and NFkB (Vaughan and Walsh, 2012) have been reported to be associated with placental insufficiencies such as PE, IUGR and recurrent pregnancy loss based on studies done using placental tissue or from maternal serum. Bioinformatics pathway analysis of the differentially expressed genes in pregnancies with EPL represented several interesting pathways, including inflammation, apoptosis and placental disease (Figure 27). These are not unexpected findings, and they support the validity of our data. TRIC provides the platform to now study these genes on a global aspect. Transcriptome signatures associated with poor placentation will identify novel targets for preclinical testing with very high sensitivity and specificity. This avenue of translational investigation will significantly accelerate our ability to diagnose and monitor perinatal disease, and is likely to facilitate experimental and clinical breakthroughs beneficial to patients who succumb to obstetrical disorders that arise from uteroplacental insufficiency.

Due to the fact that EVT invasion and conversion of maternal spiral arteries occurs in the first and early second trimesters, the unique transcriptomes of patients with disease arising from poor placentation will help to identify new biomarkers for assessment of disease risk. Though, the heterogeneous nature of these pathologies and variations in patient genetics and environmental factors gives rise to differences in expression of some genes among individual

specimens within each cohort. Yet this platform has, for the first time, made it possible to tract the changes in EVT physiology and identifies many new potential biomarkers. This study will help unravel molecular mechanisms governing uteroplacental insufficiency and the lay the foundation for subsequent studies to evaluate larger cohorts. TRIC is a novel platform for noninvasive, real time placental assessment, and pre-clinical prediction of specific abnormal pregnancy outcomes. It provides the means to identify patients at high risk for disease as a research tool for evaluating first trimester interventions and new patient management strategies.

## CHAPTER 6 - CONCLUSION

Two approaches were undertaken to investigate the etiology of placental insufficiency. The first involved a focused study of HBEGF, which was known to regulate trophoblast survival and invasion, and becomes dysregulated in PE (Brosens et al., 1972; DiFederico et al., 1999). Secondly, an unbiased global approach based on NGS and systems biology to explore the EVT transcriptome by leveraging a novel, innovative approach to capture EVT like cells non-invasively from ongoing pregnancies.

Previous studies indicated that HBEGF is post-transcriptionally regulated by  $O_2$  through a dual mechanism in which proHBEGF is cleaved by metalloproteinases at low  $O_2$ , and the released sHBEGF induces downstream signaling through MAPKs to mobilize its dormant mRNA (Armant et al., 2006; Jessmon et al., 2010). Using an established trophoblast cell line and a villous explant model, we have established a role for HSPA6 (HSP70B'), a HIF-regulated gene, in the upregulation of MMP2 required for HBEGF shedding and subsequent survival signaling at low  $O_2$  (Chapter 2). These key components of the trophoblast survival pathway could be required during early placentation and their disruption could contribute to placental insufficiency.

To further investigate the upregulation of HBEGF by low  $O_2$ , we examined the pathway downstream of its shedding, which autoregulates its accumulation. The goal was to determine how dormant HBEGF mRNA becomes translated, hypothesizing that miRNA is involved. Global analysis of miRNA by RNAseq demonstrated that the mechanism did not involve a change in miRNA expression. Demonstration for a role of the miRNA through DGCR8 knockdown with siRNA suggested that other components of the RISC could contribute to the regulation of HBEGF mRNA translation (Chapter 3). The elucidation of this complex regulatory

mechanism could provide important insights into trophoblast survival during early placentation, and its disruption in pregnancies with developmental pathologies. However, HBEGF and other components of the EGF signaling system are disrupted in placentas of women with PE (Armant et al., 2015; Leach et al., 2002a). Previous studies have shown that the survival and invasive function of EVT cells is under the regulation of numerous pathways involving growth factors, cell surface proteins and extracellular matrix components (Cross et al., 1994; Fritz et al., 2014; Lala and Hamilton, 1996). Therefore, there is need to study trophoblast development using a global platform.

TRIC is a novel approach to non-invasively acquire EVT cells hypothesized to be central for proper placentation during the first half of pregnancy. Using rigorous genetic analysis of cells isolated by TRIC, we have shown that they are indeed fetal in origin (Chapter 4). Additionally, isolation of fetal cells by TRIC followed by NGS provides an advantageous platform for perinatal diagnostics as that is the first to offer noninvasive fetal genetic and perinatal disease testing as early as 5 weeks of gestation, which compares favorably to the current available options.

We applied the TRIC platform to investigate the transcriptome of fetal cells from ongoing pregnancies with known outcomes as a strategy to identify molecules contributing to placental insufficiencies (Chapter 5). Evidence was provided that cells obtained by TRIC expressed many known trophoblast markers, indicating an EVT phenotype. Therefore, TRIC can provide a novel window into the molecular mechanisms controlling EVT cells during development and pathology. Based on their expression of genes associated with the EVT phenotype, it is interesting to note that displacement to the cervix has not greatly altered these cells due to a new environment. Further analysis by direct comparison to authentic EVT cells is



necessary to establish the extent of impact from this dislocation. Our pilot study provides an initial view of transcripts that are differentially expressed between EVT cells of normal term pregnancies and those that end in an EPL. Here, we postulate that EPL is the result of severe placental insufficiency. In using TRIC, we are the first to examine EVT cells in the first trimester from pregnancies with known outcomes. We can report, based on the altered expression of 348 genes, that the EVT cells are indeed disrupted in placental insufficiencies, as long hypothesized (Burton and Jauniaux, 2004).

Fritz et al, found a half-dozen proteins that altered in EVT cells from the cervix of patients that had an EPL, compared to those with a normal term pregnancy (Fritz et al., 2015a), confirming expectations based on published changes in serum levels of those proteins at much later times during gestation. Recent studies demonstrated the same protein changes in cervical EVT cells from patients that later developed FGR or PE (Bolnick et al., in press), suggesting a relationship between those proteins and EVT failure to remodel the spiral arteries prior to placental insufficiency. It would be interesting to determine global molecular changes in EVT cells associated with disease, using transcriptomic, proteomic and other systems biology approaches. Here, we have found through bioinformatics differences between EVT and maternal cells indicative of EMT. Additionally, the differentially expressed genes in pregnancies with EPL represented several interesting pathways, including inflammation, apoptosis, placental disease and gestation trophoblastic disease. These are not unexpected findings, and they support the validity of our data. Future pre-clinical studies with greater sample numbers should be conducted to firmly establish molecular profiles of control and disease pregnancies to provide insight into changes in signaling pathways associated with placental insufficiencies.

Comparisons among cohorts of EVT cells obtained by TRIC that are associated with

normal or adverse pregnancy outcomes could provide an in-depth validation that these cells accurately reflect pathologies arising from EVT deficiencies, as supported by our data. These studies will provide a clearer view of the utility of EVT cells as a platform for perinatal testing to predict maternal risk of placenta-based disease. The current choice of biomarkers for adverse outcomes is limited to a few found in serum, usually late in gestation. Screening the fetal genome, proteome and transcriptome by TRIC during the first trimester will expand the pool of potential biomarkers by several orders of magnitude.

Although neither HBEGF nor MMP2 gene expression was altered by EPL, we did find a decrease in expression of HSP90B. HSP90 works with HSP70 (Hernandez et al., 2002; Wegele et al., 2004), a critical gene in HBEGF upregulation (Chapter 2). Based on findings in Chapters 2 and 3, we know that HBEGF is post-transcriptionally regulated. In the future, proteomics could be used to investigate components of the RISC affected by placental insufficiency that could be involved in HBEGF regulation. While the studies in this dissertation have raised many questions, the findings provide a way forward towards understanding mechanisms that regulate trophoblast survival and differentiation using the TRIC platform in conjunction with a systems biology approach.

## APPENDIX

## IRB Approval Letter

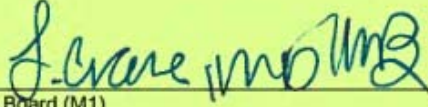
**WAYNE STATE  
UNIVERSITY**

IRB Administration Office  
87 East Canfield, Second Floor  
Detroit, Michigan 48201  
Phone: (313) 577-1628  
FAX: (313) 993-7122  
<http://lrb.wayne.edu>

---

**NOTICE OF FULL BOARD CONTINUATION APPROVAL**

**To:** David Armant  
Obstetrics/Gynecology  
339 Mott Center

**From:** Lawrence R. Crane, M.D. or designee   
Chairman, Medical Institutional Review Board (M1)

**Date:** July 07, 2016

**RE:** IRB #: 100206M1F  
Protocol Title: Use of Cervical Secretions to Predict Pregnancy Outcomes  
Funding Source: Unit: Obstetrics/Gynecology  
Protocol #: 0609004132

**Expiration Date:** July 06, 2017

**Risk Level / Category:** Research not involving greater than minimal risk

---

Continuation for the above-referenced protocol and items listed below (if applicable) were **APPROVED** following Full Board review by the Wayne State University Institutional Review Board (M1) for the period of 07/07/2016 through 07/06/2017. This approval does not replace any departmental or other approvals that may be required.

- Actively accruing participants
- Research Informed Consent with HIPAA Authorization (revision dated 6/10/15)
- Research Informed Consent - Las Vegas Site (revision dated 6/10/15)

- 
- Federal regulations require that all research be reviewed at least annually. You may receive a "Continuation Renewal Reminder" approximately two months prior to the expiration date; however, it is the Principal Investigator's responsibility to obtain review and continued approval *before* the expiration date. Data collected during a period of lapsed approval is unapproved research and can never be reported or published as research data.
  - All changes or amendments to the above-referenced protocol require review and approval by the IRB **BEFORE** implementation.
  - Adverse Reactions/Unexpected Events (AR/UE) must be submitted on the appropriate form within the timeframe specified in the IRB Administration Office Policy (<http://www.lrb.wayne.edu/policies-human-research.php>).

**NOTE:**

1. Upon notification of an impending regulatory site visit, hold notification, and/or external audit the IRB Administration Office must be contacted immediately.
2. Forms should be downloaded from the IRB website at each use.

Notify the IRB of any changes to the funding status of the above-referenced protocol.

## REFERENCES

1. (2015). Committee Opinion No. 640: Cell-Free DNA Screening For Fetal Aneuploidy. *Obstet Gynecol* 126, e31-37.
2. Abravaya, K., Myers, M. P., Murphy, S. P. and Morimoto, R. I. (1992). The human heat shock protein hsp70 interacts with HSF, the transcription factor that regulates heat shock gene expression. *Genes Dev* 6, 1153-1164.
3. Adams, B. D., Claffey, K. P. and White, B. A. (2009). Argonaute-2 expression is regulated by epidermal growth factor receptor and mitogen-activated protein kinase signaling and correlates with a transformed phenotype in breast cancer cells. *Endocrinology* 150, 14-23.
4. Adamson, S. L., Lu, Y., Whiteley, K. J., Holmyard, D., Hemberger, M., Pfarrer, C. and Cross, J. C. (2002). Interactions between trophoblast cells and the maternal and fetal circulation in the mouse placenta. *Dev Biol* 250, 358-373.
5. Adinolfi, M. and Sherlock, J. (1997). First trimester prenatal diagnosis using transcervical cells: an evaluation. *Hum Reprod Update* 3, 383-392.
6. Adinolfi M, Sherlock J. (2001). Fetal cells in transcervical samples at an early stage of gestation. *Journal of Human Genetics* 46, 99-104.
7. Aghajanova, L., Bjuresten, K., Altmae, S., Landgren, B. M. and Stavreus-Evers, A. (2008). HB-EGF but not amphiregulin or their receptors HER1 and HER4 is altered in endometrium of women with unexplained infertility. *Reprod Sci* 15, 484-492.
8. Allaire, A. D., Ballenger, K. A., Wells, S. R., McMahon, M. J. and Lessey, B. A. (2000). Placental apoptosis in preeclampsia. *Obstet Gynecol* 96, 271-276.
9. Ananthan, J., Goldberg, A. L. and Voellmy, R. (1986). Abnormal proteins serve as eukaryotic stress signals and trigger the activation of heat shock genes. *Science* 232, 522-

- 524.
10. Anders, S. and Huber, W. (2010). Differential expression analysis for sequence count data. *Genome Biol* 11, R106.
  11. Aplin, J. D., Haigh, T., Vicovac, L., Church, H. J. and Jones, C. J. (1998). Anchorage in the developing placenta: an overlooked determinant of pregnancy outcome? *Hum Fertil (Camb)* 1, 75-79.
  12. Armant, D. R., Fritz, R., Kilburn, B. A., Kim, Y. M., Nien, J. K., Maihle, N. J., Romero, R. and Leach, R. E. (2015). Reduced expression of the epidermal growth factor signaling system in preeclampsia. *Placenta* 36, 270-278.
  13. Armant, D. R., Kilburn, B. A., Petkova, A., Edwin, S. S., Duniec-Dmuchowski, Z. M., Edwards, H. J., Romero, R. and Leach, R. E. (2006). Human trophoblast survival at low oxygen concentrations requires metalloproteinase-mediated shedding of heparin-binding EGF-like growth factor. *Development* 133, 751-759.
  14. Baek, D., Villen, J., Shin, C., Camargo, F. D., Gygi, S. P. and Bartel, D. P. (2008). The impact of microRNAs on protein output. *Nature* 455, 64-71.
  15. Baird, N. A., Turnbull, D. W. and Johnson, E. A. (2006). Induction of the heat shock pathway during hypoxia requires regulation of heat shock factor by hypoxia-inducible factor-1. *J Biol Chem* 281, 38675-38681.
  16. Barad, O., Meiri, E., Avniel, A., Aharonov, R., Barzilai, A., Bentwich, I., Einav, U., Gilad, S., Hurban, P., Karov, Y., et al. (2004). MicroRNA expression detected by oligonucleotide microarrays: system establishment and expression profiling in human tissues. *Genome Res* 14, 2486-2494.
  17. Barrett, A. N., McDonnell, T. C., Chan, K. C. and Chitty, L. S. (2012). Digital PCR

- analysis of maternal plasma for noninvasive detection of sickle cell anemia. *Clin Chem* 58, 1026-1032.
18. Bartel, D. P. (2004). MicroRNAs: genomics, biogenesis, mechanism, and function. *Cell* 116, 281-297.
  19. Bass, K. E., Morrish, D., Roth, I., Bhardwaj, D., Taylor, R., Zhou, Y. and Fisher, S. J. (1994). Human cytotrophoblast invasion is up-regulated by epidermal growth factor: evidence that paracrine factors modify this process. *Dev Biol* 164, 550-561.
  20. Bastek, J. A. and Elovitz, M. A. (2013). The role and challenges of biomarkers in spontaneous preterm birth and preeclampsia. *Fertil Steril* 99, 1117-1123.
  21. Baudouin-Legros, M., Hinzpeter, A., Jaulmes, A., Brouillard, F., Costes, B., Fanen, P. and Edelman, A. (2005). Cell-specific posttranscriptional regulation of CFTR gene expression via influence of MAPK cascades on 3'UTR part of transcripts. *Am J Physiol Cell Physiol* 289, C1240-1250.
  22. Ben-Baruch, N. and Yarden, Y. (1994). Neu differentiation factors: a family of alternatively spliced neuronal and mesenchymal factors. *Proc Soc Exp Biol Med* 206, 221-227.
  23. Bianchi, D. W., Chudova, D., Sehnert, A. J., Bhatt, S., Murray, K., Prosen, T. L., Garber, J. E., Wilkins-Haug, L., Vora, N. L., Warsof, S., et al. (2015). Noninvasive Prenatal Testing and Incidental Detection of Occult Maternal Malignancies. *JAMA* 314, 162-169.
  24. Bischof, P., Aplin, J. D., Bentin-Ley, U., Brannstrom, M., Casslen, B., Castrillo, J. L., Classen-Linke, I., Critchley, H. O., Devoto, L., D'Hooghe, T., et al. (2006). Implantation of the human embryo: research lines and models. From the implantation research network 'Fruitful'. *Gynecol Obstet Invest* 62, 206-216.

25. Bischoff, F. Z. and Simpson, J. L. (2006). Endocervical fetal trophoblast for prenatal genetic diagnosis. *Curr Opin Obstet Gynecol* 18, 216-220.
26. Boisvert, F. M., Ahmad, Y., Gierlinski, M., Charriere, F., Lamont, D., Scott, M., Barton, G. and Lamond, A. I. (2012). A quantitative spatial proteomics analysis of proteome turnover in human cells. *Mol Cell Proteomics* 11, M111 011429.
27. Bolnick, J. M., Kilburn, B. A., Bajpayee, S., Reddy, N., Jeelani, R., Crone, B., Simmerman, N., Singh, M., Diamond, M. P. and Armant, D. R. (2014). Trophoblast retrieval and isolation from the cervix (TRIC) for noninvasive prenatal screening at 5 to 20 weeks of gestation. *Fertil Steril* 102, 135-142 e136.
28. Bolnick, J. M., Kilburn, B. A., Bolnick, A. D., Diamond, M. P., Singh, M., Hertz, M., Dai, J. and Armant, D. R. (2015). Sildenafil Prevents Apoptosis of Human First-Trimester Trophoblast Cells Exposed to Oxidative Stress: Possible Role for Nitric Oxide Activation of 3',5'-cyclic Guanosine Monophosphate Signaling. *Reprod Sci* 22, 718-724.
29. Brosens, I. A., Robertson, W. B. and Dixon, H. G. (1972). The role of the spiral arteries in the pathogenesis of preeclampsia. *Obstet Gynecol Annu* 1, 177-191.
30. Brown, N., Deb, K., Paria, B. C., Das, S. K. and Reese, J. (2004). Embryo-uterine interactions via the neuregulin family of growth factors during implantation in the mouse. *Biol Reprod* 71, 2003-2011.
31. Bujold, E., Roberge, S. and Nicolaides, K. H. (2014). Low-dose aspirin for prevention of adverse outcomes related to abnormal placentation. *Prenat Diagn* 34, 642-648.
32. Burden, S. and Yarden, Y. (1997). Neuregulins and their receptors: a versatile signaling module in organogenesis and oncogenesis. *Neuron* 18, 847-855.
33. Burton, G. J. (2009). Oxygen, the Janus gas; its effects on human placental development



- and function. *J Anat* 215, 27-35.
34. Burton, G. J. and Jauniaux, E. (2004). Placental oxidative stress: from miscarriage to preeclampsia. *J Soc Gynecol Investig* 11, 342-352.
  35. Burton, G. J., Jauniaux, E. and Watson, A. L. (1999). Maternal arterial connections to the placental intervillous space during the first trimester of human pregnancy: the Boyd collection revisited. *Am J Obstet Gynecol* 181, 718-724.
  36. Bussani, C., Cioni, R., Mattei, A., Fambrini, M., Marchionni, M. and Scarselli, G. (2007). Prenatal diagnosis of common aneuploidies in transcervical samples using quantitative fluorescent-PCR analysis. *Mol Diagn Ther* 11, 117-121.
  37. Bussani, C., Cioni, R., Scarselli, B., Barciulli, F., Bucciantini, S., Simi, P., Fogli, A. and Scarselli, G. (2002). Strategies for the isolation and detection of fetal cells in transcervical samples. *Prenat Diagn* 22, 1098-1101.
  38. Bustin, S. A., Benes, V., Garson, J. A., Hellemans, J., Huggett, J., Kubista, M., Mueller, R., Nolan, T., Pfaffl, M. W., Shipley, G. L., et al. (2009). The MIQE guidelines: minimum information for publication of quantitative real-time PCR experiments. *Clin Chem* 55, 611-622.
  39. Carrigan, P. E., Sikkink, L. A., Smith, D. F. and Ramirez-Alvarado, M. (2006). Domain:domain interactions within Hop, the Hsp70/Hsp90 organizing protein, are required for protein stability and structure. *Protein Sci* 15, 522-532.
  40. Cartharius, K., Frech, K., Grote, K., Klocke, B., Haltmeier, M., Klingenhoff, A., Frisch, M., Bayerlein, M. and Werner, T. (2005). MatInspector and beyond: promoter analysis based on transcription factor binding sites. *Bioinformatics* 21, 2933-2942.
  41. Castellucci, M., Kaufmann, P. and Bischof, P. (1990). Extracellular matrix influences



- hormone and protein production by human chorionic villi. *Cell Tissue Res* 262, 135-142.
42. Chaddha, V., Viero, S., Huppertz, B. and Kingdom, J. (2004). Developmental biology of the placenta and the origins of placental insufficiency. *Semin Fetal Neonatal Med* 9, 357-369.
  43. Chao, A., Tsai, C. L., Wei, P. C., Hsueh, S., Chao, A. S., Wang, C. J., Tsai, C. N., Lee, Y. S., Wang, T. H. and Lai, C. H. (2010). Decreased expression of microRNA-199b increases protein levels of SET (protein phosphatase 2A inhibitor) in human choriocarcinoma. *Cancer Lett* 291, 99-107.
  44. Chen, S. and Smith, D. F. (1998). Hop as an adaptor in the heat shock protein 70 (Hsp70) and hsp90 chaperone machinery. *J Biol Chem* 273, 35194-35200.
  45. Cheng, C. Y., Tseng, H. C. and Yang, C. M. (2012). Bradykinin-mediated cell proliferation depends on transactivation of EGF receptor in corneal fibroblasts. *J Cell Physiol* 227, 1367-1381.
  46. Chitty, L. S. and Bianchi, D. W. (2013). Noninvasive prenatal testing: the paradigm is shifting rapidly. *Prenat Diagn* 33, 511-513.
  47. Chobotova, K., Karpovich, N., Carver, J., Manek, S., Gullick, W. J., Barlow, D. H. and Mardon, H. J. (2005). Heparin-binding epidermal growth factor and its receptors mediate decidualization and potentiate survival of human endometrial stromal cells. *J Clin Endocrinol Metab* 90, 913-919.
  48. Chobotova, K., Muchmore, M. E., Carver, J., Yoo, H. J., Manek, S., Gullick, W. J., Barlow, D. H. and Mardon, H. J. (2002a). The mitogenic potential of heparin-binding epidermal growth factor in the human endometrium is mediated by the epidermal growth factor receptor and is modulated by tumor necrosis factor-alpha. *J Clin Endocrinol Metab*

- 87, 5769-5777.
49. Chobotova, K., Spyropoulou, I., Carver, J., Manek, S., Heath, J. K., Gullick, W. J., Barlow, D. H., Sargent, I. L. and Mardon, H. J. (2002b). Heparin-binding epidermal growth factor and its receptor ErbB4 mediate implantation of the human blastocyst. *Mech Dev* 119, 137-144.
  50. Chow, F. L. and Fernandez-Patron, C. (2007). Many membrane proteins undergo ectodomain shedding by proteolytic cleavage. Does one sheddase do the job on all of these proteins? *IUBMB Life* 59, 44-47.
  51. Christianson, A. and Modell, B. (2004). Medical genetics in developing countries. *Annu Rev Genomics Hum Genet* 5, 219-265.
  52. Churchill, J. D., Schmedes, S. E., King, J. L. and Budowle, B. (2016). Evaluation of the Illumina((R)) Beta Version ForenSeq DNA Signature Prep Kit for use in genetic profiling. *Forensic Sci Int Genet* 20, 20-29.
  53. Cock, P. J., Antao, T., Chang, J. T., Chapman, B. A., Cox, C. J., Dalke, A., Friedberg, I., Hamelryck, T., Kauff, F., Wilczynski, B., et al. (2009). Biopython: freely available Python tools for computational molecular biology and bioinformatics. *Bioinformatics* 25, 1422-1423.
  54. Contos, J. J., Ishii, I. and Chun, J. (2000). Lysophosphatidic acid receptors. *Mol Pharmacol* 58, 1188-1196.
  55. Cross, J. C., Werb, Z. and Fisher, S. J. (1994). Implantation and the placenta: key pieces of the development puzzle. *Science* 266, 1508-1518.
  56. Damsky, C. H., Librach, C., Lim, K. H., Fitzgerald, M. L., McMaster, M. T., Janatpour, M., Zhou, Y., Logan, S. K. and Fisher, S. J. (1994). Integrin switching regulates normal

- trophoblast invasion. *Development* 120, 3657-3666.
57. Das, S. K., Chakraborty, I., Paria, B. C., Wang, X. N., Plowman, G. and Dey, S. K. (1995). Amphiregulin is an implantation-specific and progesterone-regulated gene in the mouse uterus. *Mol Endocrinol* 9, 691-705.
  58. Das, S. K., Das, N., Wang, J., Lim, H., Schryver, B., Plowman, G. D. and Dey, S. K. (1997). Expression of betacellulin and epiregulin genes in the mouse uterus temporally by the blastocyst solely at the site of its apposition is coincident with the "window" of implantation. *Dev Biol* 190, 178-190.
  59. Das, S. K., Wang, X. N., Paria, B. C., Damm, D., Abraham, J. A., Klagsbrun, M., Andrews, G. K. and Dey, S. K. (1994). Heparin-binding EGF-like growth factor gene is induced in the mouse uterus temporally by the blastocyst solely at the site of its apposition: a possible ligand for interaction with blastocyst EGF-receptor in implantation. *Development* 120, 1071-1083.
  60. Davey, D. A. and MacGillivray, I. (1988). The classification and definition of the hypertensive disorders of pregnancy. *Am. J. Obstet. Gynecol.* 158, 892-898.
  61. De Baets, G., Reumers, J., Blanco, J. D., Dopazo, J., Schymkowitz, J. and Rousseau, F. (2011). An Evolutionary Trade-Off between Protein Turnover Rate and Protein Aggregation Favors a Higher Aggregation Propensity in Fast Degrading Proteins. *Plos Comput Biol* 7.
  62. Dethlefsen, S. M., Raab, G., Moses, M. A., Adam, R. M., Klagsbrun, M. and Freeman, M. R. (1998). Extracellular calcium influx stimulates metalloproteinase cleavage and secretion of heparin-binding EGF-like growth factor independently of protein kinase C. *J Cell Biochem* 69, 143-153.

63. DiFederico, E., Genbacev, O. and Fisher, S. J. (1999). Preeclampsia is associated with widespread apoptosis of placental cytotrophoblasts within the uterine wall. *Am J Pathol* 155, 293-301.
64. Dilworth, M. R. and Sibley, C. P. (2013). Review: Transport across the placenta of mice and women. *Placenta* 34 Suppl, S34-39.
65. Dong, J. and Wiley, H. S. (2000). Trafficking and proteolytic release of epidermal growth factor receptor ligands are modulated by their membrane-anchoring domains. *J Biol Chem* 275, 557-564.
66. Donker, R. B., Mouillet, J. F., Nelson, D. M. and Sadovsky, Y. (2007). The expression of Argonaute2 and related microRNA biogenesis proteins in normal and hypoxic trophoblasts. *Mol Hum Reprod* 13, 273-279.
67. Ekambaram, P. (2011). HSP70 expression and its role in preeclamptic stress. *Indian J Biochem Biophys* 48, 243-255.
68. Eleuterio, N. M., Palei, A. C. T., Machado, J. S. R., Tanus-Santos, J. E., Cavalli, R. C. and Sandrim, V. C. (2015). Positive correlations between circulating adiponectin and MMP2 in preeclampsia pregnant. *Pregnancy Hypertens* 5, 205-208.
69. Fabian, M. R., Sonenberg, N. and Filipowicz, W. (2010). Regulation of mRNA translation and stability by microRNAs. *Annu Rev Biochem* 79, 351-379.
70. Falls, D. L. (2003). Neuregulins: functions, forms, and signaling strategies. *Exp Cell Res* 284, 14-30.
71. Filipowicz, W., Bhattacharyya, S. N. and Sonenberg, N. (2008). Mechanisms of post-transcriptional regulation by microRNAs: are the answers in sight? *Nat Rev Genet* 9, 102-114.

72. Fritz, R., Jain, C. and Armant, D. R. (2014). Cell signaling in trophoblast-uterine communication. *Int J Dev Biol* 58, 261-271.
73. Fritz, R., Kohan-Ghadr, H. R., Bolnick, J. M., Bolnick, A. D., Kilburn, B. A., Diamond, M. P., Drewlo, S. and Armant, D. R. (2015a). Noninvasive detection of trophoblast protein signatures linked to early pregnancy loss using trophoblast retrieval and isolation from the cervix (TRIC). *Fertil Steril* 104, 339-346 e334.
74. Fritz, R., Kohan-Ghadr, H. R., Sacher, A., Bolnick, A. D., Kilburn, B. A., Bolnick, J. M., Diamond, M. P., Drewlo, S. and Armant, D. R. (2015b). Trophoblast retrieval and isolation from the cervix (TRIC) is unaffected by early gestational age or maternal obesity. *Prenat Diagn* 35, 1218-1222.
75. Fukushima, A., Kawahara, H., Isurugi, C., Syoji, T., Oyama, R., Sugiyama, T. and Horiuchi, S. (2005). Changes in serum levels of heat shock protein 70 in preterm delivery and pre-eclampsia. *J Obstet Gynaecol Res* 31, 72-77.
76. Fulda, S., Gorman, A. M., Hori, O. and Samali, A. (2010). Cellular stress responses: cell survival and cell death. *Int J Cell Biol* 2010, 214074.
77. Genbacev, O., Joslin, R., Damsky, C. H., Polliotti, B. M. and Fisher, S. J. (1996). Hypoxia alters early gestation human cytotrophoblast differentiation/invasion *in vitro* and models the placental defects that occur in preeclampsia. *J Clin Invest* 97, 540-550.
78. Genbacev, O., Schubach, S. A. and Miller, R. K. (1992). Villous culture of first trimester human placenta--model to study extravillous trophoblast (EVT) differentiation. *Placenta* 13, 439-461.
79. Genbacev, O., Zhou, Y., Ludlow, J. W. and Fisher, S. J. (1997). Regulation of human placental development by oxygen tension. *Science* 277, 1669-1672.

80. Gil, M. M., Quezada, M. S., Revello, R., Akolekar, R. and Nicolaides, K. H. (2015). Analysis of cell-free DNA in maternal blood in screening for fetal aneuploidies: updated meta-analysis. *Ultrasound Obstet Gynecol* 45, 249-266.
81. Goff, S. A. and Goldberg, A. L. (1985). Production of abnormal proteins in *E. coli* stimulates transcription of *lon* and other heat shock genes. *Cell* 41, 587-595.
82. Goldman-Wohl, D. S., Ariel, I., Greenfield, C., Hochner-Celnikier, D., Cross, J., Fisher, S. and Yagel, S. (2000). Lack of human leukocyte antigen-G expression in extravillous trophoblasts is associated with pre-eclampsia. *Mol Hum Reprod* 6, 88-95.
83. Graham, C. H., Fitzpatrick, T. E. and McCrae, K. R. (1998). Hypoxia stimulates urokinase receptor expression through a heme protein-dependent pathway. *Blood* 91, 3300-3307.
84. Graham, C. H., Hawley, T. S., Hawley, R. G., MacDougall, J. R., Kerbel, R. S., Khoo, N. and Lala, P. K. (1993). Establishment and characterization of first trimester human trophoblast cells with extended lifespan. *Exp Cell Res* 206, 204-211.
85. Gregory, R. I., Yan, K. P., Amuthan, G., Chendrimada, T., Doratotaj, B., Cooch, N. and Shiekhattar, R. (2004). The Microprocessor complex mediates the genesis of microRNAs. *Nature* 432, 235-240.
86. Gsponer, J. and Babu, M. M. (2012). Cellular strategies for regulating functional and nonfunctional protein aggregation. *Cell Rep* 2, 1425-1437.
87. Gsponer, J., Futschik, M. E., Teichmann, S. A. and Babu, M. M. (2008). Tight regulation of unstructured proteins: from transcript synthesis to protein degradation. *Science* 322, 1365-1368.
88. Haimovici, F. and Anderson, D. J. (1993). Effects of Growth-Factors and Growth Factor-

- Extracellular Matrix Interactions on Mouse Trophoblast Outgrowth in-Vitro. *Biol Reprod* 49, 124-130.
89. Hamatani, T., Daikoku, T., Wang, H., Matsumoto, H., Carter, M. G., Ko, M. S. and Dey, S. K. (2004). Global gene expression analysis identifies molecular pathways distinguishing blastocyst dormancy and activation. *Proc Natl Acad Sci U S A* 101, 10326-10331.
  90. Han, J., Lee, Y., Yeom, K. H., Kim, Y. K., Jin, H. and Kim, V. N. (2004). The Drosha-DGCR8 complex in primary microRNA processing. *Genes Dev* 18, 3016-3027.
  91. Head, S. R., Komori, H. K., LaMere, S. A., Whisenant, T., Van Nieuwerburgh, F., Salomon, D. R. and Ordoukhanian, P. (2014). Library construction for next-generation sequencing: overviews and challenges. *Biotechniques* 56, 61-64, 66, 68, passim.
  92. Hefler, L. A., Tempfer, C. B., Unfried, G., Schneeberger, C., Lessl, K., Nagele, F. and Huber, J. C. (2001). A polymorphism of the interleukin-1beta gene and idiopathic recurrent miscarriage. *Fertil Steril* 76, 377-379.
  93. Hentze, M. W. and Preiss, T. (2013). Circular RNAs: splicing's enigma variations. *EMBO J* 32, 923-925.
  94. Hernandez, M. P., Sullivan, W. P. and Toft, D. O. (2002). The assembly and intermolecular properties of the hsp70-Hop-hsp90 molecular chaperone complex. *J Biol Chem* 277, 38294-38304.
  95. Hitchon, C. A., Danning, C. L., Illei, G. G., El-Gabalawy, H. S. and Boumpas, D. T. (2002). Gelatinase expression and activity in the synovium and skin of patients with erosive psoriatic arthritis. *J Rheumatol* 29, 107-117.
  96. Hofmann, G. E., Drews, M. R., Scott, R. T., Jr., Navot, D., Heller, D. and Deligdisch, L.

- (1992). Epidermal growth factor and its receptor in human implantation trophoblast: immunohistochemical evidence for autocrine/paracrine function. *J Clin Endocrinol Metab* 74, 981-988.
97. Holbro, T. and Hynes, N. E. (2004). ErbB receptors: Directing key signaling networks throughout life. *Annu Rev Pharmacol* 44, 195-217.
  98. Horman, S. R., Janas, M. M., Litterst, C., Wang, B., MacRae, I. J., Sever, M. J., Morrissey, D. V., Graves, P., Luo, B., Umesalma, S., et al. (2013). Akt-mediated phosphorylation of argonaute 2 downregulates cleavage and upregulates translational repression of MicroRNA targets. *Mol Cell* 50, 356-367.
  99. Hossain, N. and Paidas, M. J. (2007). Adverse pregnancy outcome, the uteroplacental interface, and preventive strategies. *Semin Perinatol* 31, 208-212.
  100. Hung, T. H. and Burton, G. J. (2006). Hypoxia and reoxygenation: a possible mechanism for placental oxidative stress in preeclampsia. *Taiwan J Obstet Gynecol* 45, 189-200.
  101. Imudia, A. N., Kilburn, B. A., Petkova, A., Edwin, S. S., Romero, R. and Armant, D. R. (2008). Expression of heparin-binding EGF-like growth factor in term chorionic villous explants and its role in trophoblast survival. *Placenta* 29, 784-789.
  102. Imudia, A. N., Kumar, S., Diamond, M. P., DeCherney, A. H. and Armant, D. R. (2010). Transcervical retrieval of fetal cells in the practice of modern medicine: a review of the current literature and future direction. *Fertil Steril* 93, 1725-1730.
  103. Imudia, A. N., Suzuki, Y., Kilburn, B. A., Yelian, F. D., Diamond, M. P., Romero, R. and Armant, D. R. (2009). Retrieval of trophoblast cells from the cervical canal for prediction of abnormal pregnancy: a pilot study. *Hum Reprod* 24, 2086-2092.
  104. Isaka, K., Usuda, S., Ito, H., Sagawa, Y., Nakamura, H., Nishi, H., Suzuki, Y., Li, Y. F.



- and Takayama, M. (2003). Expression and activity of matrix metalloproteinase 2 and 9 in human trophoblasts. *Placenta* 24, 53-64.
105. Ishihara, N., Matsuo, H., Murakoshi, H., Laoag-Fernandez, J. B., Samoto, T. and Maruo, T. (2002). Increased apoptosis in the syncytiotrophoblast in human term placentas complicated by either preeclampsia or intrauterine growth retardation. *Am J Obstet Gynecol* 186, 158-166.
  106. Iwasaki, S., Kobayashi, M., Yoda, M., Sakaguchi, Y., Katsuma, S., Suzuki, T. and Tomari, Y. (2010). Hsc70/Hsp90 chaperone machinery mediates ATP-dependent RISC loading of small RNA duplexes. *Mol Cell* 39, 292-299.
  107. Jauniaux, E., Jurkovic, D. and Campbell, S. (1991). *In vivo* investigations of the anatomy and the physiology of early human placental circulations. *Ultrasound Obstet Gynecol* 1, 435-445.
  108. Jauniaux, E., Watson, A. and Burton, G. (2001). Evaluation of respiratory gases and acid-base gradients in human fetal fluids and uteroplacental tissue between 7 and 16 weeks' gestation. *Am J Obstet Gynecol* 184, 998-1003.
  109. Jessmon, P., Kilburn, B. A., Romero, R., Leach, R. E. and Armant, D. R. (2010). Function-Specific Intracellular Signaling Pathways Downstream of Heparin-Binding EGF-Like Growth Factor Utilized by Human Trophoblasts. *Biol Reprod* 82, 921-929.
  110. Jessmon, P., Leach, R. E. and Armant, D. R. (2009). Diverse functions of HBEGF during pregnancy. *Mol Reprod Dev* 76, 1116-1127.
  111. Jiang, B. H., Zheng, J. Z., Leung, S. W., Roe, R. and Semenza, G. L. (1997). Transactivation and inhibitory domains of hypoxia-inducible factor 1alpha. Modulation of transcriptional activity by oxygen tension. *J Biol Chem* 272, 19253-19260.

112. Jiao, J., Herl, L. D., Farese, R. V. and Gao, F. B. (2010). MicroRNA-29b regulates the expression level of human progranulin, a secreted glycoprotein implicated in frontotemporal dementia. *PLoS One* 5, e10551.
113. Jirecek, S., Hohlagschwandtner, M., Tempfer, C., Knofler, M., Husslein, P. and Zeisler, H. (2002). Serum levels of heat shock protein 70 in patients with preeclampsia: a pilot-study. *Wien Klin Wochenschr* 114, 730-732.
114. Jopling, C. L., Schutz, S. and Sarnow, P. (2008). Position-dependent function for a tandem microRNA miR-122-binding site located in the hepatitis C virus RNA genome. *Cell Host Microbe* 4, 77-85.
115. Jopling, C. L., Yi, M., Lancaster, A. M., Lemon, S. M. and Sarnow, P. (2005). Modulation of hepatitis C virus RNA abundance by a liver-specific MicroRNA. *Science* 309, 1577-1581.
116. Jovanovic, M., Stefanoska, I., Radojicic, L. and Vicovac, L. (2010). Interleukin-8 (CXCL8) stimulates trophoblast cell migration and invasion by increasing levels of matrix metalloproteinase (MMP)2 and MMP9 and integrins alpha5 and beta1. *Reproduction* 139, 789-798.
117. Katz-Jaffe, M. G., Mantzaris, D. and Cram, D. S. (2005). DNA identification of fetal cells isolated from cervical mucus: potential for early non-invasive prenatal diagnosis. *BJOG* 112, 595-600.
118. Kearse, M., Moir, R., Wilson, A., Stones-Havas, S., Cheung, M., Sturrock, S., Buxton, S., Cooper, A., Markowitz, S., Duran, C., et al. (2012). Geneious Basic: an integrated and extendable desktop software platform for the organization and analysis of sequence data. *Bioinformatics* 28, 1647-1649.

119. Khong, T. Y., De Wolf, F., Robertson, W. B. and Brosens, I. (1986). Inadequate maternal vascular response to placentation in pregnancies complicated by pre-eclampsia and by small-for-gestational age infants. *Br J Obstet Gynaecol* 93, 1049-1059.
120. Kidd, K. K., Pakstis, A. J., Speed, W. C., Grigorenko, E. L., Kajuna, S. L., Karoma, N. J., Kungulilo, S., Kim, J. J., Lu, R. B., Odunsi, A., et al. (2006). Developing a SNP panel for forensic identification of individuals. *Forensic Sci Int* 164, 20-32.
121. Kilburn, B. A., Wang, J., Duniec-Dmuchowski, Z. M., Leach, R. E., Romero, R. and Armant, D. R. (2000). Extracellular matrix composition and hypoxia regulate the expression of HLA-G and integrins in a human trophoblast cell line. *Biol Reprod* 62, 739-747.
122. Kim, D., Pertea, G., Trapnell, C., Pimentel, H., Kelley, R. and Salzberg, S. L. (2013). TopHat2: accurate alignment of transcriptomes in the presence of insertions, deletions and gene fusions. *Genome biology* 14, R36.
123. Kim, V. N. and Nam, J. W. (2006). Genomics of microRNA. *Trends Genet* 22, 165-173.
124. Knofler, M. and Pollheimer, J. (2013). Human placental trophoblast invasion and differentiation: a particular focus on Wnt signaling. *Front Genet* 4, 190.
125. Koritzinsky, M., Seigneure, R., Magagnin, M. G., van den Beucken, T., Lambin, P. and Wouters, B. G. (2005). The hypoxic proteome is influenced by gene-specific changes in mRNA translation. *Radiother Oncol* 76, 177-186.
126. Koumenis, C., Naczki, C., Koritzinsky, M., Rastani, S., Diehl, A., Sonenberg, N., Koromilas, A. and Wouters, B. G. (2002). Regulation of protein synthesis by hypoxia via activation of the endoplasmic reticulum kinase PERK and phosphorylation of the translation initiation factor eIF2 $\alpha$ . *Mol Cell Biol* 22, 7405-7416.

127. Kramer, M. S. (1987). Determinants of low birth weight: methodological assessment and meta-analysis. *Bull World Health Organ* 65, 663-737.
128. Kristensen, A. R., Gsponer, J. and Foster, L. J. (2013). Protein synthesis rate is the predominant regulator of protein expression during differentiation. *Mol Syst Biol* 9, 689.
129. Lala, P. K. and Hamilton, G. S. (1996). Growth factors, proteases and protease inhibitors in the maternal-fetal dialogue. *Placenta* 17, 545-555.
130. Landthaler, M., Yalcin, A. and Tuschl, T. (2004). The human DiGeorge syndrome critical region gene 8 and Its D. melanogaster homolog are required for miRNA biogenesis. *Curr Biol* 14, 2162-2167.
131. Larsen, E. C., Christiansen, O. B., Kolte, A. M. and Macklon, N. (2013). New insights into mechanisms behind miscarriage. *BMC Med* 11, 154.
132. Leach, R. E., Jessmon, P., Coutifaris, C., Kruger, M., Myers, E. R., Ali-Fehmi, R., Carson, S. A., Legro, R. S., Schlaff, W. D., Carr, B. R., et al. (2012). High throughput, cell type-specific analysis of key proteins in human endometrial biopsies of women from fertile and infertile couples. *Hum Reprod* 27, 814-828.
133. Leach, R. E., Khalifa, R., Ramirez, N. D., Das, S. K., Wang, J., Dey, S. K., Romero, R. and Armant, D. R. (1999). Multiple roles for heparin-binding epidermal growth factor-like growth factor are suggested by its cell-specific expression during the human endometrial cycle and early placentation. *J Clin Endocrinol Metab* 84, 3355-3363.
134. Leach, R. E., Kilburn, B., Wang, J., Liu, Z., Romero, R. and Armant, D. R. (2004). Heparin-binding EGF-like growth factor regulates human extravillous cytotrophoblast development during conversion to the invasive phenotype. *Dev Biol* 266, 223-237.
135. Leach, R. E., Kilburn, B. A., Petkova, A., Romero, R. and Armant, D. R. (2008).

- Diminished survival of human cytotrophoblast cells exposed to hypoxia/reoxygenation injury and associated reduction of heparin-binding epidermal growth factor-like growth factor. *Am J Obstet Gynecol* 198, 471 e471-477; discussion 471 e477-478.
136. Leach, R. E., Romero, R., Kim, Y. M., Chaiworapongsa, T., Kilburn, B., Das, S. K., Dey, S. K., Johnson, A., Qureshi, F., Jacques, S., et al. (2002a). Pre-eclampsia and expression of heparin-binding EGF-like growth factor. *Lancet* 360, 1215-1219.
  137. Leach, R. E., Romero, R., Kim, Y. M., Chaiworapongsa, T., Kilburn, B., Das, S. K., Dey, S. K., Johnson, A., Qureshi, F., Jacques, S., et al. (2002b). Pre-eclampsia and expression of heparin-binding EGF-like growth factor. *Lancet* 360, 1215-1219.
  138. Lee, D. S., Yanagimoto Ueta, Y. and Suzuki, H. (2006). Expression of amphiregulin during the pre- and post-implantation period in the mouse reproductive tract. *J Reprod Dev* 52, 781-787.
  139. Legewie, S., Herzel, H., Westerhoff, H. V. and Bluthgen, N. (2008). Recurrent design patterns in the feedback regulation of the mammalian signalling network. *Mol Syst Biol* 4, 190.
  140. Librach, C. L., Werb, Z., Fitzgerald, M. L., Chiu, K., Corwin, N. M., Esteves, R. A., Grobely, D., Galaray, R., Damsky, C. H. and Fisher, S. J. (1991). 92-kD type IV collagenase mediates invasion of human cytotrophoblasts. *J Cell Biol* 113, 437-449.
  141. Lim, H. J. and Dey, S. K. (2009). HB-EGF: a unique mediator of embryo-uterine interactions during implantation. *Exp Cell Res* 315, 619-626.
  142. Lindell, T. J., Weinberg, F., Morris, P. W., Roeder, R. G. and Rutter, W. J. (1970). Specific Inhibition of Nuclear Rna Polymerase Ii by Alpha-Amanitin. *Science* 170, 447-9
  143. Lisy, K. and Peet, D. J. (2008). Turn me on: regulating HIF transcriptional activity. *Cell*

- Death Differ* 15, 642-649.
144. Liu, Y., Li, N., You, L., Liu, X., Li, H. and Wang, X. (2008). HSP70 is associated with endothelial activation in placental vascular diseases. *Mol Med* 14, 561-566.
  145. Liu, Z. and Armant, D. R. (2004). Lysophosphatidic acid regulates murine blastocyst development by transactivation of receptors for heparin-binding EGF-like growth factor. *Exp Cell Res* 296, 317-326.
  146. Loffek, S., Schilling, O. and Franzke, C. W. (2011). Series "matrix metalloproteinases in lung health and disease": Biological role of matrix metalloproteinases: a critical balance. *Eur Respir J* 38, 191-208.
  147. Luetkeke, N. C., Qiu, T. H., Fenton, S. E., Troyer, K. L., Riedel, R. F., Chang, A. and Lee, D. C. (1999). Targeted inactivation of the EGF and amphiregulin genes reveals distinct roles for EGF receptor ligands in mouse mammary gland development. *Development* 126, 2739-2750.
  148. Luetkeke, N. C., Qiu, T. H., Peiffer, R. L., Oliver, P., Smithies, O. and Lee, D. C. (1993). TGF alpha deficiency results in hair follicle and eye abnormalities in targeted and waved-1 mice. *Cell* 73, 263-278.
  149. Maccani, M. A. and Marsit, C. J. (2009). Epigenetics in the placenta. *Am J Reprod Immunol* 62, 78-89.
  150. Machida, T., Taga, M. and Minaguchi, H. (1995). Effects of epidermal growth factor and transforming growth factor alpha on the mouse trophoblast outgrowth *in vitro*. *Eur J Endocrinol* 133, 741-746.
  151. Mann, G. B., Fowler, K. J., Gabriel, A., Nice, E. C., Williams, R. L. and Dunn, A. R. (1993). Mice with a null mutation of the TGF alpha gene have abnormal skin

- architecture, wavy hair, and curly whiskers and often develop corneal inflammation. *Cell* 73, 249-261.
152. Mantzaris, D. and Cram, D. S. (2015). Potential of syncytiotrophoblasts isolated from the cervical mucus for early non-invasive prenatal diagnosis: evidence of a vanishing twin. *Clin Chim Acta* 438, 309-315.
  153. Martin, K. L., Barlow, D. H. and Sargent, I. L. (1998). Heparin-binding epidermal growth factor significantly improves human blastocyst development and hatching in serum-free medium. *Hum Reprod* 13, 1645-1652.
  154. Meis, P. J., Goldenberg, R. L., Mercer, B. M., Iams, J. D., Moawad, A. H., Miodovnik, M., Menard, M. K., Caritis, S. N., Thurnau, G. R., Bottoms, S. F., et al. (1998). The preterm prediction study: risk factors for indicated preterm births. Maternal-Fetal Medicine Units Network of the National Institute of Child Health and Human Development. *Am. J. Obstet. Gynecol.* 178, 562-567.
  155. Meyer, D., Yamaai, T., Garratt, A., Riethmacher-Sonnenberg, E., Kane, D., Theill, L. E. and Birchmeier, C. (1997). Isoform-specific expression and function of neuregulin. *Development* 124, 3575-3586.
  156. Miettinen, P. J., Berger, J. E., Meneses, J., Phung, Y., Pedersen, R. A., Werb, Z. and Derynck, R. (1995). Epithelial immaturity and multiorgan failure in mice lacking epidermal growth factor receptor. *Nature* 376, 337-341.
  157. Mignone, F., Gissi, C., Liuni, S. and Pesole, G. (2002). Untranslated regions of mRNAs. *Genome Biol* 3, REVIEWS0004.
  158. Mohammad, M. A., Ismael, N. R., Shaarawy, S. M. and El-Merzabani, M. M. (2010). Prognostic value of membrane type 1 and 2 matrix metalloproteinase expression and

- gelatinase A activity in bladder cancer. *Int J Biol Marker* 25, 69-74.
159. Molvarec, A., Prohaszka, Z., Nagy, B., Szalay, J., Fust, G., Karadi, I. and Rigo, J., Jr. (2006). Association of elevated serum heat-shock protein 70 concentration with transient hypertension of pregnancy, preeclampsia and superimposed preeclampsia: a case-control study. *J Hum Hypertens* 20, 780-786.
  160. Molvarec, A., Rigo, J., Jr., Lazar, L., Balogh, K., Mako, V., Cervenak, L., Mezes, M. and Prohaszka, Z. (2009). Increased serum heat-shock protein 70 levels reflect systemic inflammation, oxidative stress and hepatocellular injury in preeclampsia. *Cell Stress Chaperones* 14, 151-159.
  161. Monk, J. M., Leonard, S., McBey, B. A. and Croy, B. A. (2005). Induction of murine spiral artery modification by recombinant human interferon-gamma. *Placenta* 26, 835-838.
  162. Montagnana, M., Lippi, G., Albiero, A., Scevarolli, S., Salvagno, G. L., Franchi, M. and Guidi, G. C. (2009). Evaluation of metalloproteinases 2 and 9 and their inhibitors in physiologic and pre-eclamptic pregnancy. *J Clin Lab Anal* 23, 88-92.
  163. Mouillet, J. F., Chu, T., Nelson, D. M., Mishima, T. and Sadovsky, Y. (2010). MiR-205 silences MED1 in hypoxic primary human trophoblasts. *FASEB J* 24, 2030-2039.
  164. Mouillet, J. F., Chu, T. and Sadovsky, Y. (2011). Expression patterns of placental microRNAs. *Birth Defects Res A Clin Mol Teratol* 91, 737-743.
  165. Mujezinovic, F. and Alfirevic, Z. (2007). Procedure-related complications of amniocentesis and chorionic villous sampling: a systematic review. *Obstet Gynecol* 110, 687-694.
  166. Myatt, L., Clifton, R. G., Roberts, J. M., Spong, C. Y., Hauth, J. C., Varner, M. W.,



- Wapner, R. J., Thorp, J. M., Jr., Mercer, B. M., Grobman, W. A., et al. (2012). The utility of uterine artery Doppler velocimetry in prediction of preeclampsia in a low-risk population. *Obstet Gynecol* 120, 815-822.
167. Myers, J. E., Merchant, S. J., Macleod, M., Mires, G. J., Baker, P. N. and Davidge, S. T. (2005). MMP-2 levels are elevated in the plasma of women who subsequently develop preeclampsia. *Hypertens Pregnancy* 24, 103-115.
168. Narumiya, H., Zhang, Y. L., Fernandez-Patron, C., Guilbert, L. J. and Davidge, S. T. (2001). Matrix metalloproteinase-2 is elevated in the plasma of women with preeclampsia. *Hypertens Pregnancy* 20, 185-194.
169. Nicolaides, K. H., Syngelaki, A., Gil, M., Atanasova, V. and Markova, D. (2013). Validation of targeted sequencing of single-nucleotide polymorphisms for non-invasive prenatal detection of aneuploidy of chromosomes 13, 18, 21, X, and Y. *Prenat Diagn* 33, 575-579.
170. Niranjana Kumari, S., Lasda, E., Brazas, R. and Garcia-Blanco, M. A. (2002). Reversible cross-linking combined with immunoprecipitation to study RNA-protein interactions *in vivo*. *Methods* 26, 182-190.
171. Nollen, E. A. and Morimoto, R. I. (2002). Chaperoning signaling pathways: molecular chaperones as stress-sensing 'heat shock' proteins. *J Cell Sci* 115, 2809-2816.
172. Norwitz, E. R., Schust, D. J. and Fisher, S. J. (2001). Implantation and the survival of early pregnancy. *N Engl J Med* 345, 1400-1408.
173. Obenaus, J. C., Cantley, L. C. and Yaffe, M. B. (2003). Scansite 2.0: Proteome-wide prediction of cell signaling interactions using short sequence motifs. *Nucleic Acids Res* 31, 3635-3641.

174. Onogi, A., Naruse, K., Sado, T., Tsunemi, T., Shigetomi, H., Noguchi, T., Yamada, Y., Akasaki, M., Oi, H. and Kobayashi, H. (2011). Hypoxia inhibits invasion of extravillous trophoblast cells through reduction of matrix metalloproteinase (MMP)-2 activation in the early first trimester of human pregnancy. *Placenta* 32, 665-670.
175. Orendi, K., Kivity, V., Sammar, M., Grimpel, Y., Gonen, R., Meiri, H., Lubzens, E. and Huppertz, B. (2011). Placental and trophoblastic *in vitro* models to study preventive and therapeutic agents for preeclampsia. *Placenta* 32 Suppl, S49-54.
176. Orom, U. A., Nielsen, F. C. and Lund, A. H. (2008). MicroRNA-10a binds the 5'UTR of ribosomal protein mRNAs and enhances their translation. *Mol Cell* 30, 460-471.
177. Ortiz-Barahona, A., Villar, D., Pescador, N., Amigo, J. and del Peso, L. (2010). Genome-wide identification of hypoxia-inducible factor binding sites and target genes by a probabilistic model integrating transcription-profiling data and in silico binding site prediction. *Nucleic Acids Res* 38, 2332-2345.
178. Pang, A. L., Peacock, S., Johnson, W., Bear, D. H., Rennert, O. M. and Chan, W. Y. (2009). Cloning, characterization, and expression analysis of the novel acetyltransferase retrogene *Ard1b* in the mouse. *Biol Reprod* 81, 302-309.
179. Pang, R. T., Leung, C. O., Ye, T. M., Liu, W., Chiu, P. C., Lam, K. K., Lee, K. F. and Yeung, W. S. (2010). MicroRNA-34a suppresses invasion through downregulation of Notch1 and Jagged1 in cervical carcinoma and choriocarcinoma cells. *Carcinogenesis* 31, 1037-1044.
180. Papageorgiou, A. T., Yu, C. K. and Nicolaides, K. H. (2004). The role of uterine artery Doppler in predicting adverse pregnancy outcome. *Best Pract Res Clin Obstet Gynaecol* 18, 383-396.

181. Paria, B. C., Das, S. K., Andrews, G. K. and Dey, S. K. (1993). Expression of the epidermal growth factor receptor gene is regulated in mouse blastocysts during delayed implantation. *Proc Natl Acad Sci U S A* 90, 55-59.
182. Paria, B. C., Elenius, K., Klagsbrun, M. and Dey, S. K. (1999). Heparin-binding EGF-like growth factor interacts with mouse blastocysts independently of ErbB1: a possible role for heparan sulfate proteoglycans and ErbB4 in blastocyst implantation. *Development* 126, 1997-2005.
183. Paria, B. C., Ma, W., Tan, J., Raja, S., Das, S. K., Dey, S. K. and Hogan, B. L. (2001). Cellular and molecular responses of the uterus to embryo implantation can be elicited by locally applied growth factors. *Proc Natl Acad Sci U S A* 98, 1047-1052.
184. Park, J. K., Kang, T. G., Kang, M. Y., Park, J. E., Cho, I. A., Shin, J. K., Choi, W. J., Lee, S. A., Choi, W. S., Kwon, H. M., et al. (2014). Increased NFAT5 expression stimulates transcription of Hsp70 in preeclamptic placentas. *Placenta* 35, 109-116.
185. Park, P. J. (2009). ChIP-seq: advantages and challenges of a maturing technology. *Nat Rev Genet* 10, 669-680.
186. Parsell, D. A. and Sauer, R. T. (1989). Induction of a heat shock-like response by unfolded protein in Escherichia coli: dependence on protein level not protein degradation. *Genes Dev* 3, 1226-1232.
187. Pfaffl, M. W. (2001). A new mathematical model for relative quantification in real-time RT-PCR. *Nucleic Acids Res* 29, e45.
188. Pfeifer, I., Benachi, A., Saker, A., Bonnefont, J. P., Mouawia, H., Broncy, L., Frydman, R., Brival, M. L., Lacour, B., Dachez, R., et al. (2016). Cervical trophoblasts for non-invasive single-cell genotyping and prenatal diagnosis. *Placenta* 37, 56-60.

189. Phelps, E. D., Updike, D. L., Bullen, E. C., Grammas, P. and Howard, E. W. (2006). Transcriptional and posttranscriptional regulation of angiopoietin-2 expression mediated by IGF and PDGF in vascular smooth muscle cells. *Am J Physiol Cell Physiol* 290, C352-361.
190. Pijnenborg, R., Vercruysse, L. and Hanssens, M. (2006). The uterine spiral arteries in human pregnancy: facts and controversies. *Placenta* 27, 939-958.
191. Pillai, R. S., Bhattacharyya, S. N. and Filipowicz, W. (2007). Repression of protein synthesis by miRNAs: how many mechanisms? *Trends Cell Biol* 17, 118-126.
192. Powell, W. C., Fingleton, B., Wilson, C. L., Boothby, M. and Matrisian, L. M. (1999). The metalloproteinase matrilysin proteolytically generates active soluble Fas ligand and potentiates epithelial cell apoptosis. *Curr Biol* 9, 1441-1447.
193. Prakash, S., Tian, L., Ratliff, K. S., Lehotzky, R. E. and Matouschek, A. (2004). An unstructured initiation site is required for efficient proteasome-mediated degradation. *Nat Struct Mol Biol* 11, 830-837.
194. Pratt, W. B., Gestwicki, J. E., Osawa, Y. and Lieberman, A. P. (2015). Targeting Hsp90/Hsp70-based protein quality control for treatment of adult onset neurodegenerative diseases. *Annu Rev Pharmacol Toxicol* 55, 353-371.
195. Pratt, W. B. and Toft, D. O. (2003). Regulation of signaling protein function and trafficking by the hsp90/hsp70-based chaperone machinery. *Exp Biol Med (Maywood)* 228, 111-133.
196. Raab, G., Kover, K., Paria, B. C., Dey, S. K., Ezzell, R. M. and Klagsbrun, M. (1996). Mouse preimplantation blastocysts adhere to cells expressing the transmembrane form of heparin-binding EGF-like growth factor. *Development* 122, 637-645.

197. Ramma, W. and Ahmed, A. (2014). Therapeutic potential of statins and the induction of heme oxygenase-1 in preeclampsia. *J Reprod Immunol* 101-102, 153-160.
198. Rappolee, D. A., Brenner, C. A., Schultz, R., Mark, D. and Werb, Z. (1988). Developmental expression of PDGF, TGF-alpha, and TGF-beta genes in preimplantation mouse embryos. *Science* 241, 1823-1825.
199. Redline, R. W. and Lu, C. Y. (1989). Localization of fetal major histocompatibility complex antigens and maternal leukocytes in murine placenta. Implications for maternal-fetal immunological relationship. *Lab Invest* 61, 27-36.
200. Redman, C. W. and Sargent, I. L. (2005). Latest advances in understanding preeclampsia. *Science* 308, 1592-1594.
201. Reese, J., Brown, N., Das, S. K. and Dey, S. K. (1998). Expression of neu differentiation factor during the periimplantation period in the mouse uterus. *Biol Reprod* 58, 719-727.
202. Riese, D. J., 2nd and Stern, D. F. (1998). Specificity within the EGF family/ErbB receptor family signaling network. *Bioessays* 20, 41-48.
203. Roberts, J. M., Creasy, R. K. and Resnik, R. (1998). Pregnancy related hypertension. In *Maternal Fetal Medicine*, pp. 833-872. Philadelphia: W.B. Saunders.
204. Rodeck, C., Tutschek, B., Sherlock, J. and Kingdom, J. (1995). Methods for the transcervical collection of fetal cells during the first trimester of pregnancy. *Prenat Diagn* 15, 933-942.
205. Rodesch, F., Simon, P., Donner, C. and Jauniaux, E. (1992). Oxygen measurements in endometrial and trophoblastic tissues during early pregnancy. *Obstet Gynecol* 80, 283-285.
206. Roelle, S., Grosse, R., Aigner, A., Krell, H. W., Czubayko, F. and Gudermann, T. (2003).

- Matrix metalloproteinases 2 and 9 mediate epidermal growth factor receptor transactivation by gonadotropin-releasing hormone. *J Biol Chem* 278, 47307-47318.
207. Rossello, A., Nuti, E., Orlandini, E., Carelli, P., Rapposelli, S., Macchia, M., Minutolo, F., Carbonaro, L., Albini, A., Benelli, R., et al. (2004). New N-arylsulfonyl-N-alkoxyaminoacetohydroxamic acids as selective inhibitors of gelatinase A (MMP-2). *Bioorg Med Chem* 12, 2441-2450.
  208. Rout, U. K., Wang, J., Paria, B. C. and Armant, D. R. (2004). Alpha5beta1, alphaVbeta3 and the platelet-associated integrin alphaIIbbeta3 coordinately regulate adhesion and migration of differentiating mouse trophoblast cells. *Dev Biol* 268, 135-151.
  209. Rudel, S., Wang, Y., Lenobel, R., Korner, R., Hsiao, H. H., Urlaub, H., Patel, D. and Meister, G. (2011). Phosphorylation of human Argonaute proteins affects small RNA binding. *Nucleic Acids Res* 39, 2330-2343.
  210. Salmena, L., Poliseno, L., Tay, Y., Kats, L. and Pandolfi, P. P. (2011). A ceRNA hypothesis: the Rosetta Stone of a hidden RNA language? *Cell* 146, 353-358.
  211. Sanchez, J. J., Phillips, C., Borsting, C., Balogh, K., Bogus, M., Fondevila, M., Harrison, C. D., Musgrave-Brown, E., Salas, A., Syndercombe-Court, D., et al. (2006). A multiplex assay with 52 single nucleotide polymorphisms for human identification. *Electrophoresis* 27, 1713-1724.
  212. Schlecht, R., Scholz, S. R., Dahmen, H., Wegener, A., Sirrenberg, C., Musil, D., Bomke, J., Eggenweiler, H. M., Mayer, M. P. and Bukau, B. (2013). Functional analysis of Hsp70 inhibitors. *PLoS One* 8, e78443.
  213. Schwanhausser, B., Busse, D., Li, N., Dittmar, G., Schuchhardt, J., Wolf, J., Chen, W. and Selbach, M. (2011). Global quantification of mammalian gene expression control.

- Nature* 473, 337-342.
214. Schwarz, D. S., Hutvagner, G., Du, T., Xu, Z., Aronin, N. and Zamore, P. D. (2003). Asymmetry in the assembly of the RNAi enzyme complex. *Cell* 115, 199-208.
  215. Selbach, M., Schwanhaussner, B., Thierfelder, N., Fang, Z., Khanin, R. and Rajewsky, N. (2008). Widespread changes in protein synthesis induced by microRNAs. *Nature* 455, 58-63.
  216. Semenza, G. L. (2003). Targeting HIF-1 for cancer therapy. *Nat Rev Cancer* 3, 721-732.
  217. Sermon, K., Van Steirteghem, A. and Liebaers, I. (2004). Preimplantation genetic diagnosis. *Lancet* 363, 1633-1641.
  218. Shen, J., Xia, W., Khotskaya, Y. B., Huo, L., Nakanishi, K., Lim, S. O., Du, Y., Wang, Y., Chang, W. C., Chen, C. H., et al. (2013). EGFR modulates microRNA maturation in response to hypoxia through phosphorylation of AGO2. *Nature* 497, 383-387.
  219. Shettles, L. B. (1971). Use of the Y chromosome in prenatal sex determination. *Nature* 230, 52-53.
  220. Shimoya, K., Moriyama, A., Matsuzaki, N., Ogata, I., Koyama, M., Azuma, C., Saji, F. and Murata, Y. (1999). Human placental cells show enhanced production of interleukin (IL)-8 in response to lipopolysaccharide (LPS), IL-1 and tumour necrosis factor (TNF)-alpha, but not to IL-6. *Mol Hum Reprod* 5, 885.
  221. Shiohama, A., Sasaki, T., Noda, S., Minoshima, S. and Shimizu, N. (2003). Molecular cloning and expression analysis of a novel gene DGCR8 located in the DiGeorge syndrome chromosomal region. *Biochem Biophys Res Commun* 304, 184-190.
  222. Sibilio, M. and Wagner, E. F. (1995). Strain-dependent epithelial defects in mice lacking the EGF receptor. *Science* 269, 234-238.

223. Sims, J. D., McCready, J. and Jay, D. G. (2011). Extracellular heat shock protein (Hsp)70 and Hsp90alpha assist in matrix metalloproteinase-2 activation and breast cancer cell migration and invasion. *PLoS One* 6, e18848.
224. Sitras, V., Paulssen, R., Leirvik, J., Vartun, A. and Acharya, G. (2009). Placental gene expression profile in intrauterine growth restriction due to placental insufficiency. *Reprod Sci* 16, 701-711.
225. Soleymanlou, N., Jurisica, I., Nevo, O., Ietta, F., Zhang, X., Zamudio, S., Post, M. and Caniggia, I. (2005). Molecular evidence of placental hypoxia in preeclampsia. *J Clin Endocrinol Metab* 90, 4299-4308.
226. Sorensen, B. S., Ornskov, D. and Nexø, E. (2006). The chemotherapeutic agent VP16 increases the stability of HB-EGF mRNA by a mechanism involving the 3'-UTR. *Exp Cell Res* 312, 3651-3658.
227. Spruce, T., Pernaute, B., Di-Gregorio, A., Cobb, B. S., Merckenschlager, M., Manzanares, M. and Rodriguez, T. A. (2010). An early developmental role for miRNAs in the maintenance of extraembryonic stem cells in the mouse embryo. *Dev Cell* 19, 207-219.
228. Stachecki, J. J. and Armant, D. R. (1996). Regulation of blastocoele formation by intracellular calcium release is mediated through a phospholipase C-dependent pathway in mice. *Biol Reprod* 55, 1292-1298.
229. Staff, A. C., Benton, S. J., von Dadelszen, P., Roberts, J. M., Taylor, R. N., Powers, R. W., Charnock-Jones, D. S. and Redman, C. W. (2013). Redefining preeclampsia using placenta-derived biomarkers. *Hypertension* 61, 932-942.
230. Stamenkovic, I. (2003). Extracellular matrix remodelling: the role of matrix metalloproteinases. *J Pathol* 200, 448-464.



231. Staun-Ram, E., Goldman, S., Gabarin, D. and Shalev, E. (2004). Expression and importance of matrix metalloproteinase 2 and 9 (MMP-2 and -9) in human trophoblast invasion. *Reprod Biol Endocrinol* 2, 59.
232. Sternlicht, M. D. and Werb, Z. (2001). How matrix metalloproteinases regulate cell behavior. *Annu Rev Cell Dev Bi* 17, 463-516.
233. Stirpe, F. and Fiume, L. (1967). Effect of alpha-amanitin on ribonucleic acid synthesis and on ribonucleic acid polymerase in mouse liver. *Biochem J* 103, 67P-68P.
234. Sugihara, K., Sugiyama, D., Byrne, J., Wolf, D. P., Lowitz, K. P., Kobayashi, Y., Kabir-Salmani, M., Nadano, D., Aoki, D., Nozawa, S., et al. (2007). Trophoblast cell activation by trophinin ligation is implicated in human embryo implantation. *Proc Natl Acad Sci U S A* 104, 3799-3804.
235. Suh, N., Baehner, L., Moltzahn, F., Melton, C., Shenoy, A., Chen, J. and Belloch, R. (2010). MicroRNA function is globally suppressed in mouse oocytes and early embryos. *Curr Biol* 20, 271-277.
236. Suzuki, N., Nakayama, J., Shih, I. M., Aoki, D., Nozawa, S. and Fukuda, M. N. (1999). Expression of trophinin, tastin, and bystin by trophoblast and endometrial cells in human placenta. *Biol Reprod* 60, 621-627.
237. Tamada, H., Das, S. K., Andrews, G. K. and Dey, S. K. (1991). Cell-type-specific expression of transforming growth factor-alpha in the mouse uterus during the peri-implantation period. *Biol Reprod* 45, 365-372.
238. Tamada, H., Sakamoto, M., Sakaguchi, H., Inaba, T. and Sawada, T. (1997). Evidence for the involvement of transforming growth factor-alpha in implantation in the rat. *Life Sci* 60, 1515-1522.

239. Tamura, N., Sugihara, K., Akama, T. O. and Fukuda, M. N. (2011). Trophinin-mediated cell adhesion induces apoptosis of human endometrial epithelial cells through PKC-delta. *Cell Cycle* 10, 135-143.
240. Tamura, Y., Watanabe, F., Nakatani, T., Yasui, K., Fuji, M., Komurasaki, T., Tsuzuki, H., Maekawa, R., Yoshioka, T., Kawada, K., et al. (1998). Highly selective and orally active inhibitors of type IV collagenase (MMP-9 and MMP-2): N-sulfonylamino acid derivatives. *J Med Chem* 41, 640-649.
241. Tanimura, K., Nakago, S., Murakoshi, H., Takekida, S., Moriyama, T., Matsuo, H., Hashimoto, K. and Maruo, T. (2004). Changes in the expression and cytological localization of betacellulin and its receptors (ErbB-1 and ErbB-4) in the trophoblasts in human placenta over the course of pregnancy. *Eur J Endocrinol* 151, 93-101.
242. Tavaría, M., Gabriele, T., Kola, I. and Anderson, R. L. (1996). A hitchhiker's guide to the human Hsp70 family. *Cell Stress Chaperones* 1, 23-28.
243. Thiery, J. P., Acloque, H., Huang, R. Y. and Nieto, M. A. (2009). Epithelial-mesenchymal transitions in development and disease. *Cell* 139, 871-890.
244. Thiery, J. P. and Sleeman, J. P. (2006). Complex networks orchestrate epithelial-mesenchymal transitions. *Nat Rev Mol Cell Biol* 7, 131-142.
245. Threadgill, D. W., Dlugosz, A. A., Hansen, L. A., Tennenbaum, T., Lichti, U., Yee, D., LaMantia, C., Mourton, T., Herrup, K., Harris, R. C., et al. (1995). Targeted disruption of mouse EGF receptor: effect of genetic background on mutant phenotype. *Science* 269, 230-234.
246. Torres, C. G., Pino, A. M. and Sierralta, W. D. (2009). A cyclized peptide derived from alpha fetoprotein inhibits the proliferation of ER-positive canine mammary cancer cells.

- Oncol Rep* 21, 1397-1404.
247. Tsuchida, S., Arai, Y., Takahashi, K. A., Kishida, T., Terauchi, R., Honjo, K., Nakagawa, S., Inoue, H., Ikoma, K., Ueshima, K., et al. (2014). HIF-1 $\alpha$ -induced HSP70 regulates anabolic responses in articular chondrocytes under hypoxic conditions. *J Orthop Res* 32, 975-980.
  248. Tsui, N. B., Kadir, R. A., Chan, K. C., Chi, C., Mellars, G., Tuddenham, E. G., Leung, T. Y., Lau, T. K., Chiu, R. W. and Lo, Y. M. (2011). Noninvasive prenatal diagnosis of hemophilia by microfluidics digital PCR analysis of maternal plasma DNA. *Blood* 117, 3684-3691.
  249. Umata, T., Hirata, M., Takahashi, T., Ryu, F., Shida, S., Takahashi, Y., Tsuneoka, M., Miura, Y., Masuda, M., Horiguchi, Y., et al. (2001). A dual signaling cascade that regulates the ectodomain shedding of heparin-binding epidermal growth factor-like growth factor. *J Biol Chem* 276, 30475-30482.
  250. Vaughan, J. E. and Walsh, S. W. (2012). Activation of NF-kappaB in placentas of women with preeclampsia. *Hypertens Pregnancy* 31, 243-251.
  251. Vicovac, L. and Aplin, J. D. (1996). Epithelial-mesenchymal transition during trophoblast differentiation. *Acta Anat (Basel)* 156, 202-216.
  252. Walsh, N., Larkin, A., Swan, N., Conlon, K., Dowling, P., McDermott, R. and Clynes, M. (2011). RNAi knockdown of Hop (Hsp70/Hsp90 organising protein) decreases invasion via MMP-2 down regulation. *Cancer Lett* 306, 180-189.
  253. Wang, E., Batey, A., Struble, C., Musci, T., Song, K. and Oliphant, A. (2013). Gestational age and maternal weight effects on fetal cell-free DNA in maternal plasma. *Prenat Diagn* 33, 662-666.

254. Wang, G. L. and Semenza, G. L. (1993). General Involvement of Hypoxia-Inducible Factor-I in Transcriptional Response to Hypoxia. *P Natl Acad Sci USA* 90, 4304-4308.
255. Wang, J., Mayernik, L. and Armant, D. R. (2007). Trophoblast adhesion of the peri-implantation mouse blastocyst is regulated by integrin signaling that targets phospholipase C. *Dev Biol* 302, 143-153.
256. Wang, J., Mayernik, L., Schultz, J. F. and Armant, D. R. (2000). Acceleration of trophoblast differentiation by heparin-binding EGF-like growth factor is dependent on the stage-specific activation of calcium influx by ErbB receptors in developing mouse blastocysts. *Development* 127, 33-44.
257. Wang, X., Wang, H., Matsumoto, H., Roy, S. K., Das, S. K. and Paria, B. C. (2002). Dual source and target of heparin-binding EGF-like growth factor during the onset of implantation in the hamster. *Development* 129, 4125-4134.
258. Wapner, R. J. (2005). Invasive prenatal diagnostic techniques. *Semin Perinatol* 29, 401-404.
259. Wegele, H., Muller, L. and Buchner, J. (2004). Hsp70 and Hsp90--a relay team for protein folding. *Rev Physiol Biochem Pharmacol* 151, 1-44.
260. White, A. R., Du, T., Laughton, K. M., Volitakis, I., Sharples, R. A., Xilinas, M. E., Hoke, D. E., Holsinger, R. M., Evin, G., Cherny, R. A., et al. (2006). Degradation of the Alzheimer disease amyloid beta-peptide by metal-dependent up-regulation of metalloprotease activity. *J Biol Chem* 281, 17670-17680.
261. Wilczynska, A. and Bushell, M. (2015). The complexity of miRNA-mediated repression. *Cell Death Differ* 22, 22-33.
262. Wong, F. C. and Lo, Y. M. (2016). Prenatal Diagnosis Innovation: Genome Sequencing

- of Maternal Plasma. *Annu Rev Med* 67, 419-432.
263. Xie, H., Wang, H., Tranguch, S., Iwamoto, R., Mekada, E., Demayo, F. J., Lydon, J. P., Das, S. K. and Dey, S. K. (2007). Maternal heparin-binding-EGF deficiency limits pregnancy success in mice. *Proc Natl Acad Sci U S A* 104, 18315-18320.
  264. Xu, P., Wang, Y. L., Zhu, S. J., Luo, S. Y., Piao, Y. S. and Zhuang, L. Z. (2000). Expression of matrix metalloproteinase-2, -9, and -14, tissue inhibitors of metalloproteinase-1, and matrix proteins in human placenta during the first trimester. *Biol Reprod* 62, 988-994.
  265. Yen, H. C., Xu, Q., Chou, D. M., Zhao, Z. and Elledge, S. J. (2008). Global protein stability profiling in mammalian cells. *Science* 322, 918-923.
  266. Yoo, H. J., Barlow, D. H. and Mardon, H. J. (1997). Temporal and spatial regulation of expression of heparin-binding epidermal growth factor-like growth factor in the human endometrium: a possible role in blastocyst implantation. *Dev Genet* 21, 102-108.
  267. Yukawa, K., Tanaka, T., Tsuji, S. and Akira, S. (1999). Regulation of transcription factor C/ATF by the cAMP signal activation in hippocampal neurons, and molecular interaction of C/ATF with signal integrator CBP/p300. *Brain Res Mol Brain Res* 69, 124-134.
  268. Yung, H. W., Atkinson, D., Campion-Smith, T., Olovsson, M., Charnock-Jones, D. S. and Burton, G. J. (2014). Differential activation of placental unfolded protein response pathways implies heterogeneity in causation of early- and late-onset pre-eclampsia. *J Pathol* 234, 262-276.
  269. Zhao, W., Liu, M. and Kirkwood, K. L. (2008). p38alpha stabilizes interleukin-6 mRNA via multiple AU-rich elements. *J Biol Chem* 283, 1778-1785.
  270. Zhou, Y., Fisher, S. J., Janatpour, M., Genbacev, O., Dejana, E., Wheelock, M. and

- Damsky, C. H. (1997). Human cytotrophoblasts adopt a vascular phenotype as they differentiate. A strategy for successful endovascular invasion? *J. Clin. Invest.* 99, 2139-2151.
271. Zhu, X. M., Han, T., Wang, X. H., Li, Y. H., Yang, H. G., Luo, Y. N., Yin, G. W. and Yao, Y. Q. (2010). Overexpression of miR-152 leads to reduced expression of human leukocyte antigen-G and increased natural killer cell mediated cytotoxicity in JEG-3 cells. *Am J Obstet Gynecol* 202, 592 e591-597.

**ABSTRACT****MOLECULAR REGULATION OF TROPHOBLAST SURVIVAL DURING PLACENTATION AND PATHOLOGIES OF PLACENTAL INSUFFICIENCY**

by

**CHANDNI V. JAIN****December 2016****Advisor:** David Randall Armant, Ph.D.**Major:** Physiology (Reproductive Sciences Concentration)**Degree:** Doctor of Philosophy

HBEGF, is present in the uterus at the time of embryo implantation and protects first trimester TB cells from apoptosis and promotes their invasion. The hypertensive disease, PE, in which TB invasion of the uterine arteries is reduced and TB apoptosis is elevated, is characterized by a reduction in HBEGF expression. In this study using a first trimester cell line and villous explant culture key components involved in HBEGF survival signaling pathway were identified. Specific MMP inhibitors established the requirement for MMP2 in HBEGF shedding and upregulation. NGS identified a HIF regulated gene, HSPA6 (HSP70B') and using specific inhibitors it was established that HSP70 regulates MMP2 mediated shedding of HBEGF at low O<sub>2</sub> and is functional upstream of MAPKs signaling cascade. To further investigate HBEGF upregulation at low O<sub>2</sub> using NGS and siRNA knockdown of DGCR8 it was demonstrated that other components of RISC may be involved in regulation of HBEGF mRNA translation. These findings suggest that trophoblast survival during early pregnancy requires this signaling pathway and disruption of any component could lead to placental insufficiency. However, a global platform is needed to study the pathophysiology of trophoblast cells and their role in placental insufficiency.

TRIC is an innovative platform to noninvasively acquire fetal cells. DNA was extracted from fetal cells isolated from 20 specimens with gestational age as early as 5 weeks to 19 weeks. This was followed by targeted sequencing using the Forenseq (Illumina) platform to identify informative SNPs. Using the Forenseq software  $89\% \pm 12\%$  of the 94 SNPs were called correctly in the fetal samples. Using the STR analysis out of the 20 fetal samples, 9 males were confirmed. Therefore, TRIC not only provides fetal cells but also opens new venues of perinatal testing.

TRIC provides ample RNA from isolated fetal cells for extensive transcriptomic analysis. Using qPCR it was demonstrated that the fetal cells have higher expression for EVT specific markers such as HLA-G and KRT7 and markers for invasion/migration such as CDH5 and MMP9, whereas the maternal cells have a higher expression for epithelial markers such as CDH1 and ITGA6. This suggests that not only are the fetal cells EVT like but may also undergo an epithelial mesenchymal transition. Comparison of fetal and maternal cells from normal group using NGS identified 409 genes, of which top 5 upregulated and downregulated genes were validated by qPCR. Pathway analysis of the differentially regulated identified pathways related to invasion/migration, proliferation and differentiation, further suggesting the EVT like expression of the fetal cells. NGS revealed 348 differential expressed genes on comparison of the EVT like fetal cells from the EPL group to those from the normal group that were further validated by qPCR. Bioinformatic analysis identified pathways related to apoptosis, inflammation and placental disease.

The exact origin and biology of cervical EVT cells, and their relationship to the human placenta and pregnancy outcomes, are widely unknown. Based on our study so far it can be hypothesized that as the placenta grows, EVT cells are naturally shed into the cervical canal, and



their overall phenotype is comparable to the EVT cells residing in the placenta. These studies will provide a clearer view of the utility of EVT cells obtained by TRIC from ongoing pregnancies for investigating early placentation and mechanisms of pathology, and their potential as a platform for prenatal tests to predict maternal risk of placenta-based disease.

## AUTOBIOGRAPHICAL STATEMENT

**Chandni V. Jain**

### **EDUCATION**

07/2008	B.Sc. Punjab University, Ldh, India
06/2010	M.Sc. Lovely Professional University, Jal, India
01/12-to date	Ph.D. Wayne State University, Michigan, USA

### **AWARDS, HONORS, DISTINCTIONS**

10/200	Participated in Inter College Paper Presentation Competition
09/2009	Awarded <b>2<sup>nd</sup> Prize</b> in Bio-Horizon Debate held at Lovely Professional University
10/2009	Awarded <b>1<sup>st</sup> prize</b> in Biotechnology Debate held at Lovely Professional University.
04/2012	Presented a poster at the 3 <sup>rd</sup> annual Michigan Alliance of Reproductive Technologies and Science (MARTS) meet 2012.
08/2012	Presented a poster at the Society of Study of Reproduction (SSR) annual meeting on 14 <sup>th</sup> August 2012 at University of Pennsylvania.
08/2012	Awarded <b>LEMTFF travel grant</b> by the SSR.
09/2012	Awarded <b>3<sup>rd</sup> prize</b> at WSU-Graduate Student Research Day held on Sept. 27, 2012
10/2012	Presented a poster at the NIH Research Festival held from October 9-12, 2012.
05/2014	Presented a poster at the Annual Mott Centre Retreat held on May 7 <sup>th</sup> , 2014.
07/2014	Presented a poster at the Society of Study of Reproduction (SSR) annual meeting to be held from the July 18-23, 2014 at Grand Rapids, MI.
05/2015	Presented a poster at the Annual Mott Centre Retreat held on May 8 <sup>th</sup> , 2015.
05/2015	Awarded the 2015-2016 <b>Thomas C. Rumble University Graduate Fellowship</b> WSU
03/2016	Awarded <b>3<sup>rd</sup> prize</b> at WSU-Graduate Research Symposium held on Mar 23 <sup>rd</sup> 2016

### **SCHOLARLY BIBLIOGRAPHY**

1. **Chandni V. Jain**, Philip Jessmon, Charbel T. Barrak, Alan D. Bolnick, Brian A. Kilburn, Michael Hertz, D. Randall Armant. Trophoblast survival signaling during human placentation requires HIF-induced transcription of HSP70. **Manuscript submitted to "Development"**.
2. **Chandni V. Jain\***, Leena Kadam\*, Marie van Dijk, Hamid-Reza Kohan-Ghadr, Brian A. Kilburn, Craig Hartman, Vicki Mazzorana, Allerdien Visser, Michael Hertz, Alan D. Bolnick, Rani Fritz, D. Randall Armant and Sascha Drewlo. Fetal genome profiling at five weeks of gestation after noninvasive isolation of trophoblast cells from the endocervical canal **Manuscript submitted to "Science Translational Medicine"**.
3. **Chandni V. Jain**, Philip Jessmon, Brian A. Kilburn, Meritxell Jodar, Edward Sendler, Stephen A. Krawetz, D. Randall Armant. Regulation of HBEGF by Micro-RNA for survival of developing human trophoblast cells. **Manuscript in process of revision to "PLOS ONE"**.
4. Jay M Bolnick, Yan Zhou, **Chandni V. Jain**, Alan Bolnick, Brian A Kilburn, Michael Hertz, Jing Dai, Michael P. Diamond, Susan J. Fisher, and D.Randall Armant. HBEGF and survival of first trimester villous explants during oxygen fluctuations. **Manuscript in process of revision to "Biology of Reproduction"**.
5. Fritz R, **Jain C**, Armant DR. (2014) Cell signaling in trophoblast-uterine communication. *Int. J Dev Biol* 58, 261-71.
6. Kohan-Ghadr HR, Kadam L, **Jain C**, Armant DR, Drewlo S. (2016) Potential role of epigenetic mechanisms in regulation of trophoblast differentiation, migration, and invasion in the human placenta. *Cell Adh Migr*. 8, 1-10.
7. Bolnick AD, Fritz R, **Jain C**, Kadam L, Bolnick JM, Kilburn BA, Singh M, Diamond MP, Drewlo S, Armant DR. (2016) Trophoblast retrieval and isolation from the cervix for noninvasive, first trimester, fetal gender determination in a carrier of congenital adrenal hyperplasia. *Reprod Sci*. pii. 1993719116632922.